

Regulation of Interferon-kappa Expression in Normal and HPV-positive Human Keratinocytes

Dissertation

der Mathematisch-Naturwissenschaftlichen Fakultät

der Eberhard Karls Universität Tübingen

zur Erlangung des Grades eines

Doktors der Naturwissenschaften

(Dr. rer. nat.)

vorgelegt von

Katrin Klein

aus Reutlingen

Tübingen

2020

Gedruckt mit Genehmigung der Mathematisch-Naturwissenschaftlichen Fakultät der Eberhard Karls
Universität Tübingen.

Tag der mündlichen Qualifikation: 28.05.2020

Dekan: Prof. Dr. Wolfgang Rosenstiel

1. Berichterstatter: Prof. Dr. Stefan Stevanović

2. Berichterstatter: Prof. Dr. Frank Stubenrauch

Table of Contents

List of Abbreviations.....	VII
List of Figures.....	XII
List of Tables.....	XIV
1. Summary.....	15
2. Introduction.....	19
2.1. Interferons in General	19
2.1.1. Human Interferon Classes	20
2.1.1.1. Type I IFNs	20
2.1.1.2. Type II and Type III IFNs.....	21
2.1.2. Regulation of Type I and Type III IFN Expression	22
2.1.2.1. Inducible IFNs	22
2.1.2.2. cGAS/STING Pathway	22
2.1.2.3. Constitutively Expressed IFNs.....	24
a) IFN Epsilon.....	24
b) IFN Kappa.....	24
2.1.3. IFN- κ in Disease	25
2.1.3.1. IFN- κ in Cutaneous Lupus Erythematosus	25
2.1.3.2. IFN- κ in Papillomavirus Infection	26
2.2. Papillomaviruses.....	26
2.2.1. Classification of Human Papillomaviruses and Clinical Relevance	27
2.2.2. Structure of the HPV Genome.....	28
2.2.3. Viral Life Cycle	29
2.2.4. Viral Proteins	30
2.2.4.1. The E1 Helicase.....	30
2.2.4.2. The E2 and the E8 ^{E2} Protein	30
2.2.4.3. The E4 Protein	31
2.2.4.4. The E5 Protein	31
2.2.4.5. The E6 Oncoprotein.....	32
2.2.4.6. The E7 Oncoprotein.....	32
2.2.4.7. The Capsid Proteins L1 and L2.....	32
2.2.5. HPV Vaccination	33
2.3. Objective.....	34
3. Material and Methods.....	35

3.1. Materials.....	35
3.1.1. Chemicals in General.....	35
3.1.2. Buffers	35
3.1.3. Media & Solutions	37
3.1.3.1. Bacterial Culture.....	37
3.1.3.2. Eukaryotic Cell Culture	37
3.1.3.3. Inhibitors, Activators	39
3.1.4. Used Kits and Reagents	40
3.1.5. Enzymes.....	41
3.1.6. Antibodies	41
3.1.7. Used Cell Types.....	44
3.1.7.1. Eukaryotic Cells.....	44
3.1.7.2. Bacterial Strains.....	44
3.1.8. Used Nucleic Acids	45
3.1.9. Plasmids.....	50
3.1.10. Devices	53
3.1.11. Consumption Items	55
3.2. Methods	56
3.2.1. DNA-Methods.....	56
3.2.1.1. Standard Methods.....	56
3.2.1.2. Preparative Isolation of Plasmid DNA from Bacteria	56
3.2.1.3. Amplification of DNA.....	56
3.2.1.4. Isolation of DNA after Electrophoretic Separation.....	57
3.2.1.5. Ligation of DNA Fragments.....	57
3.2.1.6. Molecular Cloning.....	58
3.2.1.7. Choosing Candidate Binding Motifs for Transcription Factors.....	58
3.2.1.8. Validation of used DNA Sequences	59
3.2.2. Microbiological Methods	59
3.2.2.1. Production of Chemical Competent Bacteria.....	59
3.2.2.2. Transformation of Plasmid DNA.....	60
3.2.2.3. Culture of Bacteria for DNA Amplification and Isolation	60
3.2.3. Cell Culture Methods.....	60
3.2.3.1. Retrieval of NHK from Human Foreskin	60
3.2.3.2. Culture of Cells	61
3.2.3.3. Mitomycin C Treatment of Feeder Cells.....	61

3.2.3.4.	Freezing and Thawing of Mammalian Cells	62
3.2.3.5.	Test for <i>Mycoplasma</i> Contamination	62
3.2.3.6.	Harvesting Cells	64
3.2.3.7.	Treatment of Cells	64
3.2.3.8.	Transfection of Cells	64
3.2.4.	Analysis of Eukaryotic Cells	66
3.2.4.1.	Luciferase Reporter Assays.....	66
3.2.4.2.	Nuclear Extract Preparation	67
3.2.4.3.	Electrophoretic Mobility Shift Assay (EMSA)	68
3.2.4.4.	RNA Interference	69
3.2.4.5.	Compound Treatments	69
3.2.4.6.	Western Blot Analysis.....	70
3.2.4.7.	Chromatin Immunoprecipitation (ChIP).....	71
3.2.4.8.	Immunofluorescence.....	72
3.2.5.	RNA Methods	72
3.2.5.1.	Isolation of Total RNA from Mammalian Cells	72
3.2.5.2.	Synthesis of complementary DNA (cDNA)	73
3.2.5.3.	Quantitative Real-Time PCR (qPCR).....	73
3.2.6.	Statistical Analysis and Creation of Figures.....	74
4.	Results	75
4.1.	Regulation of the <i>IFNK</i> Gene	75
4.1.1.	Contribution of three DNase I Hypersensitive Regions to Reporter Activity	75
4.1.2.	Identification and Analysis of putative Transcription Factor Binding Sites.....	76
4.1.3.	Analysis of Protein Binding to Identified Binding Sites	80
4.1.4.	Effect of Different Signaling Pathways on Endogenous <i>IFNK</i> RNA Expression.....	82
4.1.5.	Effects of MAPK and TGF- β Signaling on <i>IFNK</i> RNA Expression in NHK	83
4.1.6.	Effects of MAPK and TGF- β Signaling on <i>IFNK</i> RNA Expression in HK 16E7	85
4.1.7.	Analysis of IFN- κ on Protein Level.....	87
4.1.7.1.	Analysis of IFN- κ , phospho-STAT1 and IFIT1 Expression in NHK.....	88
4.1.8.	Regulation of putatively involved AP-1 Transcription Factors	88
4.1.9.	Identification of Transcription Factors involved in <i>IFNK</i> Gene Activation	90
4.1.9.1.	Role of putative p53/p63 Binding Site in <i>IFNK</i> Enhancer	93
4.1.10.	Analysis of Transcription Factor Binding to the <i>IFNK</i> Enhancer in vivo	94
4.1.11.	Effect of identified Transcription Factors on other Type I IFNs	95

4.2.	Regulation of <i>IFNK</i> Expression in Pathological Settings	96
4.2.1.	<i>IFNK</i> Expression in HR-HPV-positive Keratinocytes.....	96
4.3.	Influence of HR-HPV Proteins on cGAS/STING Signaling.....	99
4.3.1.	Establishment of a cGAS/STING/ <i>IFNB1</i> -Promoter Reporter Assay	99
4.3.2.	Influence of HR-HPV Proteins on STING-dependent <i>IFNB1</i> Reporter	103
4.3.3.	Localization of HPV E5 and STING	104
5.	Discussion	107
5.1.	Regulation of IFN- κ Expression	107
5.1.1.	Putative Role of HMG-I Factors in <i>IFNK</i> Expression	109
5.1.2.	Signaling Pathways and Transcription Factors involved in <i>IFNK</i> Expression.....	110
5.1.3.	<i>IFNK</i> in the Context of Infections	111
5.1.4.	IFN- κ in Skin Disorders	113
5.2.	HR-HPV and cGAS/STING Signaling	114
5.2.1.	Strategies of Immune Evasion.....	114
5.2.2.	The cGAS/STING Pathway in HPV Infection	114
5.2.3.	<i>IFNB1</i> Induction in various Cell Types	115
5.2.4.	Impact of HPV Proteins on <i>IFNB1</i> Reporter.....	116
5.2.5.	HPV E5 and STING Signaling	116
6.	Appendix.....	CXVIII
6.1.	Supplemental Figures.....	CXVIII
6.1.1.	Internal Deletions of <i>IFNK</i> Reporter Constructs.....	CXVIII
6.1.2.	Binding of Keratinocyte Proteins to the putative HOX BS.....	CXIX
6.1.3.	Effects of reduced Amounts of TGF- β on <i>IFNK</i> Transcription	CXXI
6.2.	Curriculum Vitae.....	CXXII
6.3.	Publications	CXXIII
6.4.	Acknowledgement.....	CXXIV
7.	References.....	CXXV

List of Abbreviations

Gene symbols (if used in this work) are shown in italic typesetting, corresponding protein names thereafter

Abbreviation	Meaning
(ds)/(c)DNA	(double-stranded)/(complementary) deoxyribonucleic acid
(E)/(S)YFP	(enhanced)/(super) yellow fluorescent protein
(F)CS	(fetal) calf serum
(H)PV	(human) papillomavirus
(q)PCR	(quantitative real-time) polymerase chain reaction
(si)RNA	(short interfering) ribonucleic acid
(v/v)	volume per volume
(w/v)	weight per volume
°C	degree Celsius
µg	microgram
µl	microliter
µM	micromolar
∞	for ever
>/≥	more than/equal or more than
≈	approximately
Δ	delta (indicating either a difference or a missing part)
A	adenine
AG	'Aktiengesellschaft'
AP-1	activator protein 1
ATF-2	activating transcription factor 2
ATM	ataxia telangiectasia mutated
ATP	adenosine triphosphate
Bap31	B-cell receptor-associated protein 31
bp	base pairs
BS	binding site
BSA	bovine serum albumin
C	cytosine
cAMP	cyclic adenosine monophosphate
CAPS	N-cyclohexyl-3-aminopropanesulfonic acid
cGAMP	cyclic GMP-AMP
cGAS	cyclic guanosine monophosphate (GMP)- adenosine monophosphate (AMP) synthase
ChIP	chromatin immunoprecipitation
CIN	cervical intraepithelial neoplasia
CLE	cutaneous lupus erythymatosus
CMV	cytomegalovirus
c-myc	myc proto-oncogene protein
Co. KG	'Compagnie Kommanditgesellschaft'
CP	crossing point
CpG	cytosine-guanine (connected via phosphodiester bound)
C-terminal	carboxy-terminal
CTZ	coelenterazine
DAPI	4',6-diamidino-2-phenylindole
DDR	DNA damage response
del	deletion
DH5α	Doug Hanahan 5 alpha (bacterial strain)

Gene symbols (if used in this work) are shown in italic typesetting, corresponding protein names thereafter

Abbreviation	Meaning
diGMP	(cyclic) di-guanosine monophosphate
DMEM	Dulbecco's Modified Eagle Medium
DMF	dimethylformamide
DMSO	dimethyl sulfoxide
DNase I	deoxyribonuclease I
dNTP	deoxynucleotide triphosphate
<i>DPH3</i>	diphthamide biosynthesis 3
Dr.	Doctor (academic grade)
E6-AP	(human papillomavirus) E6-associated protein
EDTA	ethylenediaminetetraacetic acid
EGF(R)	epidermal growth factor (receptor)
ELK3	ETS domain-containing protein Elk-3
EMCV	encephalomyocarditis virus
EMSA	electrophoretic mobility shift assay
ER	endoplasmic reticulum
ERK(i)	extracellular signal-regulated kinase (inhibitor)
EtBr	ethidium bromide
F	forward
FLuc	Firefly luciferase
fM	femtomol
<i>FOS/Fos</i>	proto-oncogene c-Fos
<i>FOSB/FosB</i>	protein FosB
<i>FOSL1/Fra1</i>	FOS like 1/Fos-related antigen 1
<i>FOSL2/Fra2</i>	FOS like 2/Fos-related antigen 2
FOX	forkhead box protein
G	guanine
g	gram or gravity of earth
<i>GAPDH</i>	glyceraldehyde 3-phosphate dehydrogenase
GFP	green fluorescent protein
GLuc	<i>Gaussia</i> luciferase
GmbH	'Gesellschaft mit beschränkter Haftung'
GRHL2	grainyhead-like protein 2 homolog
h	hours
HC	HyClone serum
HEK 293T	human embryonic kidney cells, containing the large T antigen of SV40
HEPES	4-(2-hydroxyethyl)-1-piperazineethanesulfonic acid
HK	human keratinocytes
HK 16E7	human keratinocytes expressing the HPV16 E7 protein
HK HPV16/31	human keratinocytes carrying HPV16/HPV31 genomes
HMGA	high mobility group A protein
HOX	homeobox protein
HR-	high risk-
hs	<i>Homo sapiens</i> (human)
HS	(DNase I) hypersensitive region
HSV-2	herpes simplex virus 2
IARC	International Agency for Research on Cancer
<i>IFI16/IFI16</i>	gamma-interferon-inducible protein 16
<i>IFIT1/IFIT1</i>	interferon-induced protein with tetratricopeptide repeats 1
IFN	interferon
<i>IFNA/IFN-α</i>	interferon alpha

Gene symbols (if used in this work) are shown in italic typesetting, corresponding protein names thereafter

Abbreviation	Meaning
IFNAR	interferon alpha receptor
<i>IFNB1</i> , -E, G/ <i>IFN-β</i> , -ε, -γ	interferon beta, epsilon, gamma
IFNGR	interferon gamma receptor
<i>IFNK</i> , -L/ <i>IFN-κ</i> , -λ	interferon kappa, lambda
IFNLR1	interferon lambda receptor 1
<i>IFNW1</i> / <i>IFN-ω</i>	interferon omega
IgG	immunoglobulin G
IL10RB	interleukin 10 receptor subunit beta
IL-6	interleukin 6
Inc.	Incorporated
IRF	interferon-regulatory factor
ISG	interferon-stimulated gene
J2	NIH-3T3-J2 (fibroblast cell line)
JAK	Janus kinase (tyrosine-protein kinase JAK)
JNK(i)	c-Jun amino-terminal kinase (inhibitor)
<i>JUN</i> /Jun	proto-oncogene c-Jun
<i>JUNB</i> /jun-B	transcription factor jun-B
<i>JUND</i> /jun-D	transcription factor jun-D
kb	kilobases
kDa	kilodalton
KGaA	'Kommanditgesellschaft auf Aktien'
KLF5	Krueppel-like factor 5
l	liter
L1, L2	late proteins of papillomaviruses
LB	Luria-Bertani
Log10	logarithm of x to the base 10
Luc	<i>Gaussia</i> or <i>Renilla</i> Luciferase
LR-	low risk-
M	molar (mol/l)
MAF	transcription factor Maf
MAPK	mitogen-activated protein kinase
mCherry	monomeric red fluorescent protein
MDM2	mouse double minute 2 homolog
MEK	MAPK/ERK kinase 1
mg	milligram
min	minute(s)
ml	milliliter
mM	millimolar
mm	<i>Mus musculus</i> (mouse)
mt	mutation/mutant/mutated
<i>NFAT5</i> / <i>NFAT5</i>	nuclear factor of activated T cells 5
NF-κB	nuclear factor-κB
NHK	normal human keratinocytes
NIKS	normal immortal keratinocytes
nm	nanometer
nM	nanomolar
N-terminal	amino-terminal
OD ₍₆₀₀₎	optical density (at 600 nm)
oligo	oligonucleotide
ORF	open reading frame

Gene symbols (if used in this work) are shown in italic typesetting, corresponding protein names thereafter

Abbreviation	Meaning
PAA	polyacrylamide
PAGE	polyacrylamide gel electrophoresis
PARP-1	poly [ADP-ribose] polymerase 1, ADP = adenosine diphosphate
PaVE	Papillomavirus Episteme (database)
PBS/PBS-T	phosphate-buffered saline/with Tween20
PE	early promoter
PES	polyethersulfone
PET	polyethylene terephthalate
<i>PGK1</i>	phosphoglycerate kinase 1
pH	decimal logarithm of reciprocal of hydrogen ion activity in a solution
p.i.	post infection
pInd	pInducer (inducible expression plasmid)
PL	late promoter
pmol	picomol
poly(dA:dT)	poly(deoxyadenylic:deoxythymidylic) acid
poly(dI:dC)	poly(deoxyinosinic-deoxycytidylic) acid
poly(I:C)	poly(inosinic:polycytidylic) acid
PP	polypropylene
prep	preparation
Prof.	Professor (academic grade)
Prom	promoter
PRR	pattern-recognition receptor
PS	polystyrene
R	reverse
<i>RB1/pRb</i>	RB transcriptional corepressor 1 (Retinoblastoma)
<i>RFX/RFX</i>	regulatory factor X
RIG-I	retinoic acid-inducible gene I
RIPA buffer	radioimmunoprecipitation assay buffer
RLU	relative luminescent units
RLuc	<i>Renilla</i> luciferase
rpm	rounds per minute
RTS3b	renal transplant squamous cells (cell line)
s	seconds
SDS	sodium dodecyl sulfate
<i>SERPINE1/PAI-1</i>	serpin family E member 1/plasminogen activator inhibitor 1
SEM	standard error of the means
SLE	systemic lupus erythematosus
<i>SMAD/SMAD</i>	mothers against decapentaplegic homolog 3
SOC	Super Optimal broth with Catabolite repression (medium)
sp.	species
<i>SP100/Sp-100</i>	nuclear autoantigen Sp-100
<i>STAT/STAT</i>	signal transducer and activator of transcription
SV40	simian virus 40
SYBR	Synergy Brands, Inc. (stock symbol)
T	thymine
TAE	Tris- acetic acid - EDTA
Taq polymerase	<i>Thermus aquaticus</i> polymerase
TBE	Tris -borate - EDTA
TBK1	TANK-binding kinase 1
TBS/TBS-T	Tris-buffered saline/with Tween20

Gene symbols (if used in this work) are shown in italic typesetting, corresponding protein names thereafter

Abbreviation	Meaning
Tech.	Technology (part of company name)
TERT	telomerase reverse transcriptase
<i>TFAP2A</i> , -B, -C, -D, -E/ AP-2 α , - β , - γ , - δ , - ϵ	transcription factor AP-2 alpha, beta, gamma, delta, epsilon
TF(BS)	transcription factor (binding site)
TGFBR1(i)	transforming growth factor beta receptor 1 (inhibitor)
TGF- β (1)	transforming growth factor beta (1)
TLR	Toll-like receptor
<i>TMEM173</i> /STING	transmembrane protein 173/stimulator of interferon genes
<i>TP53</i> /p53	tumor protein p53
<i>TP63</i> /p63	tumor protein p63
<i>TP73</i> /p73	tumor protein p73
TPA	12-O-tetra-decanoylphorbol-13-acetate
TRE	TPA response element
Tyr701	tyrosine at position 701
U	Unit (enzymatic activity) or uracil (nucleotide)
URR	upstream regulatory region
US	United States (of America)
UV(B)	ultra violet B (irradiation)
V	Volt
VLP	virus-like particle
VSV	vesicular stomatitis virus
wt	wildtype

List of Figures

Figure 1: Pathways of Type I IFN induction and IFNA receptor signaling	19
Figure 2: Schematic representation of human chromosome 9, showing the type I IFN cluster and the adjacent <i>IFNK</i> gene.....	21
Figure 3: Two different modes of activation of STING in human keratinocytes	23
Figure 4: Genome organization of high risk alpha HPVs	29
Figure 5: Deletion of DNase I HS regions from the putative regulatory element decreases reporter activity in NHK as well as in immortalized keratinocytes.....	76
Figure 6: Mutation of several putative transcription factor binding motifs decreases <i>IFNK</i> promoter activity in keratinocytes	78
Figure 7: Proteins present in nuclear extracts from keratinocytes bind specifically to the putative binding sites for AP-1, SMAD and p63.....	81
Figure 8: <i>IFNK</i> expression in HK 16E7 cells is not different from expression in NHK.....	82
Figure 9: Analysis of NHK transcription reveals that endogenous <i>IFNK</i> is regulated by TGF- β 1 and ERK1/2 pathways.....	85
Figure 10: Influence of MAPK signaling on transcription in HK 16E7 differs from effects seen in NHK	87
Figure 11: Stimulation of the TGF- β - and inhibition of the ERK1/2 pathway induces IFN- κ expression and is accompanied by increased phosphorylation of STAT1 and induction of the antiviral IFIT1 protein.....	88
Figure 12: Manipulating the TGF- β pathway in NHK transfected with <i>IFNK</i> reporter constructs reveals that the AP-1 and SMAD binding sites constitute a TGF- β responsive element.....	89
Figure 13: Inhibition of ERK1/2 in NHK transfected with different <i>IFNK</i> reporter constructs	90
Figure 14: RNA interference experiments demonstrate that transcription of <i>IFNK</i> relies on jun-B, SMAD4 and p63.....	92
Figure 15: Compound treatments suggest that p53 represses and p63 activates <i>IFNK</i> expression in NHK.....	93
Figure 16: ChIP analysis in NHK showing enrichment of AP-2 α , jun-B and SMAD4 in the <i>IFNK</i> enhancer	94
Figure 17: Effect of TGF- β 1 and ERK1/2 pathway or <i>TFAP2</i> and <i>TP63</i> knockdown on expression of other type I IFN genes	95
Figure 18: Analysis of transcription in HPV16-positive keratinocytes demonstrates that TGF- β 1 and ERKi induce <i>IFNK</i> and reduce viral transcription	97

Figure 19: Analysis of transcription in HPV31-positive keratinocytes reveals the effect of TGF- β 1 and/or ERKi on <i>IFNK</i> and viral transcription.....	98
Figure 20: Impact of cGAMP and etoposide treatment on endogenous <i>IFNB1</i> expression in NHK	99
Figure 21: Co-transfection of different HPV16 protein expression plasmids with <i>IFNB1</i> Prom reporter in NHK.....	101
Figure 22: Effect of cGAS and STING expression on <i>IFNB1</i> Prom reporter in 293T cells	101
Figure 23: The C33A keratinocyte cell line relies on transfection of a STING expression plasmid to induce the <i>IFNB1</i> Prom reporter	102
Figure 24: Influence of co-transfected expression plasmids for different HR-HPV proteins on <i>IFNB1</i> Prom reporter activity in C33A cells.....	103
Figure 25: Immunofluorescence showing localization of STING or HR-HPV E5 proteins in C33A cells	105
Figure 26: Model for the regulation of the <i>IFNK</i> gene in human keratinocytes	108
Figure 27: Deletion of sequences stretches encompassing putative TFBS influences reporter gene activity in human keratinocytes	CXIX
Figure 28: EMSA experiment with putative HOX binding site.....	CXX
Figure 29: Treatment with 5 ng/ml TGF- β 1 results in similar induction of <i>IFNK</i> and <i>SERPINE1</i> transcription as achieved with 20 ng/ml TGF- β 1	CXXI

List of Tables

Table 1: Compounds used for Cell Culture Experiments.....	39
Table 2: List of Kits and Ready-to-use Reagents	40
Table 3: Primary Antibodies	42
Table 4: Secondary Antibodies.....	43
Table 5: Cloning Primers.....	45
Table 6: QPCR Primers.....	46
Table 7: Oligonucleotides used for EMSA Analyses	48
Table 8: siRNAs used for Knockdown of the listed Target Genes	49
Table 9: pGL3 <i>IFNK</i> Prom Reporter Plasmids generated for this Work.....	51
Table 10: Used Devices.....	53
Table 11: List of Consumables	55
Table 12: PCR Program used for High-Fidelity Amplification.....	57
Table 13: <i>Mycoplasma</i> Test PCR Program.....	63
Table 14: Candidate Transcription Factors derived from JASPAR Analysis.....	77

1. Summary

Type I interferons (IFNs) are proteins involved in the immune response to viral infections. Upon infection, different pattern-recognition receptors (PRRs) recognize viral molecules and mediate the synthesis of type I IFN-alpha (IFN- α) and -beta (IFN- β). These IFNs are secreted and bind to the IFN- α receptor (IFNAR) on the surface of the affected and surrounding cells. Activation of the IFNAR results in the expression of IFN-stimulated genes (ISGs), which confer antiviral activity. IFN- α and - β are only expressed at very low levels in non-stimulated cells but can be rapidly produced by different cell types upon PRR stimulation. In contrast to PRR-inducible IFNs, IFN-kappa (IFN- κ), which also belongs to the type I IFNs, is constitutively expressed in non-stimulated keratinocytes and only weakly induced upon viral infection. Nonetheless, IFN- κ has been demonstrated to possess antiviral activity, also against high risk human papillomaviruses (HR-HPVs), which infect human keratinocytes (NHK). HR-HPVs represent a major health issue as they are one of the most frequently sexually transmitted infectious agents and cause virtually all cervical carcinomas, the world's third most common cancer in women, which leads to more than 300,000 deaths per year. Furthermore, different skin pathologies have been linked to dysregulated IFN- κ expression, thus the mechanisms regulating *IFNK* expression should be uncovered.

In the present work, the contribution of a putative *IFNK* enhancer element and of enclosed, putative transcription factor binding sites (TFBS) to the expression of *IFNK* have been assessed. This revealed that putative BS for members of the AP-2, HOX, SMAD, AP-1 and p53 TF families are important for promoter activity. The activity of SMAD and AP-1 members can be regulated by signal transduction cascades. Consistent with the SMAD BS being important, activation of the TGF- β 1 signaling pathway induces whereas its inhibition reduces IFN- κ and ISG expression in NHK. Surprisingly, inhibition of extracellular signal-regulated kinases (ERKs), which can activate AP-1 family members, induces IFN- κ and ISG expression. Additional experiments revealed that the AP-1 BS in the *IFNK* enhancer is part of a TGF- β response element, which includes the AP-1 and SMAD BS. Interestingly, combining TGF- β 1 and ERK inhibitor (ERKi) markedly increased IFN- κ and ISG expression in NHK. RNA interference and chromatin immunoprecipitation analyses revealed that the enhancer is regulated by AP-2 α , jun-B (AP-1 factor), SMAD4 and p63. Together with AP-2 α , p63 is involved in major aspects of keratinocyte biology and might therefore explain the cell type-specific expression pattern for this IFN. Other type I IFNs are not regulated by the same TFs and pathways.

Importantly, *IFNK* and ISG expression can also be induced in HPV16-positive keratinocytes (HK HPV16) by TGF- β 1 and ERKi, suggesting that IFN- κ expression can also be manipulated in pathological settings. Notably, the induction of *IFNK* in HK HPV16 decreased viral transcription. In accordance with the increased likelihood of encountering HPV infections upon wounding and the fact that TGF- β is an

SUMMARY

integral part of wound healing, increased *IFNK* expression might serve as a protective barrier against infection. In summary, it could be shown that *IFNK* is a TGF- β target gene, whose activity is negatively regulated by ERK signaling pathways. Thus, its constitutive expression, which might be mediated via AP-2 α and p63, can be fine-tuned by environmental cues.

In the second part of this work the impact of different HR-HPV proteins on a central DNA sensing pathway was analyzed. The cyclic GMP-AMP synthase/stimulator of IFN genes (cGAS/STING) pathway has been found to be of major importance to withstand viral infections by inducing the production of IFN- β . Previous studies have indicated that the HPV E7 protein interferes with this pathway. To test all early HPV proteins in an unbiased manner, a cGAS/STING-dependent *IFNB1* reporter assay was established in HPV-negative C33A cells. Initial findings suggest that the E5 protein of HPV31 but not of HPV16 decreases *IFNB1* reporter activity. The E5 protein is a putative transmembrane protein which, in case of HPV16, is located in endoplasmic reticulum (ER) membranes. STING is also an ER-resident transmembrane protein. Consistent with this, immunofluorescence analysis revealed a perinuclear co-localization of HPV16 and HPV31 E5 proteins with STING in C33A cells. This indicates functional differences among HR-HPV E5 proteins which might contribute to immunoevasion and persistence of HPV infections.

Zusammenfassung

Typ I Interferone (IFNs) sind Proteine, die an der Immunantwort auf Virusinfektionen beteiligt sind. Nach einer Infektion erkennen verschiedene sogenannte „pattern-recognition receptors“ (PRRs) virale Moleküle und vermitteln die Synthese von Typ-I-IFN-alpha (IFN- α) und -beta (IFN- β). Diese IFNs werden sezerniert und binden an den IFN- α -Rezeptor (IFNAR) auf der Oberfläche der betroffenen und umgebenden Zellen. Die Aktivierung des IFNAR führt zur Expression von IFN-stimulierten Genen (ISGs), die antivirale Aktivität besitzen. IFN- α und - β werden in nicht-stimulierten Zellen nur in sehr geringen Mengen exprimiert, können aber bei PRR-Stimulation von verschiedenen Zelltypen schnell produziert werden. Im Gegensatz zu PRR-induzierbaren IFNs wird IFN-kappa (IFN- κ), welches ebenfalls zu den Typ I IFNs gehört, konstitutiv in nicht-stimulierten Keratinozyten exprimiert und bei einer Virusinfektion nur schwach induziert. Dennoch wurde eine antivirale Aktivität von IFN- κ auch gegen die Hochrisikotypen der humanen Papillomviren (HR-HPV), die menschliche Keratinozyten (NHK) infizieren, nachgewiesen. HR-HPVs stellen ein großes Gesundheitsproblem dar, da sie zu den am häufigsten sexuell übertragenen Infektionserregern gehören und praktisch alle Zervixkarzinome, die weltweit dritthäufigste Krebserkrankung bei Frauen, die zu mehr als 300.000 Todesfällen pro Jahr führt, verursachen. Darüber hinaus wurden verschiedene Hautpathologien mit der deregulierten Expression von IFN- κ in Verbindung gebracht, so dass die Mechanismen, die die *IFNK*-Expression regulieren, aufgedeckt werden sollten.

In der vorliegenden Arbeit wurde der Beitrag eines zuvor identifizierten, mutmaßlichen *IFNK*-Enhancer-Elements und der darin enthaltenen, mutmaßlichen Transkriptionsfaktor-Bindungsstellen (TFBS) zur *IFNK* Expression untersucht. Dabei zeigte sich, dass mutmaßliche BS für Mitglieder der TF-Familien AP-2, HOX, SMAD, AP-1 und p53 für die Promotoraktivität wichtig sind. Die Aktivität der SMAD- und AP-1-Proteine können durch Signaltransduktionskaskaden reguliert werden. Im Einklang mit der Bedeutung des SMAD BS induziert die Aktivierung des TGF- β 1-Signalweges IFN- κ , während dessen Hemmung IFN- κ und ISG-Expression in NHK reduziert. Überraschenderweise induziert die Hemmung der „extracellular signal-regulated kinases“ (ERKs), die Mitglieder der AP-1-Familie aktivieren können, die IFN- κ und ISG-Expression. Zusätzliche Experimente zeigten, dass die AP-1 BS im *IFNK*-Enhancer Teil eines „TGF- β Response Elements“ ist, zu dem die AP-1 und die SMAD BS gehören. Interessanterweise erhöhte die Kombination von TGF- β 1 und ERK-Inhibitor (ERKi) die Expression von IFN- κ und ISG in NHK deutlich. RNA-Interferenz und Chromatin-Immunpräzipitationsanalysen zeigten, dass das Enhancer-Element durch AP-2, jun-B (AP-1-Faktor) und SMAD4 reguliert wird. Zusammen mit AP-2 ist p63 an wichtigen Aspekten der Keratinozytenbiologie beteiligt und könnte daher das zelltypspezifische Expressionsmuster dieses IFNs erklären. Andere Typ I IFNs werden nicht durch dieselben TFs und Signalwege reguliert.

SUMMARY

Wichtig ist außerdem, dass die *IFNK*- und ISG-Transkription auch in HPV16-positiven Keratinozyten (HK HPV16) induziert werden konnte. Dies deutet darauf hin, dass die IFN- κ Expression auch in pathologischen Kontexten manipuliert werden kann. Erwähnenswert ist, dass die Induktion von *IFNK* in HK HPV16 die virale Transkription verringerte. Entsprechend der erhöhten Wahrscheinlichkeit durch eine Wunde HPV-Infektionen zu erleiden und der Tatsache, dass TGF- β ein integraler Bestandteil der Wundheilung ist, könnte eine erhöhte *IFNK*-Expression als Schutzbarriere gegen eine Infektion dienen. Zusammenfassend konnte in dieser Arbeit gezeigt werden, dass *IFNK* ein TGF- β Zielgen ist, dessen Aktivität durch ERK-Signalwege negativ reguliert wird. Seine konstitutive Expression, die vermutlich über AP-2 und p63 vermittelt wird, kann über externe Signale fein abgestimmt werden.

Im zweiten Teil dieser Arbeit wurde der Einfluss verschiedener HR-HPV-Proteine auf einen zentralen DNA-Erkennungssignalweg analysiert. Der „cyclic GMP-AMP-synthase“/“stimulator of IFN genes“ (cGAS/STING) Signalweg spielt eine wichtige Rolle bei der Abwehr viraler Infektionen, indem er IFN- β Produktion bewirkt. Frühere Studien weisen darauf hin, dass das HPV E7 Protein diesen Signalweg manipuliert. Um alle frühen HPV-Proteine unvoreingenommen testen zu können, wurde ein cGAS/STING-abhängiger *IFNB1*-Reporter-Assay in HPV-negativen C33A-Zellen etabliert. Erste Ergebnisse deuten darauf hin, dass das E5-Protein von HPV31, aber nicht von HPV16, die *IFNB1*-Reporteraktivität verringert. Das E5-Protein ist ein mutmaßliches Transmembranprotein, das sich im Falle von HPV16 in Membranen des Endoplasmatischen Retikulums (ER) befindet. STING ist ebenfalls ein im ER lokalisiertes Transmembranprotein. In Übereinstimmung damit ergab die Immunfluoreszenzanalyse eine perinukleäre Ko-Lokalisierung von HPV16- und HPV31-E5-Proteinen mit STING in C33A-Zellen. Dies deutet auf funktionelle Unterschiede zwischen HR-HPV-E5-Proteinen hin, die zur Immunevasion und Persistenz von HPV-Infektionen beitragen könnten.

2. Introduction

2.1. Interferons in General

More than 60 years ago, Jean Lindenmann, a virologist from Switzerland, discovered a factor which interferes with replication of the influenza virus. Hence, the yet-to-be-characterized substance was called 'interferon' (IFN) [1]. In the following years it was found that the identified factor is made up of small proteins belonging to the cytokine family. Cytokines are small intercellular signaling molecules involved in the immune response [2].

Upon viral infection IFNs confer protection against replication and spread of viruses. In a nutshell, they function as following: Upon recognition of viral nucleic acids or other pathogen- or danger-associated molecular patterns by pattern-recognition receptors (PRRs) transcription factors (TFs) are activated and induce the expression of IFN genes. Subsequently, IFNs are synthesized, secreted and bind to their respective receptors on the surface of the infected and surrounding cells. Receptor binding results in the activation of the JAK-STAT signaling pathway, which induces or enhances the expression of hundreds of IFN-stimulated genes (ISGs) [3, 4]. ISGs inhibit a variety of steps during the infection and replication of many viruses; however, they also modulate the immune response against other pathogens, influence inflammatory processes and have anti-tumor activities [5, 6].

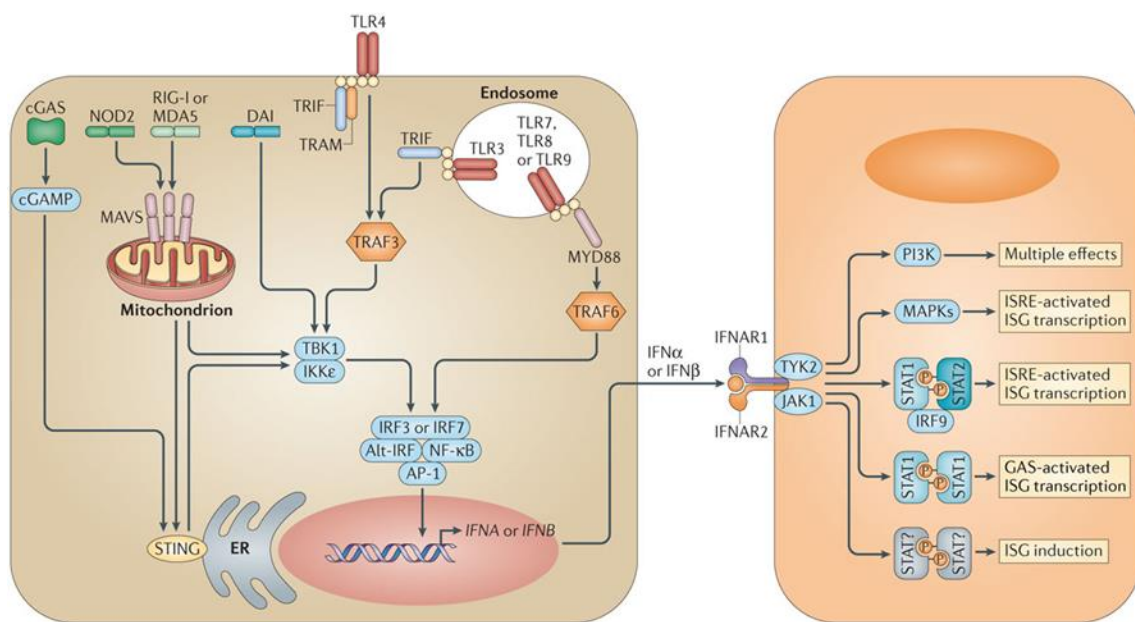


Figure 1: Pathways of Type I IFN induction and IFNA receptor signaling

Legend on the next page

INTRODUCTION

Figure 1: Pathways of Type I IFN induction and IFNA receptor signaling

Recognition of viruses or microorganisms by various cell surface or intracellular PRRs leads to the activation of distinct signaling cascades which result in the induction of *IFNA* and/or *IFNB* genes. IFN- α and - β are synthesized, secreted and bind to IFNAR1/2 on the surface of the infected as well as neighboring cells. Ligand binding can induce different signaling pathways in the IFN-stimulated cell (orange), which causes the synthesis of a particular subset of ISGs. Depending on the received stimulus, a defined biological response is mediated by the ISG products. Figure taken from [4].

NOD2 = NOD-containing protein 2, MDA5 = melanoma differentiation-associated gene 5, MAVS = mitochondrial antiviral signaling protein, DAI = DNA-dependent activator of IRFs, TRIF = TIR domain-containing adaptor protein inducing IFN- β , TRAM = TLR adaptor molecule, TRAF = TNF receptor-associated factor, MYD88 = myeloid differentiation primary response protein 88, IKK ϵ = I κ B kinase- ϵ ; Alt-IRF = IRFs other than IRF3 or IRF7, TYK2 = tyrosine kinase 2, PI3K = phosphoinositide 3-kinase, ISRE = IFN-stimulated response element, GAS = (IFN) γ -activated sequence.

Figure 1 gives an overview of the induction and action of IFNs using the well-studied IFN-alpha (IFN- α) and -beta (IFN- β) as an example. The TFs involved in the activation of the respective genes, as well as the cell surface receptor the different IFNs bind to differ between the distinct IFN family members.

2.1.1. Human Interferon Classes

Interferons are classified based upon the cell surface receptor used: Type I IFNs bind to the IFNAR1/2 receptor, type II IFNs to the IFNGR1/2 receptor and type III IFNs to the IFNLR1/IL10RB receptor. Whereas the IFNAR1/2 receptor is ubiquitously expressed, enabling nearly all cell types of the body to respond to type I IFNs, only few cell types express both subunits of the IFNL receptor. Most of these IFN-lambda (IFN- λ)-responsive cells are of epithelial origin [3, 4, 7].

In the subsequent sections, the composition of the different classes will be described, emphasizing the type I IFNs.

2.1.1.1. Type I IFNs

In humans the type I IFN family consists of 13 *IFNA* and single *IFNB1*, -epsilon (-E), -kappa (-K) and -omega (-W1) genes. On top, several pseudogenes of *IFNA* and *IFNW* exist. The different family members are encoded on chromosome 9 [7]. Whereas all other type I IFNs are encoded in a gene cluster on chromosomal band 9p21, the *IFNK* locus is located approximately 6.5 megabases proximal to the centromere relative to the existing type I IFN cluster, at chromosomal band 9p21.2 (Figure 2, [7-9]). Another interesting feature, discriminating the *IFNK* gene from the other, intron-less type I IFNs is the existence of an intron in its 3' untranslated region [9].

INTRODUCTION

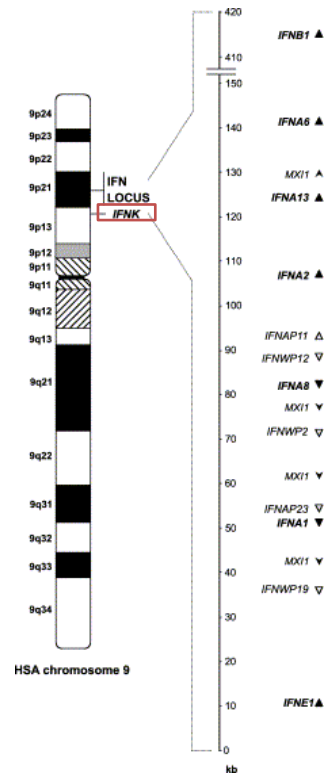


Figure 2: Schematic representation of human chromosome 9, showing the type I IFN cluster and the adjacent *IFNK* gene

The type I IFN cluster (labeled as IFN Locus) spans a region of about 400 kb and includes the *IFNA*, *-B1*, *-E* and *-W1* genes (closed triangles) as well as several pseudogenes (open triangles) and non-IFN genes (*MXI1*). The apex of the triangle points in the direction of transcription. The genes shown in the enlarged section do not represent a complete list of all genes encoded in the cluster, but depict the position (in kb) and direction of transcription of selected IFNs. The red box highlights the *IFNK* gene, which is located outside of the type I IFN cluster. *IFNA/W(P)* = interferon alpha/omega (pseudo)gene, *MXI* = MAX interactor 1. HSA = *Homo sapiens*. Figure modified from [8].

2.1.1.2. Type II and Type III IFNs

The only representative of type II IFNs is IFN-gamma ($\text{IFN-}\gamma$), which is encoded by the *IFNG* gene on chromosome 12. The type III IFN gene cluster is localized on chromosome 19 and comprises four *IFNL* genes. The various IFNs are produced by different cell types. Whereas type I IFNs can be produced by many cell types of our body upon appropriate stimulation, $\text{IFN-}\gamma$ is mainly synthesized by different immune cells and type III IFNs particularly by various immune and epithelial cells [3, 4, 7, 10].

2.1.2. Regulation of Type I and Type III IFN Expression

2.1.2.1. Inducible IFNs

Type I and type III IFNs, which are produced by epithelial cells at the site of infection, play a crucial role as a first line of defense against invading pathogens, thus have to be quickly available. In the absence of stimuli, type I IFN- α and - β and type III IFN- λ are only present at very low levels. However, upon the activation of PRRs such as Toll-like receptors (TLR), RIG-I like receptors and DNA sensors such as IFI16, cGAS (cyclic GMP-AMP synthase) and RNA polymerase III they are very rapidly and strongly upregulated [3, 4]. *PRR signaling cascades activate IFN regulatory factor (IRF) 3 and 7, NF- κ B family members p50 and p65 and a heterodimeric complex of ATF-2 and Jun [3, 4]. Different combinations of these TFs are required for the induction of IFNB1 (IRF3/IRF7, p50/p65, ATF-2/Jun), IFNA (IRF7, other IRFs) and IFNL (IRF3, IRF7, p50/p65) ([11, 12], italicized section taken from the author's publication [13]).*

2.1.2.2. cGAS/STING Pathway

There are several nucleic acid sensors present in mammalian cells. One major pathway mediating induction of type I IFNs is the cGAS pathway, which signals via the adaptor protein STING (stimulator of interferon genes). However, it should be pointed out, that the IFI16 pathway, another nucleic acid sensing pathway has been found to cooperate with the cGAS pathway to fully activate the STING protein in human keratinocytes [14]. The following section is based on a recent review by Motwani and colleagues [15].

The cGAS pathway is initiated when the cytoplasmic cGAS protein recognizes foreign or self-DNA. cGAS harbors a DNA binding domain which preferentially binds dsDNA with a length >45 bp. Several cGAS proteins bind to the same DNA molecule, leading to the formation of higher-order cGAS-DNA oligomers, which accumulate in liquid-like droplets. DNA binding activates the enzymatic functions of cGAS, resulting in the generation of the second messenger molecule 2'3' cyclic guanosine monophosphate-adenosine monophosphate (cGAMP). This second messenger molecule binds to STING, an adaptor protein which is anchored in the membrane of the endoplasmic reticulum (ER). Binding of cGAMP to STING induces a conformational change which leads to activation and oligomerization of STING. In addition to cGAMP, also other dinucleotides, such as cyclic diGMP, which is produced by some bacteria, self-DNA which is localized in the cytoplasm in interphase and ER stress can activate STING. Upon oligomerization STING translocates from the ER to the perinuclear compartments. In the Golgi apparatus, STING is palmitoylated. This post-translational modification is

INTRODUCTION

needed for its ability to induce type I IFNs [16]. In the Golgi, STING interacts with TANK-binding kinase 1 (TBK1) and gets phosphorylated, which recruits IRF3 and leads to its phosphorylation. Phosphorylated IRF3 dimerizes and translocates to the nucleus. In addition to IRF3, NF- κ B, which is retained in the cytoplasm in the absence of appropriate stimuli, is relieved upon STING activation and transported into the nucleus. Inside the nucleus, these TFs participate in the activation of type I IFNs (see above; [15]).

An additional mode of activation of STING has been observed after inducing DNA double-strand breaks using the topoisomerase II toxin etoposide in human keratinocytes. This activation involves the ataxia telangiectasia mutated (ATM) kinase and the poly [ADP-ribose] polymerase 1 (PARP-1), two proteins involved in the DNA damage response (DDR) as well as the IFI16 nucleic acid sensor. It seems to rely more on NF- κ B and results in the induction of a differential set of genes compared to the classical cGAS-initiated pathway described above [17]. The two modes of activation of the STING protein in keratinocytes are illustrated in Figure 3.

Deficiencies affecting the cGAS/STING pathway are linked to increased susceptibility to different viral infections [15]. Several DNA viruses are sensed by cGAS/STING and counteracted following activation of the pathway and thus have developed means to repress this activation [18-20]. For HPV, so far only limited insights have been obtained, which will be discussed in later chapters of this work.

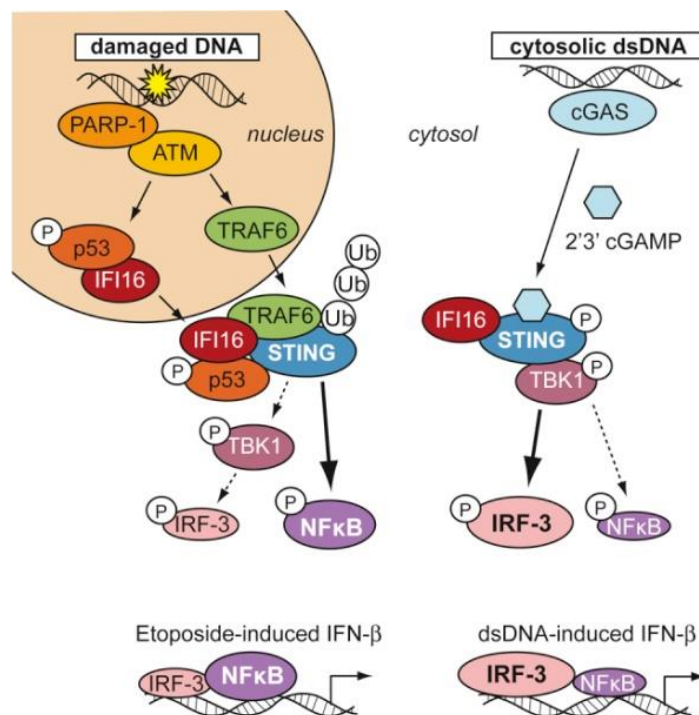


Figure 3: Two different modes of activation of STING in human keratinocytes

DNA damage as well as the presence of dsDNA in the cytoplasm results in the activation of STING and subsequent induction of the *IFNB1* gene. Figure taken from [17]. Ub = ubiquitination, P = phosphorylation, TRAF6 = TNF receptor-associated factor 6.

2.1.2.3. Constitutively Expressed IFNs

In contrast to the inducible and rather broad expression pattern observed for IFN- α , - β and - λ , IFN-epsilon (IFN- ϵ) and IFN-kappa (IFN- κ) are expressed in a cell type-dependent and constitutive manner and are not or only very weakly activated by virus infection or PRR signaling ([8, 9, 21-24], italicized section taken from the author's publication, slightly modified).

a) IFN Epsilon

*IFN- ϵ is constitutively expressed in epithelial cells of the reproductive organs and can be induced by estrogen but not by PRR signaling or overexpression of IRF3 or 7 ([21], italicized section taken from author's publication). Its expression varies with the estrous cycle and it is nearly absent in post-menopausal women. In mice, it has been shown, that IFNE-knockout renders the animals more susceptible to viral (Herpes simplex virus 2 (HSV-2)) and bacterial (*Chlamydia muridarum*) infections [21].*

b) IFN Kappa

IFN- κ is constitutively expressed in normal human keratinocytes (NHK), and to a lesser extent also in peripheral blood monocytes, and monocyte-derived dendritic cells [9, 25]. A 3- to 4-fold induction of IFNK upon infection with encephalomyocarditis virus (EMCV) was observed 5 hours (h) post infection (p.i.) which increased up to 10-fold at 15 h p.i. [9]. Stimulation of NHK with poly(I:C), an activator of RIG-I, MDA5 and TLR3 pathways, for 6 h resulted in only 1.5-fold induction of IFNK, whereas IFNB1 and -L1 were activated 1500- and 3000-fold, respectively [23]. Similarly, poly(dA:dT), which activates several cytoplasmic DNA sensors and RIG-I, induced IFNK 3- to 4-fold in the human keratinocyte NIKS cell line, whereas IFNA, -B1 and -L1 were activated 110-, 15000- and 40000-fold, respectively ([26, 27], italicized section taken from the author's publication). A recent study by Li and colleagues assessed IFNK induction 24 h after stimulation with different PRR agonists and reported approximately 5-fold induction with poly(dA:dT) and roughly 12-fold induction with poly(I:C) in undifferentiated NHK. In Ca²⁺-differentiated NHK, this induction was reduced to about 3-to 4-fold with both nucleic acids [28]. Treatment of NHK with other IFNs, like the type I IFN- β or the type II IFN- γ , for 5h induces IFNK transcription approximately 4- or 2-fold, respectively [9]. Semi-quantitative analyses also suggested a strong induction of IFN- β but not of IFN- κ protein by Sendai virus infection in human keratinocytes expressing the human papillomavirus (HPV) 16 E7 protein ([24], italicized

INTRODUCTION

section taken from the author's publication). Thus, taken together, the inducibility of the *IFNK* gene seems to be much weaker and delayed compared to the classical inducible IFNs discussed above.

Recently it has been shown that *inhibitors of the epidermal growth factor (EGF) receptor (EGFR) and of MAPK/ERK kinase (MEK) activate IFN- κ and ISG expression in NHK* ([29, 30], italicized section taken from the author's publication). Beyond this first hint, the regulatory mechanisms conferring constitutive and cell type-specific expression of IFN- κ had not been uncovered until the work presented here was finished. Afterwards the Bodily group published a study which revealed that *IFNK* transcription is not changed upon inhibiting JAK-STAT signaling in NHK [31], indicating that regulation via type I IFNs does not play a major role in *IFNK* expression and confirming some of the findings presented here (see section 5.1.3 for further details).

When IFN- κ was first discovered and classified as a type I IFN, the researchers sought to assess its antiviral activity. Indeed, they could show that application of recombinant human IFN- κ protects cultured human fibroblasts but not murine L929 cells from EMCV infection, proving its species-specific antiviral activity. Moreover, transfection with an IFN- κ expression plasmid conferred protection against vesicular stomatitis virus (VSV) infection in a human fibrosarcoma cell line [9]. Furthermore, it has been demonstrated, that IFN- κ mediates anti-HPV effects [32], which will be described in more detail in section 2.1.3.2 on page 26. Taken together, these findings show that IFN- κ possesses anti-viral activity against different RNA (EMCV, VSV) and DNA viruses (HPV), most probably by inducing different ISGs.

2.1.3. IFN- κ in Disease

IFN- κ has been found to be dysregulated in several diseases. *Increased expression of IFN- κ has been implicated in the pathology of cutaneous lupus erythematosus (CLE), whereas decreased expression has been observed for example in high-risk (HR) HPV-infected lesions* ([24, 27, 33, 34], italicized section taken from the author's publication).

2.1.3.1. IFN- κ in Cutaneous Lupus Erythematosus

CLE is an inflammatory autoimmune disease characterized by an interferon-mediated cytotoxic immune response targeting the epithelium and leading to a broad spectrum of clinical manifestations. Skin lesions arise from constant triggering of PRR pathways leading to excessive IFN production and ISG expression. Moreover, 60-80% of CLE patients have photosensitive lesions, which are caused by UVB irradiation [35]. Keratinocytes which are derived from unaffected skin of CLE patients have been found to produce significantly more pro-inflammatory IL-6 than keratinocytes

INTRODUCTION

derived from healthy donors, when stimulated with different PRR agonists or UV light. This enhanced IL-6 production can also be achieved by pre-treatment of healthy keratinocytes with IFN- κ and prevented by adding neutralizing antibodies against IFNAR1 or IFN- κ in diseased keratinocytes [34]. Moreover, it has been found that *IFNK* expression is 5-fold upregulated 6 h after UVB irradiation [36] and 8-fold 8 h after IFN- β treatment in NHK [9]. Hence, two factors linked to CLE pathogenesis are known to induce IFN- κ from other contexts. Taken together, these findings strongly suggest that the increased expression of IFN- κ in lesional CLE skin [33] is one driver of the disease. Hence, it would be useful to understand the molecular mechanisms regulating *IFNK* expression to be able to therapeutically interfere with the dysregulated gene in CLE.

2.1.3.2. IFN- κ in Papillomavirus Infection

*HR-HPVs have been shown to diminish IFN- κ expression in cultivated keratinocytes [23, 24, 26, 37, 38]. IFN- κ repression is mainly caused by the HR-HPV E6 protein and involves an increase in DNA methylation at CpG islands in the IFNK promoter [24, 38]. In addition, the E2 protein might also be involved in IFNK repression [39] and very recent evidence suggests an additional involvement of the HPV16 E5 protein [31]. Anti-HPV activity of IFN- κ has been demonstrated in CIN612-9E cells [32], an immortalized cell line derived from a cervical intraepithelial neoplastic lesion which harbors episomal HPV31 genomes. Inducing the expression of recombinant IFN- κ in these cells led to decreased cell proliferation and reduction of viral transcription, which has been observed already 4 h post induction. On top, viral copy number decreased in the presence of IFN- κ , which became evident 4-6 days post induction. Moreover, IFN- κ has been shown to modulate the expression of more than 200 genes at least 2-fold in CIN612-9E cells, 71% of which are known ISGs [32], indicating that its ability to regulate gene expression is similar to IFN- α and - β . Examples for these IFN- κ -regulated, previously known ISGs are *SP100*, *IFI16* and *IFIT1* [32]. They have been shown to limit HR-HPV replication [32, 40-44]. A recent report suggested that *TGF- β 1* specifically induces IFN- κ through demethylation of the IFNK promoter in HPV16-positive cells but not in normal keratinocytes ([38], italicized sections taken from the author's publication, slightly modified).*

2.2. Papillomaviruses

The family of *Papillomaviridae* is made up of several hundred different papillomaviruses (PVs). They infect a broad range of vertebrate species in a strictly species-specific manner and exhibit a tropism for epithelia. They are non-enveloped viruses which harbor a circular, dsDNA genome of about 5800

to 8600 bp packed in an icosahedral capsid, which is about 55 nm in diameter. All PVs encode at least five genes (<https://pave.niaid.nih.gov>, December 2019; [45-47]). The Papillomavirus Episteme (PaVE) database currently contains more than 400 papillomavirus reference genomes, of which 226 are HPV genomes classified by the International HPV Reference Center of the Karolinska Institute (<https://pave.niaid.nih.gov>, <https://hpvcenter.se>, December 2019). The classification of PVs is done according to their host and to the DNA sequence of the L1 open reading frame (ORF). The different PV types display more than 10% divergence in the L1 DNA sequence (International Committee on Taxonomy of Viruses, <https://talk.ictvonline.org/>, December 2019; [48, 49]).

2.2.1. Classification of Human Papillomaviruses and Clinical Relevance

HPVs can be assigned phylogenetically to five different genera: The alpha-, beta-, gamma-, mu- and nu-HPVs. Most of the known HPVs belong to the gamma-, alpha- or beta-genera (roughly between 50-100 types each, in descending order). In contrast to this, the mu- and nu- HPVs are only represented by three or one single type of HPV, respectively (<https://hpvcenter.se>, December 2019). HPVs cause long-lasting infections, which are most often subclinical. However, there are several HPV types that are associated with different diseases [50].

In recent years, much attention has been drawn to the alpha-HPVs. The alpha genus contains viruses with tropism for both, cutaneous and mucosal sites. The mucosal alpha-HPVs are further subdivided in high risk (HR) or low risk (LR)-HPVs according to their carcinogenic potential [45]. There are 12 HR-types which are categorized as carcinogenic for humans by the International Agency for Research on Cancer (IARC Group 1: HPV16, 18, 31, 33, 35, 39, 45, 51, 52, 56, 58 and 59) and a thirteenth HPV type is regarded as being probably carcinogenic (HPV68; <https://monographs.iarc.fr/list-of-classifications>, December 2019). Genital HPV infections are sexually transmitted. The majority of sexually active humans (50-80% worldwide) acquire an infection with one or several of these mucosal HR-HPVs during sexual intercourse [51]. More than 90% of these infections are cleared by the immune system; however, a low percentage persists and increases the risk of developing cervical cancer [50]. Almost all (99-100%) cervical carcinomas are caused by HR-HPV infection ([52, 53], <https://www.who.int/>, December 2019). In this context, HPV16 should be emphasized, as it is the causative agent for approximately 60% of cervical carcinomas worldwide (Status 2012, [53]). The second most common HR-HPV type, which is found in 15% of global cervical cancer cases, is HPV18 (Status: 2012, [53]). Cervical cancer is the third most common cancer in women worldwide (ranked by incidence, excluding non-melanoma skin cancers) and accounted for about 570,000 new cases and 311,000 deaths in 2018 (<http://gco.iarc.fr/>, December 2019). Moreover, the mucosal HR-types are associated with other types of anogenital cancers (for example squamous cell carcinomas of the vulva, vagina or

INTRODUCTION

the penis) and oropharyngeal cancers (OPCs) [50]. The incidence of HPV-positive OPCs is on the rise, with a tremendous increase from 16% in 1984-1989 to 70% in 2000 to 2004 reported in the United States [54]. This observation can be expanded on several other countries around the globe [55], suggesting that oral infection with HPVs is responsible for this trend. Interestingly, HPV16 DNA is present in more than 90% of HPV-positive OPCs [55], making this HPV type even more relevant in clinical settings. Integration of the HR-HPV genome into the host genome is observed in several of these cancers and probably drives carcinogenesis as it frequently happens at sites of active transcription [56], thereby enhancing the expression of viral oncogenes. However, invasive cervical carcinomas harboring solely episomal HPV16 genomes have also been reported [57]. The LR-HPV types cause different benign neoplasias, including genital warts and papillomas in the respiratory tract [58-60].

All genera of HPVs include viruses that target cutaneous epithelia. In immunocompetent persons they cause asymptomatic infections, even though gamma-, mu- and nu-HPVs can induce the growth of benign warts. Up to 90% of healthy individuals are colonized with beta-HPVs. Beta-HPVs are linked to squamous cell carcinomas in immunocompromised persons and growing evidence suggests that they might also be linked to the initiation of non-melanoma skin cancers at UV-irradiated sites in the immunocompetent population [50].

2.2.2. Structure of the HPV Genome

Figure 4 shows the structure of the circular, dsDNA genome of HPVs, which contains three different regions:

- The upstream regulatory region (URR) which contains the viral origin of replication and binding sites for cellular transcription factors as well as for the viral E1 and E2 proteins
- The ORFs encoding the early proteins E1, E2, E4, E5, E6, E7 and E8^{E2}
- The ORFs encoding the late, structural proteins L1 and L2

The different regions are separated by an early (between early ORFs and late ORFs) and a late polyadenylation signal (between late ORFs and URR). In the case of HPV16, the transcription of the early and late ORF region is driven by two different promoters, the early P97 (PE) and the late P670 promoter (PL). For other HPV types, promoter position and number varies, however, gene expression is regulated by early and late promoters which are regulated in dependency of the viral life cycle (see section 2.2.3 [45, 61]).

INTRODUCTION

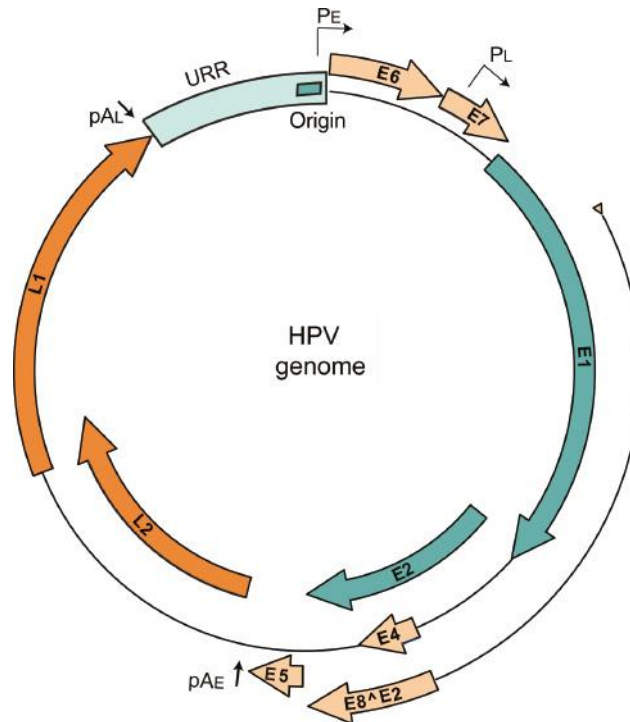


Figure 4: Genome organization of high risk alpha HPVs

Schematic overview of an alpha-HPV genome, showing the URR, the early ORFs (light orange and green) and the late ORFs (orange). URR= upstream regulatory region, PE = early promoter, PL = late promoter, pAE = early polyadenylation signal, pAL = late polyadenylation signal. Figure taken from [62].

2.2.3. Viral Life Cycle

HPVs infect the basal keratinocytes in mucosal or cutaneous epithelium. In multilayered epithelia, the virus gains access to these bottommost cells through microwounds or via hair follicles [63-66]. In the cervix, the virus probably directly accesses the epithelial cells at the squamocolumnar junction between ecto- and endocervix, which are single-layered [67]. The viruses enter the cell by receptor-mediated endocytosis and enter the nucleus during mitosis. The HPV life cycle is tightly linked to epithelial differentiation. After successful infection of the basal keratinocytes, which are undifferentiated and proliferate to re-new the layers above, the virus utilizes the cellular machinery to initiate synthesis of the viral E1 and E2 proteins. These proteins mediate an initial round of genome amplification. However, in basal keratinocytes the viral genome is amplified to low copy numbers only (50-200 per cell). This ensures the maintenance of the viral episomes during cell division. Cells which arise from the proliferating basal cells migrate to upper epithelial layers, quit the cell cycle and differentiate. In HPV-infected cells, the viral E6 and E7 proteins deregulate the cell cycle and thereby ensure that the cell maintain a permissive environment for viral replication and transcription. In addition, the late promoter is activated upon cellular differentiation and drives the expression of E1 and E2 which leads to massive amplification of the viral genomes in the upper

epithelial layers. In this so-called productive phase of the life cycle, the viral E4 and E5 proteins as well as the capsid proteins L1 and L2 are synthesized. Thus, viral genomes can be packaged into capsids and shed from the surface of the epithelium [45, 61].

2.2.4. Viral Proteins

The experiments described in the second part of this work were carried out using different proteins of HPV16 and HPV31. Thus, in the following section, a quick introduction to the different viral proteins used for these experiments will be given.

2.2.4.1. The E1 Helicase

The E1 protein is the only enzyme encoded by the virus. It displays the highest conservation of all PV proteins, highlighting its essential role in the viral life cycle. It is an ATP-dependent DNA-helicase, which binds to the origin of replication and unwinds the viral DNA. E1 interacts with several cellular factors needed for DNA replication. The E1 ORF is the largest of all PV ORFs encoding a protein of 600-650 amino acids and fulfilling its function in a double-hexameric form. The assembly of this functional E1-double-hexamers on the viral DNA depends on the interaction with viral E2 proteins [68].

Overexpression of HPV16 E1 proteins has been found to induce DNA damage pathways [69], which has been found to activate STING in keratinocytes [17], thus indicating that E1 overexpression might have an effect on STING target genes like *IFNB1*.

2.2.4.2. The E2 and the E8^{E2} Protein

The E2 protein is a sequence-specific DNA binding protein with several key functions. It regulates viral transcription and initiates viral replication as it assists loading the E1 helicase onto the DNA. Moreover, it tethers viral episomes to host chromatin, thereby ensuring proper partitioning of viral progeny to daughter cells during cell division. A study analyzing the transcriptome of keratinocytes transduced with HPV16- or HPV18 E2 proteins suggested that the E2 protein of both HR-types down-regulates *IFNK* expression, which was confirmed in subsequent qPCR analysis. Moreover, knockdown of IFN- κ as well as expression of the amino-terminal transactivation domain of HPV18 E2 decreased expression of several ISGs. Moreover, this study revealed a suppressive effect of HR-E2 on *TMEM173* [39], which encodes the STING protein, thus implementing E2 in dampening the innate immune response to HPV. Another study performed with TERT-immortalized oral keratinocytes transduced

with HPV16 E2 confirmed the reduction of *IFNK* and ISG levels upon E2 expression but reported less than 20% reduction of *IFNK* in TERT-immortalized anogenital keratinocytes [37].

In addition to the full-length E2 protein described above, PV encode a second variant of the E2 protein, in which the C-terminal DNA binding and dimerization domain of E2 is linked to a second ORF, encoded upstream of E2, resulting in the E8^{E2} protein [70]. The E8^{E2} protein functions as a repressor of viral transcription and replication [71-74].

2.2.4.3. The E4 Protein

The most abundant form of the E4 protein of HPVs is translated from a spliced mRNA, which is made up of the first few amino acids of the E1 ORF connected to the E4 ORF (E1^{E4}). The E1^{E4} transcript is typically found at very high levels in productive lesions caused by different PVs and the E4 gene products are accumulating in the mid and upper layers of infected epithelium, where they can be visualized using immunofluorescence procedures. Even though the E4 ORF was characterized as an early gene in the beginning, compelling evidence for functions of the E4 gene products during the early phases of the viral life cycle is missing. In accordance with its expression in the later stages of viral infection, different findings suggest involvement of E4 in productive genome amplification, virus assembly and release [75].

2.2.4.4. The E5 Protein

Not all PVs encode E5 proteins. However, the HR-HPVs from the alpha genus encode one E5 protein (designated E5 α) with approximately 80 amino acids, which is hydrophobic and contains putative transmembrane regions. HPV16 E5 has been shown to localize mainly to the ER membrane and at higher expression levels also to other membrane structures. E5 has been demonstrated to bind to or influence a huge set of cellular proteins. Due to its weak transforming activity in vitro E5 is referred to as the 'minor' oncoprotein. However, an important contribution to malignant transformation in vivo is suspected. In HPV16, E5 seem to contribute to transformation by increasing the level of EGFR expression on the cell surface and supporting EGFR signaling pathways. In addition to this function, HPV16 E5 has been shown to be involved in immune escape and apoptosis avoidance. It also seems to play a role in productive amplification of the viral genome, late viral gene expression and possibly also in viral egress. However, as beta-HPVs, which lack a comparable E5 ORF, are also capable to traverse their life cycle, these functions might be fulfilled also by other means [76].

Very recently, the group of Jason Bodily reported that the HPV16 E5 protein contributes to the IFN- κ repression observed in HPV16-positive keratinocytes [31]. They provided evidence that the E5

protein might play a pivotal role in immune escape by downregulating IFN- κ -mediated ISG expression. Moreover, their data indicated that the E5 protein might be utilized by the virus to stabilize the genome and circumvent genome integration [31].

2.2.4.5. The E6 Oncoprotein

As for E5, not all PVs encode an E6 protein. Moreover, the E6 protein differs between different PVs. However, there are some conserved functions of the E6 protein in HR-HPVs, which all contain an E6 ORF. HR-E6 and -E7 are the major oncoproteins, responsible for the carcinogenic potential of these viruses. They are both expressed from the early promoter right from the beginning of viral infection. By interacting with different cellular proteins, HR-E6 deregulates the cell cycle, avoids senescence and apoptosis, escapes the immune system and affects other aspects of cell biology. To keep it short, only its most prominent functions will be mentioned here: It interacts with the E6-associated protein (E6-AP), an E3 ubiquitin ligase, which mediates the degradation of p53 and thereby prevents p53-mediated cell cycle arrest or cell death upon DNA damage or other danger signals. In addition to this, the interaction with E6-AP participates in the upregulation of TERT by E6. TERT activity increases the cellular lifespan [77]. Moreover, E6 has been found to bind to IRF3 and prevent IFN- β production upon viral infection [78].

2.2.4.6. The E7 Oncoprotein

As described above for E6, E7 is not expressed by all PVs, but by all HR-HPVs and has the capability to deregulate a huge amount of cellular processes by interacting with different cellular proteins. It is the second major oncoprotein and capable to immortalize human keratinocytes on its own. Even though it has several other functions, HR-E7 is best known for its interaction with proteins of the retinoblastoma (pRb) family. These proteins are involved in the G1/S cell cycle checkpoint and prevent premature progressing to S phase; however, in the presence of HR-HPV E7 this brake is relieved [79]. Recently, E7 proteins of HPV16 as well as of HPV18 have been found to repress STING activity [80, 81].

2.2.4.7. The Capsid Proteins L1 and L2

The major capsid protein L1 and the minor capsid protein L2 form the icosahedral HPV capsid which encloses the viral genome. L1 proteins on their own can assemble into highly immunogenic virus-like particles (VLPs) which are the basis of the currently used HPV vaccines. L1 is essential for viral entry

INTRODUCTION

as it interacts with heparan sulfate proteoglycans for initial attachment of the virus to the basement membrane of the affected epithelium. The minor capsid protein L2 cannot form VLPs on its own but supports capsid assembly as well as encapsidation of the viral genome and is involved in endosomal escape of the virus after uptake into the infected cell [82, 83].

2.2.5. HPV Vaccination

As mentioned above, currently licensed HPV vaccines are made up of empty and thus non-infectious VLPs which self-assemble from recombinant L1 proteins of some of the clinical most important HPV types. The bivalent Cervarix[®] vaccine (GlaxoSmithCline) contains L1-VLPs from HPV16 and 18; the quadrivalent Gardasil[®] vaccine (Merck) additionally contains VLPs from the LR-types 6 and 11, which are most commonly found in benign warts. A nonavalent derivative of Gardasil[®], called Gardasil 9[®], further includes VLPs from HPV31, 33, 45, 52 and 58. All of these vaccines comprise adjuvants to elicit a strong immune response. They have been shown to induce antibody titers which are two to three orders of magnitude higher than observed for natural occurring infections and are regarded to be highly effective against the targeted HPV types. In addition to protection from the targeted HPV types, Cervarix[®] and Gardasil[®] have been shown to mediate cross-protection against further closely related HPV types (HPV31, 33, 45 or HPV31, respectively). Moreover, cellular immunity seems to play a major role in controlling natural HPV infections and the current vaccines have been shown to induce robust T cell responses. Unfortunately, infected keratinocytes in the basal layer do not express L1 and are therefore not targeted by the vaccine-mediated L1-specific immune response. Thus, current vaccines cannot be used therapeutically, but continuous efforts are made to develop therapeutic HPV vaccines [84].

2.3. Objective

The production of type I IFNs represents the first line of defense against invading viruses [3, 4]. As outlined in section 2.1.2 on page 22, the regulation of the type I *IFNK* and *-E* genes differs from the regulation of the well-studied type I *IFNAs* and *-B*, pointing at the existence of other, yet-unknown regulatory mechanisms. Dysregulated expression of IFN- κ was demonstrated in several pathologies, including HPV infection (see section 2.1.3 on page 25). Thus, the aim of the presented work was to shed light on the regulation of this interesting but so far poorly investigated type I IFN.

In recent years, the importance of the cGAS/STING signaling pathway (see section 2.1.2.2) for counteracting viral infections has been uncovered. This pathway is one of the major players mediating type I IFN- β production upon sensing of cytoplasmic DNA [15] and is responsible for antiviral activity against several DNA viruses, some of which counteract its activation [18-20]. For HR-HPV, not much is known concerning its impact on cGAS/STING signaling until now. Hence, the second minor project presented in this thesis intended to establish a reporter assay which can be used to analyze the influence of different HPV proteins on cGAS/STING-dependent IFN- β production.

3. Material and Methods

3.1. Materials

In the following chapter, all materials which have been utilized for the making of this work are listed.

3.1.1. Chemicals in General

Unless otherwise indicated used chemicals had molecular biology grade or were designated as “*pro analysi*”. They were purchased from the following companies:

- AppliChem GmbH (Darmstadt, Germany)
- Bio-Rad Laboratories, Inc. (Hercules, US)
- Biozym Scientific GmbH (Hessisch Oldendorf, Germany)
- Carl Roth GmbH + Co. KG (Karlsruhe, Germany)
- F. Hoffmann-La Roche AG (Roche; Basle, Switzerland)
- Honeywell Specialty Chemicals Seelze GmbH (Seelze, Germany)
- Lonza Group AG (Basle, Switzerland)
- Merck KGaA (Darmstadt, Germany)
- PerkinElmer, Inc. (Waltham, US)
- PJK GmbH (Kleinblittersdorf, Germany)
- Thermo Fisher Scientific (Thermo Fisher; Waltham, US)

3.1.2. Buffers

The list below contains the composition of the buffers used for the different experiments described in the method section. The keyword or number in brackets indicates either the purpose of the buffer or the concentration of the described stock solutions, respectively.

- **Annealing Buffer (Oligonucleotides):** 200 mM potassium acetate, 60 mM HEPES-KOH pH 7.5, 4 mM magnesium acetate
- **Assay Buffer (Luciferase Assay):** 100 mM potassium phosphate buffer pH 7.8; 15 mM MgSO₄; before usage: 5 mM ATP

MATERIAL & METHODS

- **Binding Buffer (EMSA):** 100 mM HEPES pH 7.9; 2.5 mM EDTA pH 8.0; 25% (v/v) glycerol; before usage: 1 mM DTT
- **Blocking Buffer (Western Blot):** either PBS-T or TBS-T, supplied with either 5% (w/v) nonfat dried milk powder or 5% (w/v) BSA
- **CAPS Transfer Buffer (Western Blot):** 10 mM CAPS; 10% (v/v) Methanol; pH 10.3
- **DAPI solution (Immunofluorescence):** 0.01 µg/ml in PBS
- **DNA-Loading Buffer (10x):** 20% (w/v) Ficoll 400; 0.1 M Na₂-EDTA pH 8.0; 1% (w/v) SDS; 0.25% (w/v) bromphenol blue; 0.25% (w/v) xylene cyanol
- **Elution Buffer (Nuclear Extract Preparation):** 10 mM HEPES pH 7.9, 20% (v/v) glycerol, 500 mM NaCl, 0.5 mM EDTA; before usage: protease and phosphatase inhibitor cocktails, 1 mM DTT
- **Mounting Medium (Immunofluorescence):** VECTASHIELD® H-1000 (Vector Laboratories, Inc., Burlingame, US)
- **Lysis Buffer (Luciferase Assay):** 100 mM potassium phosphate buffer pH 7.8; 1% (v/v) Triton-X 100; 1 mM DTT
- **Lysis Buffer (Nuclear Extract Preparation):** 10 mM HEPES pH 7.9, 300 mM saccharose, 50 mM NaCl, 0.5 % (v/v) Igepal CA 630, 1 mM EDTA; before usage: protease and phosphatase inhibitor cocktails, 1 mM DTT
- **Luciferin Solution:** 1 mM D-luciferin (PJK) diluted in Assay Buffer
- **PBS (10x):** 137 mM NaCl, 2.7 mM KCl, 1.5 mM KH₂PO₄ pH 7.2
 - **PBS-T:** 0.05% (v/v) Tween-20 in 1x PBS
- **Protein Loading Buffer (4x):** Roti®-Load 1 (Carl Roth)
- **RIPA buffer (Western Blot, according to Ausubel):** 1% (v/v) Igepal CA 630, 1% (w/v) sodium deoxycholate, 0.1% SDS (v/v), 150 mM NaCl, 10 mM sodium phosphate pH 7.2, 2 mM EDTA, 50 mM sodium fluoride, before usage: protease inhibitor cocktails
- **SDS-PAGE Running Buffer (5x):** 125 mM Tris-HCl; 0.96 M glycine; 17.3 mM SDS
- **Separation Gel Buffer (Western Blot):** 1.5 M Tris-HCl; pH 8.8
- **Stacking Gel Buffer (Western Blot):** 1.5 M Tris-HCl; pH 6.8
- **TAE Buffer (50x, DNA electrophoresis):** 2 M Tris; 1 M acetic acid; 0.1 M EDTA pH 8.5
- **TBE Buffer (10x, EMSA):** 890 mM Tris; 890 mM boric acid; 20 mM EDTA pH 8.0
- **TBS (10x, Western Blot):** 500 mM Tris; 1.5 M NaCl; pH 7.5
 - **TBS-T:** 0.1% (v/v) Tween-20 in 1x TBS

3.1.3. Media & Solutions

In the following section the media and chemicals needed for bacterial and mammalian cell culture are listed.

3.1.3.1. Bacterial Culture

All molecular cloning procedures were performed using the chemically competent *Escherichia coli* strain DH5 α (for details see section 3.2.1.6 on page 58). These bacteria were kept in the following media:

- **Freezing Medium:** 65% glycerol, 0.1 M MgSO₄, 0.025 M Tris, pH 8.0
- **LB Medium** (Luria-Bertani-Medium, for growth of liquid cultures): 25 g LB medium dissolved in 1 l H₂O; if necessary, 100 μ g/ml ampicillin or 30 μ g/ml kanamycin were added
- **LB-Agar** (for growth of colonies): 25 g LB Medium, 12 g Select Agar dissolved in 1 l H₂O; if necessary, 100 μ g/ml ampicillin or 30 μ g/ml kanamycin were added
- **SOC-Medium** (Super Optimal broth with Catabolite repression, for transformation): 2% (w/v) Bacto-Trypton, 0.5% (w/v) Bacto-Yeast Extract, 10 mM NaCl, 2.5 mM KCl, 10 mM MgCl₂, 10 mM MgSO₄, 20 mM glucose; pH 7.0

3.1.3.2. Eukaryotic Cell Culture

Cell culture experiments were performed with different cell types, resulting in the use of different growth media, depending on the cell type and the intended procedure. All media, which were used for culturing the different mammalian cell types, are itemized below.

- **DMEM** (Dulbecco's Modified Eagle Medium): Thermo Fisher
Ready-to-use cell culture medium for culture of different cell types, supplied with 50 mg/l gentamycin and 10% (v/v) serum. Depending on the cell type, different sera were used: For culture of the NIH3T3-J2 mouse fibroblast feeder cell line bovine serum was added (CS; Life Technologies); for culture of HEK 293T or C33A cells, Fetal Calf Serum (FCS, Thermo Fisher) was added.

- **E-Medium:** 500 ml DMEM + 500 ml DMEM/Ham's F12 (Thermo Fisher)
Self-made medium for growing cells which harbor viral expression vectors or episomal HPV genomes or the HPV-negative RTS3b cell line. E-Medium is supplemented with 100 U/ml or μ g/ml penicillin and streptomycin respectively, adenine (1.8 mM), hydrocortisone (417 μ g/ml), insulin (50 μ g/ml),

MATERIAL & METHODS

transferrin (50 µg/ml), triiodothyronine T3 (20 pM), cholera toxin (10 nM) and 5 ng/µl EGF. For HPV-containing cells, the medium was supplied with 5% (v/v) HyClone, a chemically defined Fetal Calf Serum, (GE Healthcare, Chicago, US). For culturing RTS3b cells, E-medium was supplied with 10% FCS (Thermo Fisher).

- **KSFM** (Keratinocyte Serum-Free Medium): Thermo Fisher

Serum-free media for culture of primary keratinocytes, supplemented with bovine pituitary gland extract, recombinant human EGF and 50 mg/l gentamycin.

- **Mitomycin C**: Medac (Wedel, Germany)

Stock solution: 0.4 mg/ml in PBS. Eighty µg/ml mitomycin C are used to achieve growth arrest of feeder cells (see section 3.2.3.3 on page 61).

- **Opti-MEM™ I Reduced Serum Media (Transfection Medium)**: Thermo Fisher

Medium with reduced serum, which is a modification of Eagle's Minimum Essential Media, buffered with HEPES and sodium bicarbonate and supplemented with hypoxanthine, thymidine, sodium pyruvate, L-glutamine, trace elements and growth factors.

- **Phosphate Buffered Saline** (Dulbecco's, PBS): Thermo Fisher

Balanced salt solution without calcium and magnesium

- **Trypsin-EDTA (0.25%)**: Thermo Fisher

Enzyme used to separate adherent cells from the culture dish and from each other

- **Versene**: For detachment of feeder cells

PBS supplemented with 0.5 M EDTA (Thermo Fisher)

3.1.3.3. Inhibitors, Activators

To analyze the impact of different signaling pathways on endogenous gene expression, cultured cells were treated with different substances. These substances are listed in Table 1.

Table 1: Compounds used for Cell Culture Experiments

C₆H₈O₇ = citric acid

Compound	Company	Vehicle	Final amount	Function
cGAMP	InvivoGen (San Diego, US)	H ₂ O	5 µg/ml	activates STING
Etoposide	Merck KGaA	DMSO	50 µM	induction of DNA double-strand breaks
JNK-IN-8	Selleckchem.com (Munich, Germany)	DMSO	4 µM	inhibition of JNK1/2/3
Nutlin-3a	Cayman Chemical (Ann Arbor, US)	DMF	10 µM, 20 µM	hinders binding of p53 to MDM2 → p53 stabilization
12-O-tetra- decanoylphorbol- 13-acetate (TPA)	Cayman Chemical	DMSO	50 ng/ml	activates MAPK signaling
recombinant human TGF-β1	PeproTech GmbH (Hamburg, Germany) ¹⁾	0.1% BSA, 10 mM C ₆ H ₈ O ₇	20 ng/ml	activates TGF-β signaling
SCH 772984	Cayman Chemical	DMSO	1 µM	inhibition of ERK1/2
SB-431542	MedChemExpress Europe (Sollentuna, Sweden)	DMSO	10 µM	inhibition of TGFBR1
T-5224	MedChemExpress Europe	DMSO	40 µM	hinders binding of JUN or FOS family members to the DNA

¹⁾ Due to delivery issues, few experiments were carried out using TGF-β1 bought from R&D Systems (Minneapolis, US). However, comparison of TGF-β1 from both companies did not show deviations in pathway activation (*SERPINE1* expression) or *IFNK* induction (data not shown)

3.1.4. Used Kits and Reagents

Table 2 displays the kits and reagents from different companies, which were used for the applications listed in the last column.

Table 2: List of Kits and Ready-to-use Reagents

Name	Company	Application
cComplete™ protease inhibitor cocktail, EDTA-free	Roche	protein extract preparation
EZ1 DNA Tissue Kit	Qiagen (Hilden, Germany)	DNA extraction
FuGENE® HD Transfection Reagent	Promega (Madison, US)	transfection plasmid DNA
Gaussia Juice Big Kit	PJK	determining luciferase activity
Gene Ruler 1 kb Plus DNA Ladder	Thermo Fisher	marker standard DNA electrophoresis
Gene Ruler 100 bp DNA Ladder	Thermo Fisher	marker to evaluate DNA fragmentation (ChIP)
jetPRIME® transfection reagent	Polyplus-transfection SA (Illkirch, France)	transfection with cGAMP
LightCycler® SYBR Green I Master	Roche	qPCR
Lipofectamine RNAiMAX Reagent	Thermo Fisher	siRNA transfection
PageRuler™ Prestained Protein Ladder	Thermo Fisher	marker protein electrophoresis
PhosSTOP	Roche	Protein extract preparation
QIAGEN® Plasmid Plus Maxi Kit	Qiagen	plasmid DNA isolation
QIAGEN® Plasmid Plus Midi Kit	Qiagen	plasmid DNA isolation
QIAprep® Spin Miniprep Kit	Qiagen	plasmid DNA isolation
QIAquick® Gel Extraction Kit	Qiagen	DNA extraction from agarose gels
QIAshredder® Kit	Qiagen	homogenizing cell lysates
QuantiTect® Reverse Transcription Kit	Qiagen	cDNA synthesis
Rapid DNA Ligation Kit	Thermo Fisher	DNA ligation
RNeasy® Mini Kit	Qiagen	RNA isolation
SimpleChIP® Enzymatic Chromatin IP Kit (Magnetic Beads)	Cell Signaling Tech. (Danvers, US)	chromatin immunoprecipitation

3.1.5. Enzymes

Restriction enzymes and respective buffers have been bought from New England Biolabs (Ipswich, US) or Thermo Fisher. In addition, the following enzymes have been used:

- Dispase® II (neutral protease, grade II; Roche)
- FastAP Thermosensitive Alkaline Phosphatase (Thermo Fisher)
- GoTaq® G2 DNA Polymerase (Promega)
- Pyrobest® DNA Polymerase (Takara Bio Inc.; Kusatsu, Japan)
- T4 DNA Ligase (Thermo Fisher)

3.1.6. Antibodies

The antibodies listed in Table 3 on the next page have been used to detect the respective target protein during Western blot (WB) analysis or for precipitating their target protein during chromatin immunoprecipitation (ChIP). Antigen names are given as stated by the respective company and do not necessarily reflect the appropriate protein name assigned by public databases.

MATERIAL & METHODS

Table 3: Primary Antibodies

Antigen names are given as stated by the respective company, order no. = order number, buffer composition: see 3.1.2 on page 35

Antigen (Clone)	Species Clonality	Company (order no.)	Application	Dilution, Buffer
alpha-Tubulin (DM1A)	Mouse Monoclonal	Calbiochem (Merck) (CP06)	WB	1:1000, PBS-T
AP2 alpha	Rabbit Polyclonal	Abcam (Cambridge, US) (ab52222)	WB	1:500-1:1000, PBS-T
AP-2 γ (6E4/4)	Mouse Monoclonal	Santa Cruz (Dallas, US) (sc-12762)	WB	1:500-1:1000, PBS-T
c-Fos (9F6)	Rabbit Monoclonal	Cell Signaling Tech. (#2250)	WB	1:500, 5% (w/v) milk in TBS-T
c-Jun (H-79)	Rabbit Polyclonal	Santa Cruz (sc-1694)	WB	1:300, PBS-T
c-Jun (60A8)	Rabbit Monoclonal	Cell Signaling Tech. (#9165)	ChIP	1:50, ChIP buffer (SimpleChIP® Kit)
FosB (F-7)	Mouse Monoclonal	Santa Cruz (sc-398595)	WB	1:500, PBS-T
FRA1 (D80B4)	Rabbit Monoclonal	Cell Signaling Tech. (#5281)	WB	1:500, 5% (w/v) BSA in TBS-T
Fra2 (D2F1E)	Rabbit Monoclonal	Cell Signaling Tech. (#19967)	WB	1:500, 5% (w/v) BSA in TBS-T
GAPDH (V-18)	Goat polyclonal	Santa Cruz (sc-20357)	WB	1:200-1:500, PBS-T
Histone H3 (D2B12) XP®	Rabbit Monoclonal	Cell Signaling Tech. (# 4620)	ChIP	1:50, ChIP buffer (SimpleChIP® Kit)
IFIT1	Rabbit Polyclonal	GeneTex (Irvine, US) (GTX103452)	WB	1:500, TBS-T
IFNK (1B7)	Mouse Monoclonal	Abnova (Taipei, Taiwan) (H00056832-M01)	WB	1:120 (NHK) or 1:500 (9E pInd IFNK), PBS-T
JunB (C-11)	Mouse Monoclonal	Santa Cruz (sc-8051)	WB	1:500, PBS-T
JunB (C37F9)	Rabbit Monoclonal	Cell Signaling Tech. (#3753)	ChIP	1:50, ChIP buffer (SimpleChIP® Kit)

MATERIAL & METHODS

Table 3 continued: Primary Antibodies

Antigen names are given as stated by the respective company, order no. = order number, buffer composition: see 3.1.2 on page 35

Antigen (clone)	Species Clonality	Company (order no.)	Application	Dilution, Buffer
JunD (D-9)	Mouse Monoclonal	Santa Cruz (sc-271938)	WB	1:500, PBS-T
Normal Rabbit IgG	Rabbit Polyclonal	Cell Signaling Tech. (#2729)	ChIP	1:250, ChIP buffer (SimpleChIP® Kit)
Phospho-Stat1 (Tyr701) (58D6)	Rabbit Monoclonal	Cell Signaling Tech. (#9167)	WB	1:500, 5% BSA (w/v) in TBS-T
p53 (DO-1)	Mouse monoclonal	Santa Cruz (sc-126)	WB	1:500-1:1000, PBS-T
p63 (H-137)	Rabbit polyclonal	Santa Cruz (sc-8343)	WB	1:500, PBS-T
Smad3 (C67H9)	Rabbit Monoclonal	Cell Signaling Tech. (#9523)	WB	1:500, 5% BSA (w/v) in TBS-T
SMAD4 (D3R4N) XP®	Rabbit Monoclonal	Cell Signaling Tech. (#46535)	ChIP	1:50, ChIP buffer (SimpleChIP® Kit)
Stat1 p84/p91 (E-23)	Rabbit Polyclonal	Santa Cruz (sc-346)	WB	1:1000, PBS-T

Table 4 contains the fluorescence-coupled secondary antibodies used for detection of target proteins by WB. All of the secondary antibodies were bought from LI-COR Biosciences (Lincoln, US) and used for detection with the LI-COR Odyssey® Fc Imaging System. The secondary antibodies were applied in a 1:15000 dilution in either PBS-T or TBS-T, depending on the preferences of the primary antibody.

Table 4: Secondary Antibodies

Antigen	Fluorescent Dye	Species
Goat	IRDye® 680RD	Donkey
Mouse	IRDye® 680RD	Goat
Mouse	IRDye® 800CW	Goat
Rabbit	IRDye® 680RD	Goat
Rabbit	IRDye® 800CW	Goat

3.1.7. Used Cell Types

3.1.7.1. Eukaryotic Cells

In this section, the cell lines and primary cells used for the cell culture experiments are introduced.

- **C33A:** HPV-negative cervical carcinoma cell line, carrying mutations in *TP53* and *RB1* [85-87].
- **Normal Human Keratinocytes (NHK):** NHK were isolated from human foreskin after routine circumcision upon informed consent of patients which was approved by the ethics committee of the medical faculty of the University Tübingen (6199/2018BO2) and performed according to the principles of the Declaration of Helsinki. For the preparation protocol, see section 3.2.3.1 on page 60.
- **NIH-3T3-J2 (J2):** Murine fibroblast cell line [88]. Used as feeder cell layer for keratinocytes containing expression vectors for viral proteins or whole HPV genomes.
- **HEK 293T cells (293T):** Human Embryonic Kidney cell line expressing adenoviral proteins and the large T antigen of Simian Virus 40 (SV40; [89, 90]).
- **HPV16-positive Human Keratinocytes (HK HPV16):** These cell lines were generated in our laboratory [91, 92] by stably transfecting NHK derived from different donors with HPV16 wildtype genomes. The immortalized cell lines contain episomal replicating HPV16 genomes.
- **HPV16 E7-positive Human Keratinocytes (HK 16E7):** This cell line was produced in our laboratory by transducing NHK with an expression vector for the HPV16 E7 protein using a retroviral approach.
- **HPV31-positive Human Keratinocytes (HK HPV31):** For generation of this cell line, NHK were stably transfected with HPV31 wildtype genomes in our laboratory. This immortalized cell line contains episomal replicating HPV31 genomes.
- **RTS3b:** Spontaneously immortalized, former β -HPV-positive (episomes are lost during culture), p53-deficient squamous cell carcinoma cell line derived from lesions of a renal allograft recipient [93].

3.1.7.2. Bacterial Strains

Cloning procedures and DNA amplification was performed using the *Escherichia coli* DH5 α strain (Clontech Laboratories Inc., Mountain View, US).

3.1.8. Used Nucleic Acids

In the following section the sequences of used primers, oligonucleotides (oligos) for electrophoretic mobility shift assays (EMSA) and siRNAs are listed. Unmodified, self-designed oligos have been purchased from Thermo Fisher in the standard format (desalted). DY681-modified oligos for EMSA have been ordered from the biomers.net GmbH (Ulm, Germany). SiRNAs have been purchased from different companies, which are listed in the respective table.

In the first table of this section, the sequences of primers used for cloning purposes are shown. The names of the primer refer either to the deletion (del) they are introducing into the reporter construct or the putative TFBS they are disrupting. In case of the deletions, the numbers refer to the position of the respective nucleotide relative to the start codon of the luciferase gene, which replaces the *IFNK* gene. In case of the TFBS, the primer name is derived from the respective TF or TF family, which was predicted to bind the site which is mutated by the cloning procedure.

Table 5: Cloning Primers

Primer name	Sequence (5' -> 3')
del (-4135/-4101) F	GTCTAGACTGAAATCATTACAGTTA
del (-4135/-4101) R	TAACTGTAATGATTTTCAGTCTAGAC
del (-4159/-4101) F	CCTCAGCTGAATCACATTACAGTTA
del (-4159/-4101) R	TAACTGTAATGTGATTCAGCTGAGG
del (-4195/-4159) F	AGCAATAAATCCAGCTATATCG
del (-4195/-4159) R	CGATATAGCTGGATTTATTGCT
del (-4250/-4195) F	AATATGGATGATTATCAGTAGA
del (-4250/-4195) R	TCTACTGATAATCATCCATATT
del (-4786/-4741) F	GAGAAAGCAAAGAGAGAAAGG
del (-4786/-4741) R	CCTTTCTCTTTTTGCTTTCTC
IFNK flanking 2 R	CACTGGCCTAGGTCCTGAAG
IFNK flanking 3 F	CAGTAGATGCCAAATGCCCTCA
IFNK flanking 3 R	AACCCTATCCACCATGCAAGCT
mt AP-1 F	ATGCCCCCTCAGCgctCcacCAGCTATATCGT
mt AP-1 R	ACGATATAGCTGgtgGagcGCTGAGGGGCAT
mt FOX F	AGCATTTAAGAccgAtacgcgccaCCAGTTGTTAT
mt FOX R	ATAACAACCTGGTggcgcgtaTcggTCTTAAATGCT

MATERIAL & METHODS

Table 5 continued: Cloning Primers

Primer name	Sequence (5' -> 3')
mt FOX(2) F	TCACAGAACTTcggagactacAGAGAGAAAGG
mt FOX(2) R	CCTTTCTCTCTgtagtctccgAAGTTCTGTGA
mt HOX F	TCATGGAGAGCAcacttcgTTATCAGTAGA
mt HOX R	TCTACTGATAAcaagtgTGCTCTCCATGA
mt RFX NFAT5 F	GAACAGATATaggttgccgCATGTTAGCAT
mt RFX NFAT5 R	ATGCTAACATGcggcaacctATATCTGTTC
mt TP63 F	CTCTGAGGAcctggTGtctcgcgATAAACGA
mt TP63 R	TCGTTTATcgcgagaCAccaggTCCTCAGAG
mt TP63(2) F	CATGTTAGctcaagAGTGggaAGCCTACTG
mt TP63(2) R	CAGTAGGCTtccCACTcttgagCTAACATG
RVprimer3 (commercial)	CTAGCAAAATAGGCTGTCCC

Table 6 lists the sequences and efficiency of self-designed primers for quantitative real-time PCR (qPCR) experiments. Most primers have been designed during the making of this work; however, some of them were already available when this work was started. Additionally, the name and efficiency of used QuantiTect primers (Qiagen) are given.

Table 6: QPCR Primers

Primer name	Sequence (5' -> 3')	Primer efficiency
16E1E4 880 3358F	TGGCTGATCCTGCAGCAGC	1.933
16E4 3440R	AGGCGACGGCTTTGGTATG	
16E6 226 409F	ACAGTTACTGCGACGTGAGATG	1.822
16E6 445R	TTCTTCAGGACACAGTGG	
31 804 F	TGTTAATGGGCTCATTTGGAA	1.889
31 3373 R	GGTTTTGGAATTCGATGTGG	
31E6* F	AATTGTGTCTACTGCAAAGGTGTA	1.893
31 508 R	CCAACATGCTATGCAACGTC	
ChIP AP-1 SMAD F	TGGAACAATGTA CTTTCAAGAATTGA	1.980
ChIP AP-1 SMAD R	AATGGACAAGGCAGAAATTTGG	
ChIP SERPINE1 F	CAACCTCAGCCAGACAAGGT	1.879
ChIP SERPINE1 R	CCCACGTGTCCAGACTCTCT	

MATERIAL & METHODS

Table 6 continued: QPCR Primers

Primer name	Sequence (5' -> 3')	Primer efficiency
ChIP TFAP2 F	CAAGTCCTCCTACTGCCACC	2.000
ChIP TFAP2 R	TCAGCCTCATGTCATGCTCC	
EGFR F	ACGAGTAACAAGCTCACGCA	1.906
EGFR R	CAGCTCCTTCAGTCCGGTTT	
FOS	QuantiTect Primer Assay: Hs_FOS_1_SG	1.971
FOSB F	CGCCGGGAACGAAATAAACT	2.000
FOSB R	AAATCTCTCACCTCCGCCAG	
FOSL1 F	CAGCAGATCAGCCCGGAG	1.956
FOSL1 R	TTCTGCTTCTGCAGCTCCTC	
FOSL2	QuantiTect Primer Assay: Hs_FOSL2_1_SG	1.984
IFI16 F	GAGCCCAAAGAGCAGAAGAA	1.904
IFI16 R	ATCTCCATGTTTCGGTCAGC	
IFIT1	QuantiTect Primer Assay: Hs_IFIT1_2_SG	2.000
IFNA2 F	AATGGCCTTGACCTTTGCTT	1.863
IFNA2 R	CACAGAGCAGCTTGACTTGC	
IFNB1	QuantiTect Primer Assay: Hs_IFNB1_1_SG	2.000
IFNE	QuantiTect Primer Assay: Hs_IFNE_1_SG	2.000
IFNK 217R	GAAACTCTTGGGGCAACTCA	1.959
IFNK 60F	ATTCATTGCTGGCACCCCTAT	
IFNW1 F	TGGTAAAAGGGAGCCAGTTG	1.919
IFNW1 R	TGCAGTTGCTGATGAAGTCC	
JUN F	ATCAAGGCGGAGAGGAAGCG	1.891
JUN R	TGAGCATGTTGCCGTGGAC	
JUNB	QuantiTect Primer Assay: Hs_JUNB_1_SG	2.000
JUND F	CCCCTTCGGTCTTTTCGACC	1.907
JUND R	CGGGCGAACCAAGGATTACA	
PGK1 F	CTGTGGGGGTATTTGAATGG	1.999
PGK1 R	CTTCCAGGAGCTCCAAACTG	
SERPINE1 F	GCTTTTGTGTGCCTGGTAGAAA	1.933
SERPINE1 R	TGGCAGGCAGTACAAGAGTGA	
SMAD4 F	CAGCACTACCACCTGGACTG	1.820
SMAD4 R	TGTCGATGACTGACGCAA	

MATERIAL & METHODS

Table 6 continued: QPCR Primers

Primer name	Sequence (5' -> 3')	Primer efficiency
SP100 F	TGAGAAGCAAGCATGGTGAG	1.931
SP100 R	TTCAGGTTCTTGTGGCTGTG	
TFAP2A F	TCCAATGAGCAAGTGACAA	1.858
TFAP2A R	GAGGTTGAAGTGGGTCAAGC	
TFAP2C F	GGAAGATTGTCGCTCCTCAG	1.894
TFAP2C R	AGAGTCACATGAGCGGCTTT	
TFAP2E F	TCTCCCACCCCATCCCTAAG	1.909
TFAP2E R	TATGATGAGCAGCAGCCTGG	
TP53 F	GCCCCTCCTCAGCATCTTATC	2.000
TP53 R	TGATGATGGTGAGGATGGGC	
TP63 F	ATCCCCTCCAACACCGACTA	1.920
TP63 R	CCTGTCTCTTCCTGGGCAAG	

In Table 7 the sequences of the oligos used for EMSAs are shown. The wildtype sequence was used either in the 5'-DY681 labeled or in the non-labeled version. The mutant oligos contain the same nucleotide exchanges or deletions as introduced into the plasmids used for the luciferase reporter assays.

Table 7: Oligonucleotides used for EMSA Analyses

Poly(dI:dC) has been purchased from Thermo Fisher, poly(dA:dT) from Sigma-Aldrich (Merck KGaA)

Oligo	Sequence (5' -> 3')
AP-1 wildtype F	GCCCCTCAGCTGAATCACAGCTATATC
AP-1 mutant F	GCCCCTCAGCgctCcacCAGCTATATC
LightShift™ Poly (dI:dC)	...ICICICICICICICICICICICICICIC...
poly(dA:dT)	...ATATATATATATATATATATATATA...
SMAD wildtype F	GCTATATCGTCTAGACTGAAATGT
SMAD mutant F	GCTATATCtgtcgagtGAAATGT
TP63 #2 wildtype F	CATGTTAGCATGTCAAGTGCATAGCCTACTG
TP63 #2 mutant F	CATGTTAGctcaagAGTGggaAGCCTACTG

The last table in this section, Table 8, shows the siRNAs used for knockdown of the indicated target genes.

MATERIAL & METHODS

Table 8: siRNAs used for Knockdown of the listed Target Genes

The shown sequence either represents the genomic target sequence or the sequence of the siRNA itself

Target	Company, Product name, Catalogue number	5'-3' Sequence(s)
<i>FOS</i>	Dharmacon, ON-TARGETplus Human FOS (2353) - SMART pool, L-003265-00-0005	GGGAUAGCCUCUCUUACUA ACAGUUAUCUCCAGAAGAA GAACCUGUCAAGAGCAUCA GCAAUGAGCCUCCUCUGA
<i>FOSB</i>	Qiagen, Hs_FOSB1 + 4-6, SI00091357, SI00091378, SI04948965, SI04948972	TACAATCTGTATCTTTGACAA CTGGAGTGATTATACTGTGA TTCCTGGTTCCGAAAGGCAA CTAGGTCACGTTGGCCCTCAA
<i>FOSL1</i>	Dharmacon, siGenome Human FOSL1 (8061) - SMART pool, M-004341-04-0005	GCUCAUCGCAAGAGUAGCA GGACACAGGCAGUACCAGU AGCGAGAGAUUGAGGAGCU GCAGGCGGAGACUGACAAA
<i>FOSL2</i>	Qiagen, Hs_FOSL2_5, SI02780379	GCGGATCATGTACCAGGATTA
<i>JUN</i>	Dharmacon, ON-TARGETplus Human JUN (3725) - SMART pool, L-003268-00-0005	GAGCGGACCUUAUGGCUAC GAACAGGUGGCACAGCUUA GAAACGACCUUCUAUGACG UGAAAGCUCAGAACUCGGA
<i>JUNB</i>	Dharmacon, ON-TARGETplus Human JUNB (3726) - SMART pool, L-003269-00-0005	GGACACGCCUUCUGAACGU CAUACACAGCUACGGGAUA GAACAGCCUUCUACCACG GAGCUGGAACGCCUGAUUG
<i>JUND</i>	Sigma-Aldrich, SASI_Hs01_00200236 + SASI_Hs01_00200236_AS	GCAUCUCGCGCCUGGAAGATT UCUUCAGGCGCGAGAUGCTT
none	Qiagen, AllStars Neg. Control siRNA, 1027281	proprietary
<i>SMAD4</i>	Dharmacon, ON-TARGETplus Human SMAD4 (4089) - SMART pool, L-003902-00-0005	GCAAUUGAAAGUUUGGUAA CCCACAACCUUUAGACUGA GAAUCCAUAUCACUACGAA GUACAGAGUUACUACUAG
<i>TFAP2A</i>	Dharmacon, ON-TARGETplus Human TFAP2A (7020) - SMART pool, L-006348-02-0005	GUUUUAACAUCCAGAUCA CGUAAAGCUGCCAACGUUA CCACCUAGCCAGGGACUUU UAACAAGGACAACCUCUUC

MATERIAL & METHODS

Table 8 continued: siRNAs used for Knockdown of the listed Target Genes

The shown sequence either represents the genomic target sequence or the sequence of the siRNA itself

Target	Company, Product name, Catalogue number	5'-3' Sequence(s)
TFAP2C	Dharmacon, ON-TARGETplus Human TFAP2C (7022) - SMART pool, L-005238-00-0005	CCGAUAAUGUCAAGUACGA
		ACACUGGAGUCGCCGAAUA
		GUAAACCAGUGGCAGAAUA
		GGACAAGAUUGGGUUGAAU
TFAP2E	Dharmacon, ON-TARGETplus Human TFAP2E (339488) - SMART pool, L-018021-02-0005	GUGGUGUGUUGGUAAGUUA
		CAAUGGACGAGCCGGAAU
		AGAUAAAGCACAAAUCGCA
		GGAUUAGAGUCAGGCCAGA
TP53	ThermoFisher, TP53, S605, 4390824	GUAAUCUACUGGGACGGAATT
		UCCGUCCCAGUAGAUUACCA
TP63	Dharmacon, ON-TARGETplus Human TP63 (8626) - SMART pool, L-003330-00-0005	UCUAUCAGAUUGAGCAUUA
		GCACACAGACAAAUGAAUU
		CGACAGUCUUGUACAAUUU
		GAUGAACUGUUAUACUUAC

3.1.9. Plasmids

In this section, all plasmids used for this work are described. Some commercially available plasmids have been used for the luciferase reporter assays. They have been purchased by the companies indicated in brackets.

- pGL3-basic: promoterless luciferase reporter construct encoding the luciferase gene of the firefly *Photinus pyralis* (Promega)
- pCMV-GLuc: contains the luciferase gene of *Gaussia princeps* controlled by the constitutive active CMV promoter (New England Biolabs, Frankfurt am Main)
- pGL3-promoter: luciferase reporter construct encoding the luciferase gene of the firefly *Photinus pyralis* under the control of the SV40 promoter

Additionally, many of the plasmids generated by Christina Habiger were used [94]. These plasmids were created by amplifying the putative *IFNK* enhancer + promoter sequence from NHK and inserting it in the promoterless pGL3-basic plasmid, which encodes the Firefly luciferase (pGL3 *IFNK* Prom). The number included in the title refers to the position of the first inserted nucleotide relative to the

MATERIAL & METHODS

start codon of *IFNK*. The highlighted -5631 construct was used as a reference construct and vector backbone for all further cloning procedures. Moreover, all internal deletions and mutations of putative TFBS which were cloned by C. Habiger [94] are itemized. As the same cloning strategy was used for the constructs prepared for this work, the procedure will be explained in detail in section 3.2.1.6 on page 58.

- **pGL3 *IFNK* Prom -5631 (-5631)**
- pGL3 *IFNK* Prom -3540
- pGL3 *IFNK* Prom del HS 1 (-4811/-4660)
- pGL3 *IFNK* Prom del (-4661/-4250)
- pGL3 *IFNK* Prom del HS 2 (-4251/-4100)
- pGL3 *IFNK* Prom del HS 3 (-4046/-3895)
- pGL3 *IFNK* Prom mt_{AP-2}
- pGL3 *IFNK* Prom mt₂_{AP-2}
- pGL3 *IFNK* Prom mt_{KLF5}
- pGL3 *IFNK* Prom mt_{SMAD3/4}

Table 9 contains the *IFNK* reporter plasmids, which were generated for this work.

Table 9: pGL3 *IFNK* Prom Reporter Plasmids generated for this Work

del = deletion, mt = mutation, AP-1 = activator protein 1, FOX = forkhead box protein, HOX = homeobox protein, RFX = regulatory factor X, NFAT = nuclear factor of activated T cells, TP63 = tumor protein 63

Reporter name	Remark	inserted in -5631 via...
del (-4786/-4741)	contains putative FOX #2 BS	NheI, BlnI
del (-4253/-4194)	contains putative HOX BS	BlnI, XhoI
del (-4195/-4158)	contains putative AP-1 BS	BlnI, XhoI
del (-4159/-4100)	contains putative SMAD BS	BlnI, XhoI
del (-4135/-4100)	downstream of analyzed BS in HS 2	BlnI, XhoI
mt _{AP-1}	disrupts putative AP-1 BS	BlnI, XhoI
mt _{FOX}	disrupts putative FOX BS	NheI, BlnI
mt _{FOX #2}	disrupts second putative FOX BS	NheI, BlnI
mt _{HOX}	disrupts putative HOX BS	BlnI, XhoI
mt _{TP63}	disrupts putative p53/p63 BS	BlnI, XhoI
mt _{TP63 #2}	disrupts second putative p53/p63 BS	BlnI, XhoI
mt _{RFX/NFAT5}	disrupts putative RFX or NFAT5 BS	BlnI, XhoI

MATERIAL & METHODS

For the analysis of the cGAS/STING pathway, different plasmids available in the laboratory have been used. They are listed below:

- pCI-neo RLuc: contains the codon-optimized luciferase gene of the sea pen *Renilla reniformis* (hRLucCP, Promega) inserted into the pCI-neo mammalian expression vector (Promega); thus, RLuc expression is controlled by the constitutively active CMV promoter
- pGL3 *IFNB1* Prom: *IFNB1* promoter fragment inserted in pGL3 basic, received from Pamela Österlund [95]
- different HR-HPV protein genes inserted in the pSG5 expression vector, which drives protein expression via the SV40 promoter
 - pSG HPV16 E1
 - pSG HPV16 E2
 - pSG HPV16 E1^{E4}
 - pSG HPV16 E5
 - pSG HPV16 E8^{E2}
 - pSG HPV31 E1
 - pSG HPV31 E2
 - pSG HPV31 E5
 - pSG HPV31 E8^{E2}
 - pSG YFP-HPV31 E5, which contains an N-terminal YFP-tag
- pIRESneo3-hscGAS-GFP: expression plasmid for human cGAS, GFP-tagged at the C-terminus, received from Melanie Brinkmann, who got this plasmid from Andrea Ablasser [96]
- pEFBOS-mCherry-mmSTING: expression plasmid for murine STING, mCherry-tagged at the N-terminus, received from Melanie Brinkmann, who got this plasmid from Andrea Ablasser [96]

Additionally, the codon-optimized HPV16 E6 and E7 proteins were subcloned from pEYFP-vectors into the pSG5 vector using an EcoRI and BamHI restriction enzyme-based cloning strategy. In the same way, the HPV 16E5 protein was subcloned from the pSG5 vector into the pSYFP-C1 vector using BspEI and SmaI, creating an N-terminally tagged version of the protein.

3.1.10. Devices

In Table 10 all the devices used for the presented work are listed.

Table 10: Used Devices

OD = optical density; EtBr = ethidium bromide

Device (Purpose)	Company
Autoclave HRM 242 II	Hirayama Manufacturing Cooperation (Toyono, Japan)
BioPhotometer spectrophotometer (OD measurement)	Eppendorf AG (Hamburg, Germany)
BioRobot EZ1 [®] DSP workstation (DNA extraction)	Qiagen
Certomat IS shaking incubator (bacterial culture)	B. Braun Biotech International GmbH (Melsungen, Germany)
CO ₂ incubator C200 (cell culture)	LaboTect (Rosdorf, Germany)
DeltaVision OMX SR Imaging System with AcquireSR- softWoRx and ImageJ software (immunofluorescence)	GE Healthcare (Chicago, US); Image J: open source, developed by LOCI, University of Wisconsin-Madison, US
Herasafe [™] sterile workbench (cell culture)	Thermo Fisher
Intas Gel iX20 Imager with software Intas Gel Doc version 0.2.14 (detection of EtBr-labeled DNA)	Intas Science Imaging Instruments GmbH (Göttingen, Germany)
Kelvitron [®] T incubator (solid phase bacterial culture)	Heraeus (Hanau, Germany)
LI-COR Odyssey [®] Fc Imaging System with Image Studio [™] software version 2.0 (detection of fluorescent-labeled proteins or DNA)	LI-COR Biosciences (Lincoln, US)
LightCycler [®] 480 Instrument (qPCR)	Roche
Lumat LB 9507 luminometer (measurement of luminescence)	BERTHOLD TECHNOLOGIES GmbH & Co. KG (Bad Wildbad, Germany)
Milli-Q [®] UF Plus (supplying ultrapure water)	Merck KGaA
Mini-, Wide-, Sub Cell [®] GT chambers (DNA electrophoresis)	Bio-Rad Laboratories, Inc. (Hercules, US)
Mr. Frosty [™] freezing container (freezing eukaryotic cells)	Thermo Fisher
Multipette [®] plus	Eppendorf AG
NanoDrop [™] 2000 spectrophotometer (concentration, purity of nucleic acid preparations)	Thermo Fisher

MATERIAL & METHODS

Table 10 continued: Used Devices

Device (Purpose)	Company
Neubauer Chamber 0.100 mm depth, 0.0025 mm ² (counting eukaryotic cells)	Glaswarenfabrik Karl Hecht GmbH & Co. KG (Sondheim vor der Rhön, Germany)
PCT 200 Peltier Thermal Cycler (PCR)	Bio-Rad Laboratories, Inc.
pH-meter WTW pH 526	Xylem Inc. (Rye Brook, US)
PIPETMAN Classic™ P10, P20, P200, P1000 pipette	Gilson Inc. (Middleton, US)
pipettor pipetus®	Hirschmann Laborgeräte GmbH & Co. KG (Eberstadt, Germany)
PowerPac 200 (power supply gel electrophoresis)	Bio-Rad Laboratories, Inc.
precision scales GJ and 770	KERN & SOHN GmbH (Balingen, Germany)
Reax top vortexer	Heidolph Instruments GmbH & Co. KG (Schwabach, Germany)
Research® Pro electronic pipette 5 - 100 µl	Eppendorf AG
SonoPuls Sonifier UW 2200 (shearing DNA, homogenizing samples)	Bandelin electronic GmbH & Co. KG (Berlin, Germany)
Sprout™ mini centrifuge	Heathrow Scientific (Vernon Hills, US)
tabletop centrifuges 5804R, 5810R, 5417R, 5424R	Eppendorf AG
Thermomixer comfort	Eppendorf AG
ThermoStat plus	Eppendorf AG
Trans-Blot® Cell chamber (electrophoresis proteins)	Bio-Rad Laboratories, Inc.
transmitted light microscope DM IRB (cell culture)	Leica Camera AG (Wetzlar, Germany)
UV transilluminator NU-72 KL (excision of DNA bands for subsequent cloning)	Konrad Benda Laborgeräte Ultravioletstrahler (Wiesloch, Germany)
VacuSafe scavenge pump	INTEGRA Biosciences AG (Zizers, Switzerland)
water bath WB10	Memmert GmbH & Co. KG (Schwabach, Germany)

3.1.11. Consumption Items

Table 11 specifies the used consumables.

Table 11: List of Consumables

PP = polypropylene; PET = polyethylene terephthalate, PES = polyethersulfone, PS = polystyrene

Item	Company
Blotting Paper (Western Blot)	Whatman plc (Maidstone, UK)
Cell Culture Dishes (Nunc™, 35 mm, 60 mm, 100 mm, 150 mm)	Thermo Fisher
Cell Culture Plates (Nunc™, 6 well, 12 well, 24 well)	Thermo Fisher
Cell Lifter (Corning™, Costar®)	Thermo Fisher
Coated Cell Culture Dishes (Corning™ Primaria™, 60 mm, 100 mm)	Thermo Fisher
Conical Centrifuge Tubes (CELLSTAR®, PP, 15 ml, 50 ml)	Greiner Bio-One
Cryo Tubes Bacterial Stocks (PP, 3.6 ml)	Thermo Fisher
Cryo Tubes Cell Culture (Cryo.s™, PP, 2 ml)	Greiner Bio-One (Kremsmünster, Austria)
EASYstrainer™ (PET, 100 µm)	Greiner Bio-One
Filter Pipette Tips (ART® Barrier Tips; 10, 20, 200, 1000 µl)	Thermo Fisher
High Precision Microscope Cover Glasses, 170 µm thickness	Paul Marienfeld GmbH & Co. KG (Lauda-Königshofen, Germany)
LightCycler® 480 Multiwell Plate 96, white	Roche
Nitrocellulose Membrane (Amersham™ Protran®, 0.22 µm)	Whatman plc
PCR Soft Tubes (0.2 ml)	Biozym Scientific GmbH
Pipette Tips (10 µl)	Biozym Scientific GmbH
Pipette Tips (200, 1000 µl)	Greiner Bio-One
Reaction Tubes (1.5 ml, 2.0 ml)	Eppendorf
Scalpel, disposable	B. Braun Melsungen AG
Sterile Filters 0.22 µm, 0.45 µm (Millex-GP, PES)	Merck KGaA
Transfection Tubes (PS, 3.5 ml)	Sarstedt AG & Co. KG (Nümbrecht, Germany)
Tubes for Bacterial Culture (PS, 14 ml, sterile)	Greiner Bio-One
Tubes for Luciferase Measurements (PS, 5 ml)	Sarstedt AG & Co. KG

3.2. Methods

3.2.1. DNA-Methods

In the first section of this chapter the techniques applied for isolation, amplification and modification of DNA molecules are summarized.

3.2.1.1. Standard Methods

The most commonly used methods are described in detail in the *Current protocols in molecular biology* [97] and will not be explained here. This includes the electrophoretic separation of DNA in agarose gels and the cleavage of DNA with restriction enzymes.

3.2.1.2. Preparative Isolation of Plasmid DNA from Bacteria

Isolation of plasmid DNA from bacteria was performed using different Qiagen kits. For small amounts of DNA (≈ 500 ng - 10 μ g) the QIAprep[®] Spin Miniprep Kit was used to isolate plasmid DNA from 3 ml of liquid bacterial overnight culture. To retrieve larger amounts of DNA either the QIAgen[®] Plasmid Plus Midi Kit or the QIAgen[®] Plasmid Plus Maxi Kit were utilized to prepare DNA from 50 ml or 200 ml of liquid overnight culture, respectively. All kits were used as described in the manufacturer's instructions. DNA was eluted in 50, 200 or 400 μ l EB buffer (Qiagen), respectively. The purity and concentration of the eluted DNA was determined using the NanoDrop[™] 2000 spectrophotometer (Thermo Fisher). DNA with aberrant 260/280 ratio (should be between 1.8 and 2.0) or suspicious spectral curves was discarded and freshly prepared.

3.2.1.3. Amplification of DNA

To amplify a specific DNA sequence, a polymerase chain reaction (PCR) is executed [98]. Depending on the intended use of the amplified DNA, different polymerases were employed: To test for *Mycoplasma* contamination in cell culture the GoTaq[®] G2 DNA Polymerase (Promega) from *Thermus aquaticus* was applied (see section 3.2.3.5 on page 62). This standard polymerase possesses a medium fidelity, meaning it might create single mismatches during amplification of DNA, thereby altering the DNA sequence of the product. However, as the Taq polymerase is only used to check

MATERIAL & METHODS

whether a *Mycoplasma* gene product is present, its performance is sufficient for this purpose. In contrast, for cloning purposes, in which the production of the correct DNA sequence is crucial, the high-fidelity Pyrobest® DNA Polymerase (Takara Bio Inc.) from *Pyrococcus* sp. was used. The Pyrobest® DNA Polymerase was operated following the program shown below:

Table 12: PCR Program used for High-Fidelity Amplification

initial denaturation	5 min	95°C	
denaturation	30 s	95°C	
annealing	30 s	55°C	30 cycles
elongation	60 s	72°C	
storage	∞	10°C	

3.2.1.4. Isolation of DNA after Electrophoretic Separation

After digestion of plasmid DNA with restriction enzymes or after amplification of DNA via PCR, purification of the DNA molecule of interest was done by electrophoretic separation followed by recovery of the nucleic acid from the agarose gel. This was done using the QIAquick® Gel Extraction Kit (Qiagen) according to the manufacturer's instructions. The purified DNA was eluted in 50 µl of buffer EB (Qiagen).

3.2.1.5. Ligation of DNA Fragments

Ligation of DNA fragments was done using the T4 DNA Ligase and the Rapid DNA Ligation Kit (Thermo Fisher) as described in the manual. This method was used to insert a PCR-derived DNA fragment into a plasmid. Before ligation, amplicon and plasmid DNA were digested with the same restriction enzymes to create compatible ends. To prevent re-ligation of the digested plasmid the phosphate group at the 5'-end of the DNA was removed using 1 µl of FastAP Thermosensitive Alkaline Phosphatase (1 U/µl; Thermo Fisher) for each digestion (3-5 µg plasmid DNA). After addition of the phosphatase the DNA was incubated for another 10 min at 37°C. To estimate the ratio in which the digested insert and plasmid should be used for ligation, equal volumes of both DNA preparations were run on an agarose gel. If the intensity of both DNA bands was similar, indicating similar amount of loaded DNA, a 3-fold excess of insert was applied. If one of the bands indicated less DNA, the volume of the respective DNA preparation was increased. Additionally, a vector control was implemented in each ligation. In this control, water instead of insert DNA was added to the reaction.

Colonies which arose from bacteria transformed with these controls represent re-ligation events in which the plasmid DNA was ligated without enclosure of the insert DNA.

3.2.1.6. Molecular Cloning

Molecular cloning is a process in which, by combination of various DNA sequences derived from different species, a new, recombinant DNA molecule is produced [99]. For this work different luciferase reporter plasmids containing alterations in the *IFNK* enhancer sequence were created. They are all based on the pGL3 *IFNK* Prom -5631 (-5631) plasmid. This plasmid was assembled by C. Habiger by inserting parts of the human *IFNK* gene in the promoterless pGL3 basic plasmid which contains a Firefly luciferase gene [94]. In this section, a brief recapitulation of the molecular cloning procedure is given. First, primers containing mutated sequences or bridging the part of the DNA sequence to be deleted were designed. For generation of the deletion constructs, primers which bridge the region to be omitted were generated: These primers contain \approx 10-12 bp that anneal to the last nucleotides before the deletion and \approx 10-12 bp which are complementary to the region after the deletion. The name of the deletion refers to the position of the last nucleotide before and the first nucleotide after the deleted region. The amplified product was inserted into the -5631 construct via digestion with restriction enzymes. For generation of a mutation in a putative TFBS, primers which contain the mutated sequence, flanked by \approx 12 bp of complementary sequence on both sides, were designed. As for the deletion constructs, the mutated amplicons were inserted in the -5631 construct by digestion with restriction enzymes (Table 9 on page 51) and re-ligation with the vector. The sequence of these self-designed primers can be looked-up in Table 5 on page 45. The primers were used to perform an overlap extension PCR using the -5631 construct as a template. The resulting modified DNA sequence was purified from a gel to remove primer dimers (see section 3.2.1.4 on page 57) and inserted in the -5631 construct by digestion with the same restriction enzymes and ligation of the purified digestion products as described in section 3.2.1.5 on page 57. Afterwards, the newly generated plasmid DNA was transformed in chemically competent DH5 α bacteria as described below (section 3.2.2.2 on page 60).

3.2.1.7. Choosing Candidate Binding Motifs for Transcription Factors

In order to identify TFs involved in *IFNK* gene expression, the JASPAR CORE database for vertebrates was used to choose candidate TFs for further evaluation (<http://jaspar.genereg.net>, accessed between January 2017 and September 2019, resulting in the usage of different versions of the

database). As the database contains a huge number of experimentally validated binding motifs for TFs it delivers an extensive list of candidates. Thus, the initial list had to be filtered: Only candidates with a predicted binding score above 10 were considered. Next, literature research was performed to figure out whether these candidates are known to be expressed in NHK and might be involved in aspects of keratinocyte biology. All promising candidates with a score ≥ 10 could be linked to some keratinocyte or general cellular features which are also present in keratinocytes. Initial testing of the candidate TFs was done by mutation of their predicted binding motif in the context of the pGL3 *IFNK* Prom -5631 reporter construct. To achieve the best possible abrogation of TF binding, the position weight matrices of JASPAR were used to predict the least favorable sequence for binding of the candidate. In any case, binding of the candidate TF was predicted to be abolished by the JASPAR database after mutation.

3.2.1.8. Validation of used DNA Sequences

To ensure working with the correct DNA sequences, all newly generated plasmid DNAs were sequenced before being used for the first time. This was done by Sanger sequencing performed by the Eurofins Scientific SE/ GATC Biotech AG (Luxemburg).

3.2.2. Microbiological Methods

In the following section, the microbiological methods used for cloning procedures or amplification of eukaryotic DNA in bacterial cultures are described. The procedures delineated below have been performed using the *Escherichia coli* strain DH5 α (Clontech Laboratories Inc.).

3.2.2.1. Production of Chemical Competent Bacteria

To enable bacteria to take up plasmid DNA, that is, making them competent, bacteria were treated with CaCl₂, RbCl and MnCl₂ [97]. Briefly, cells were grown in LB medium overnight, this pre-culture was diluted in fresh LB medium and grown to an OD₆₀₀ of 0.45 to 0.55. Incubation on ice and resuspension in buffers containing calcium, rubidium and manganese was followed by snap-freezing the bacteria in liquid nitrogen and storage at - 80°C.

3.2.2.2. Transformation of Plasmid DNA

To transform these competent cells, the heat shock method was applied [97]. Bacteria were thawed on ice, DNA was added and after 15 min on ice, cells were heat-shocked at 42°C for 1 min. Then, SOC medium was added and bacteria were grown half an hour at 37°C before being plated on agar plates containing the selection antibiotic. After growing overnight, clones were picked the next afternoon and inoculated for liquid culture. Uptake of the correct plasmid DNA was validated by sending isolated DNA for sequencing (see section 3.2.1.8 on page 59).

3.2.2.3. Culture of Bacteria for DNA Amplification and Isolation

To amplify DNA, bacteria harboring the plasmid of interest were cultured in liquid LB medium supplemented with the selection antibiotic the respective plasmid carries the resistance gene for. As predetermined by this resistance gene, bacteria were grown in the presence of either 100 µg/ml ampicillin or 30 µg/ml kanamycin. Depending on the amount of DNA needed, 3 (mini prep), 50 (midi prep) or 200 ml (maxi prep) of culture medium were prepared. All liquid cultures were inoculated from frozen bacteria stocks in the late afternoon and grown for 16 to 18h at 37°C and 130-160 rpm until the next morning. Frozen bacteria stocks were prepared for long-term storage, as soon as the uptake of the correct plasmid was confirmed, by mixing the bacteria 1:1 with freezing medium and transfer them to -80°C.

3.2.3. Cell Culture Methods

In the following section, all cell culture procedures are described. All working steps have been conducted under a sterile workbench using only sterile materials. The different cell types used for this work are cultured in different media which are listed in section 3.1.3.2 on page 37.

3.2.3.1. Retrieval of NHK from Human Foreskin

After routine circumcision, tissue samples were collected in PBS. Under the cell culture hood, the samples were rinsed once with PBS and covered with fresh PBS for the preparation procedure. First, the underlying fat tissue and blood vessels were cautiously removed using sterile tweezers and scissors. Afterwards, the relieved keratinocyte layer was cut into small pieces, transferred into a 60 mm cell culture dish and covered with 5 ml of dispase. After incubation for 12-16 h at 4°C, the upper layer of the skin could be removed, cut into as small pieces as possible and transferred into

MATERIAL & METHODS

3 ml of trypsin-EDTA in a 15 ml tube. To isolate the cells, they were incubated for 10 min at 37°C. During the incubation time, the tube was inverted several times. Afterwards serum-containing medium was added to inactivate trypsin and the cells were passed through a nylon cell strainer (100 µm). Then, singularized cells were collected by centrifuging at 1394 g for 5 min and resuspended in KSFM. Depending on the cell mass, the freshly isolated keratinocytes were seeded in to one or two coated cell culture dishes (Corning™ Primaria™) and allowed to grow until near-confluency.

3.2.3.2. Culture of Cells

All cells were kept in a humidified incubator (95% relative humidity) at 37°C and 5% CO₂ in Nunc™ cell culture dishes. Only freshly isolated NHK (first two passages) were grown on coated cell culture dishes. Cells were inspected every two to three days under the microscope. Determined by the cell density, the cells were either supplied with fresh medium or distributed to new dishes. To do the latter, medium was aspirated and PBS was used to wash away remnants of the medium. Afterwards, cells were covered with trypsin-EDTA and incubated at 37°C until they detached. Depending on the cell type used, this detachment step took between 2-5 min. Then, cells were collected in serum-containing medium to inactivate trypsin. For keratinocytes, which are cultivated in serum-free medium, an additional centrifugation step (1394 g, 5 min) to pellet the cells and to resuspend them in the preferred growth medium, was conducted. Other cell types were directly distributed to new dishes, using enough medium to dilute trypsin to an inactive concentration. Depending on the cell type, cells were passaged in a ratio of 1:2 up to 1:10. During the culture of keratinocytes special attention was paid to avoid isolating the cells too much or letting them grow until confluency. These cells were never divided more than 5-fold. Cells that changed their morphology (sign of stress or starting differentiation) were discarded. For the experiments, cells were used at low passage numbers to avoid creation of culture artefacts. Primary cells were used at passage 2 to 4 whereas immortalized cell lines were used at passages 7 to 45, depending on the availability of the respective cell type. Keratinocytes carrying HPV genomes or protein expression plasmids were cultured on a growth-arrested feeder layer of murine J2 fibroblasts. Hence, before distributing these cells on new dishes, a sufficient amount of feeder cells had to be treated with mitomycin C (see section 3.2.3.3) and seeded in the respective dishes.

3.2.3.3. Mitomycin C Treatment of Feeder Cells

Keratinocytes carrying viral genomes are co-cultured with fibroblasts. To avoid an overgrowth of fibroblasts, they are treated with mitomycin C before usage as feeder cell layer.

Mitomycin C interferes with the formation of the spindle apparatus and therefore inhibits cell division. The resulting non-proliferative fibroblasts are still viable and can support keratinocyte growth but cannot overgrow the keratinocyte population anymore [100]. To achieve the growth arrest, near-confluent dishes of murine J2 cells, which are kept in DMEM-CS, were treated with 80 µg/ml mitomycin C for 1 to 2 h. Afterwards they were thoroughly washed with PBS to remove remnants of the cytostatic agent. For co-cultures the fibroblasts were cultivated in E-medium supplemented with HyClone serum (HC).

3.2.3.4. Freezing and Thawing of Mammalian Cells

For long-term storage, cells of a preferably low passage are kept in liquid nitrogen. To do so, they have to be collected in freezing medium. These freezing media are made up of the growth medium of the respective cell type supplemented with an additional 10% (v/v) of the preferred serum plus either 10% (v/v) DMSO (J2, NHK and 293T cells) or 20% (v/v) glycerol (HPV genome or expression plasmid-containing HK and RTS3b). Freezing media was freshly prepared before usage and sterile filtered using a 0.22 µm filter. The cells were trypsinized, after detachment trypsin action was stopped using serum-containing medium and cells were collected by centrifuging at 1394 g for 5 min. Afterwards, the pellet was resuspended in 2 ml of freezing medium per near-confluent 100 mm dish and distributed to two cryo tubes. The cryo tubes were placed into a freezing container which has been warmed to room temperature before starting. After that, it was immediately transferred to -80 °C. The next day, cells were moved to the liquid nitrogen tank.

Vice versa, for thawing cells, they were removed from liquid nitrogen in the afternoon, thawed in the 37°C water bath and immediately transferred to 10 ml of 37°C warm medium. They were allowed to settle down overnight and medium was exchanged the next day to remove the remnants of DMSO or glycerol.

3.2.3.5. Test for *Mycoplasma* Contamination

A major obstacle during mammalian cell culture is the contamination with *Mycoplasma* sp., which are resistant against many means implemented to avoid contamination. These bacterial species is the smallest known self-replicating organism and lacks a cell wall, which renders them unresponsive to antibiotics targeting the cell wall and let them pass micro filters used to get rid of conventional bacteria. On top, their reduced metabolism (no cloudiness or change of pH of the medium) and small size prevents their recognition during routine check-up of the cells. As they do not obviously damage the cells either, they can persist for a pro-longed time [101, 102]. Hence, systematic scans for

MATERIAL & METHODS

Mycoplasma contamination have to be employed to get aware of the presence of this bacterium which influences the cells' behavior and therefore the results of any experiment performed based on cell culture systems. In our laboratory, cell lines are checked for *Mycoplasma* contamination after being thawed. To do so, they are kept in antibiotic-free medium for at least 48 h and the cell culture supernatant is used for a *Mycoplasma* test PCR. After being incubated at 95°C for 5 min the supernatant, which might contain the bacterium, is used as a template for the PCR. For each culture to be tested as well as for one negative (H₂O) and one positive control the following reaction is prepared:

32.75 µl	H ₂ O
10 µl	5x GoTaq® Green Reaction Buffer (Promega)
1 µl	dNTPs (10 mM each)
1 µl	template (culture supernatant) or H ₂ O or positive control
0.25 µl	GoTaq® Polymerase (Promega)
2.5 µl	forward primer (10 µM)
2.5 µl	reverse primer (10 µM)

Afterwards, the PCR is conducted as shown in Table 13 and the products are run on a 1% agarose gel. Appearance of a DNA band at 560 bp indicates the presence of *Mycoplasma* infection. During the making of this work, no *Mycoplasma* contamination was observed.

Table 13: *Mycoplasma* Test PCR Program

initial denaturation	5 min	95°C	
denaturation	20 s	95°C	
annealing	20 s	65°C	35 cycles
elongation	20 s	72°C	
final elongation	2 min	72°C	
storage	∞	10°C	

Sequences *Mycoplasma* primers:

Forward: CCAGACTCCTACGGGAGGCA

Reverse: TGCGAGCATACTACTCAGGC

3.2.3.6. Harvesting Cells

Depending on the type of experiment, cells were either harvested by trypsinizing, adding a lysis buffer or by scratching them off the plate with a cell lifter. For subsequent RNA extraction RLT buffer from the RNeasy® Mini Kit (Qiagen), supplemented with beta-mercaptoethanol (1:100), was added to the cells, leading to detachment of the cells. For preparing nuclear or whole cell extracts, the growth medium was removed, the cells were washed with PBS, fresh PBS was added and cells were scratched off the dish with a cell lifter and centrifuged (30 s, 20000 g, 4°C) to collect them.

Cells which are co-cultured with feeder cells were depleted from the feeder layer before harvesting. This was either done by thoroughly washing with PBS or addition of versene, depending on the stickiness of the feeder cells to the culture dish. If versene had to be used, cells were incubated for 3 min at 37°C, versene was removed, cells were washed twice with PBS and harvested afterwards.

3.2.3.7. Treatment of Cells

For treatment with different substances (see Table 1 on page 39) $2 \cdot 10^5$ keratinocytes per well were seeded in 6 well plates. The next day, the growth medium was replaced by fresh medium and the respective substances or vehicle controls were added. The different compounds were aliquoted as 1000x stocks, referring to the lowest concentration used. Thus, in most experiments the vehicle accounted for a 1 or 2‰ (v/v) and a maximum of 4‰ (v/v) of the total volume in a well. After the respective incubation period, cells were subjected to harvesting as described above or measurement of reporter activity was performed.

3.2.3.8. Transfection of Cells

Transfection of plasmid DNA using FuGENE® HD

Reporter Assays

As part of this work, different cell types have been transfected with plasmid DNA to perform reporter assays. These assays have all been done in 24 well plates. Cells were seeded approximately 16 h before transfection and should have reached roughly 80% density to achieve optimal transfection efficiency. As the used cell types differ in size, proliferation rate and tendency to settle down, various cell counts have been used. When using NHK and HK 16E7 cells, 50,000 cells/well were seeded, whereas 30,000 of RTS3b cells/well were sufficient to reach optimal density. When using C33A or 293T cells 75,000 cells/well were seeded. Transfection was done using the FuGENE® HD Transfection Reagent according to the manufacturer's instructions. Briefly, the plasmid DNA was diluted in Opti-

MATERIAL & METHODS

MEM medium and supplemented with 5 μ l of FuGENE[®] per 2 μ g of DNA. All cell types have been transfected with 0.5 ng of the pCMV-GLuc (*IFNK* experiments) or 60 ng of the pCI-Neo RLuc reporter construct (C33A) per well to correct for different transfection efficiencies. This plasmid was added to the Opti-MEM medium before distributing it to the different tubes for the separate transfection mixtures. One transfection mixture was prepared for all technical replicates. For the *IFNK* experiments, NHK and HK 16E7 were transfected with 300 ng of Firefly luciferase constructs per well. For RTS3b, which are more easily to be transfected, 100 ng of DNA were used. For the cGAS/STING experiments, NHK were transfected with 300 ng of the pGL3 *IFNB1* Prom Firefly luciferase construct (pGL3 *IFNB1* Prom) and 500 ng of the different HPV protein expression plasmids or the empty vector (pSG5). C33A or 293T were transfected with 100 ng pGL3 *IFNB1* Prom, 100 ng of cGAS- and 100 ng of STING-expression plasmid plus 100 ng of the different HPV protein expression plasmids or respective controls. To ensure equal distribution master mixes were prepared whenever applicable. Differences in the DNA amount were adjusted using the pSG5 plasmid. After adding all DNAs and the transfection reagent the whole mixture was vortexed for 10 s and incubated for 15 min at room temperature. In the meantime, the medium on the cells to be transfected was exchanged. Then, the FuGENE[®]:DNA complex was added droplet by droplet to the wells. Twenty-four hours after transfection medium was exchanged.

Immunofluorescence

Three hundred thousand C33A cells/well in a 6 well plate were transfected with the FuGENE[®] HD Transfection Reagent as described above. In this format, 400 ng/well of the mCherry-STING plasmid, 800 ng/well of the EYFP-HPV31 E5 plasmid or a combination of both was used. Differences in the DNA amount were adjusted using the pSG5 plasmid. In the second experiment, 80,000 C33A cells/well were seeded in a 12 well plate and transfected with the FuGENE[®] HD Transfection Reagent using 200 ng/well of the mCherry-STING plasmid and/or 400 ng/well of the HPV E5 expression plasmids. Once more, differences in the DNA amount were adjusted using pSG5 plasmid DNA.

Transfection of siRNAs using Lipofectamine RNAiMAX

For the knockdown experiments described in this work an RNA interference approach was used. NHK, which have been seeded on a 6 well plate (2×10^5 cells/well) approximately 16 h before, were transfected with siRNAs using the Lipofectamine RNAiMAX reagent according to the manufacturer's instructions. First, siRNA and transfection reagent were diluted in Opti-MEM. Then, diluted reagent was added to the diluted siRNA and mixed by pipetting up and down several times. After 5 min of incubation at room temperature, in which the cells were supplied with fresh growth medium, the

transfection mixtures were added droplet by droplet to the wells. Like this, 90 pmol of siRNA per well were delivered using 9 μ l of RNAiMAX each.

Transfection of cGAMP using jetPRIME®

To mimic cGAS activation, C33A have been transfected with 5 μ g/ml cGAMP using jetPRIME® according to the manufacturer's instructions. Briefly cGAMP was diluted in jetPRIME® buffer, the transfection reagent was added and incubated for 10 min at room temperature. Culture medium was exchanged and the transfection complex was slowly added to the cells.

3.2.4. Analysis of Eukaryotic Cells

In the following section, the different experiments, which were done using mammalian cells, are described.

3.2.4.1. Luciferase Reporter Assays

To analyze the contribution of a certain DNA sequence to the expression of a gene of interest, reporter assays are performed. In this kind of assays, the gene of interest is replaced by a reporter gene whose expression levels can be easily assessed. This is for example applicable to enzymes, which convert a substrate into a product that can be quantified. The assays used for this work are based on the luciferase gene of the firefly *Photinus pyralis*. When adding the substrate of this enzyme, D-luciferin, to the cell lysate containing the reporter gene product, the luciferase catalyzes the oxidation of its substrate, which results in the emission of light. As this light emission increases linearly with the quantity of enzyme present in the cell lysate, the relative luminescent units (RLU) detected by the luminometer can be used as a direct means to quantify the expression of the reporter gene. Hence, by manipulating the surrounding DNA sequences of a gene of interest, the influence of this sequence stretches on gene expression can be studied.

To identify the DNA sequences which are needed for the expression of the *IFNK* gene, different reporter plasmids have been generated and transfected into primary as well as immortalized keratinocytes (RTS3b, HK 16E7) as described in section 3.2.3.8 on page 64. Two days after transfection the activity of the co-transfected *Gaussia* luciferase, which is secreted into the cell culture medium, was measured using the *Gaussia* Juice Big Kit (PJK) according to the manufacturer's instructions: Five μ l of the supernatant of each well (24 well plate) were transferred to a tube and the luminometer added 100 μ l of coelenterazine (CTZ)-containing buffer to the medium. The oxidation of coelenterazine by the *Gaussia* luciferase causes the emission of light, which is detected

MATERIAL & METHODS

and recorded by the luminometer. To measure the expression of the intracellular Firefly reporter gene, cells had to be lysed. Hence, after two washing steps using cold PBS, 150 µl of lysis buffer were added per well and the plate was incubated gently shaking on ice for 10 min. Afterwards, 100 µl of the lysate were added to 100 µl of assay buffer and supplemented with 100 µl of D-luciferin-containing assay buffer by the luminometer. The RLU generated by the Firefly luciferase were divided by the RLU of the *Gaussia* luciferase to correct for transfection efficiency and the average of the technical duplicates was used to calculate the percentage of the respective luciferase activities relative to the activity of the pGL3 *IFNK* Prom -5631 construct, which was set to 100%. All different reporter constructs were analyzed at least three times, using keratinocytes from different donors or passages (cell lines).

For cGAS/STING experiments, the same protocol was followed. However, when working with the intracellular expressed *Renilla* luciferase instead of the *Gaussia* luciferase for normalization purposes, cells were lysed directly and Firefly luciferase expression was determined before washing the luminometer and using the Gaussia Juice Big Kit to assess expression of the *Renilla* luciferase, which also uses CTZ as substrate. Controls, which showed no signal above background generated by the Firefly luciferase upon CTZ usage and vice versa (*Renilla* luciferase - D-luciferin), were implemented in these experiments.

3.2.4.2. Nuclear Extract Preparation

As this work focuses on the regulation of a gene, different TFs had to be evaluated. Active TFs are found in the cell nucleus; hence, to analyze their expression or use them for binding assays, nuclear extracts had to be prepared. To do so, cells were harvested when reaching near-confluency: The culture dishes were placed on ice, medium was removed and cells were washed once with cold PBS. Then, 1-2 ml of PBS were added, cells were scratched off the plate and collected in a 2 ml tube. Afterwards they were centrifuged for 30 s at 20000 g and 4°C and the cell pellet was dissolved in 150-500 µl cold lysis buffer (depending on the cell mass). Incubation on ice for 5 min was followed by a second centrifugation step (5 min, 3000 g, 4°C) after which the pelleted nuclei were resuspended in 50-150 µl cold elution buffer (depending on cell mass). Elution was done by incubation on ice for 15 min. Afterwards, the eluate was centrifuged for 5 min at 20000 g and 4°C to remove the cell debris and the supernatant was aliquoted into pre-cooled tubes. The nuclear extracts were stored at -80°C, repeated thawing was avoided.

3.2.4.3. Electrophoretic Mobility Shift Assay (EMSA)

In order to show binding of proteins to a DNA sequence of interest an EMSA can be performed. This assay is based on the fact that a nucleic acid which is bound by one or several proteins migrates slower than its free counterpart during native gel electrophoresis. To visualize this so-called band shift labeled oligos are used. In this work oligos, which were labeled with the DY681 fluorophore at the 5' end, were utilized to visualize the DNA. To assess whether the observed binding event is sequence-specific, unlabeled competitor oligos are included in the analysis. The EMSAs shown in this work were performed using a 100-fold excess of unlabeled competitor oligos. Two different kind of competitors have been employed: On the one hand, the same sequence was used to prevent the formation of a shifted band and on the other hand the addition of an excess of a mutated DNA sequence (see Table 7 on page 48) was used, which - in case of sequence-specific binding - led to the reappearance of the shifted band. As a probe for EMSA either purified proteins or cell extracts containing the proteins to be tested can be used. In this work, nuclear extracts from different keratinocyte types (see section 3.2.4.2 on page 67) have been used to test DNA binding capacity.

The oligos used for EMSA have been purchased as single-stranded DNA molecules and had to be annealed in the laboratory before the first usage. For this purpose, 12.5 μ l of 100 μ M forward oligo was mixed with 12.5 μ l of 100 μ M reverse oligo and 25 μ l of 2x annealing buffer. Annealing was achieved by running the following program in a thermal cycler:

10min 95°C
10min 70°C
10min 60°C
10min 50°C
10min 40°C
10min 25°C
 ∞ 4°C

To change from one temperature level to the next, the ramp rate of the cycler was set to 0.1°C/s.

The EMSA experiment was conducted as following: Per reaction 2 μ l of binding buffer were pre-mixed with 0.5 μ l of 1 μ g/ μ l poly(dA:dT) or poly(dI:dC) - depending on the composition of the oligo to be tested - and 2.5 μ l of water and supplemented with 3 μ l of nuclear extract or water (free oligo control). Then, 1 μ l of the wildtype or the mutant competitor oligo (4 μ mol/ μ l) or water was added and incubated for 5 min at room temperature. Afterwards, 1 μ l of the labeled oligo (40 fmol/ μ l) was added and the whole mixture was incubated another 15 min at room temperature in the dark before being loaded on a 3-5% polyacrylamide (PAA) gel. The percentage of the gel was chosen based on the size of the proteins or protein complexes which were expected to bind. Gel electrophoresis was

performed in 0.5x TBE buffer at 4°C and 100V for approximately 40-50 min. Before loading the samples, the gel was adapted to the running conditions for about half an hour. After electrophoresis the band pattern was visualized using the Odyssey® Fc Imaging System (LI-COR Biosciences). Each experiment was performed several times, testing nuclear extracts derived from different donors or passages (cell lines).

3.2.4.4. RNA Interference

To evaluate the contribution of different TFs to *IFNK* expression, the expression of this candidate TFs was knocked down. For this purpose, cells ($1.5 - 2 \times 10^5$ per well on a 6 well plate) were transfected with siRNAs directed against the respective candidate genes and harvested 48 h after siRNA delivery as described in section 3.2.3.8 and 3.2.3.6 on page 64, respectively. Then, RNA was isolated, the flow-through of the columns was collected for future protein precipitation and the isolated RNA was reverse-transcribed. The resulting cDNA was used to determine the knockdown efficiency on RNA level and the influence on *IFNK* transcription (see section 3.2.5 on page 72 for detailed description). The primers used for this purpose are listed in Table 6 on page 46. The Light Cycler 480 instrument (Roche) was used for cDNA quantification, obtained CP values were converted to fold change compared to the non-targeting siRNA control according to Pfaffl [103] and *PGK1* as the reference gene transcript. In addition to the knockdown evaluation on RNA level, proteins were precipitated from the flow through of the RNeasy® columns as described in the handbook of the kit and subjected to Western blot analysis to assess the impact of the siRNA treatment on protein level. If Western blot analysis from these acetone-precipitated proteins was not feasible, nuclear extracts from siRNA-treated samples were prepared (see section 3.2.4.2 on page 67) and used for analysis of protein expression.

3.2.4.5. Compound Treatments

To assess the impact of different signaling pathways on *IFNK* expression, cells ($1.5 - 2 \times 10^5$ per well) were seeded in a 6 well plate and treated the next day with substances that interfere with these pathways or the respective vehicle controls (see Table 1 on page 39). Twenty-four hours later, cells were harvested and RNA was isolated and reverse-transcribed. The analysis of gene expression was performed using the LightCycler® 480 Instrument (Roche, see section 3.2.5 on page 72). The obtained CP values were converted to fold induction compared to the vehicle control according to Pfaffl [103] and *PGK1* as the reference gene transcript. Furthermore, the impact of the most promising

candidates for *IFNK* regulation was evaluated on protein level. To do so, a Western blot protocol (as described below) was applied.

3.2.4.6. Western Blot Analysis

Western blot analysis comprises different steps: First, proteins are separated electrophoretically according to their molecular weight under denaturing conditions in a PAA gel and then they are electrophoretically transferred from the gel onto a solid phase, for example onto a nitrocellulose membrane. Next, the proteins trapped on the solid phase can be immunologically detected by applying antisera or antibodies directed against the proteins of interest [104]. In the following section the Western blot protocol used for this work is described.

a) Sample Preparation

Samples from different sources have been subjected to Western blot analysis: Cell extracts from compound-treated cells were obtained by lysing cells in RIPA buffer (75 μ l per well, 6 well plate), for Nutlin-3a- and some siRNA treatments, the flow-through from RNeasy[®] columns was precipitated using acetone as described in the RNeasy[®] Mini Handbook (Qiagen) and for some experiments nuclear extracts had to be prepared. To use these different sample types for Western blot, all of them were either directly resuspended in Roti[®]-Load 1 (Carl Roth, 4x) or supplemented with Roti[®]-Load 1 to yield an at least 1x concentrated Roti[®]-Load 1 suspension. The samples were stored at -20°C and were heated at 95°C for 5 min before usage. To shear the viscous DNA implemented in the samples, they were sonified using the SonoPuls Sonifier UW 2200 (Bandelin) for 20 s with 20% power before loading them on a gel.

b) Polyacrylamide Gel Electrophoresis (PAGE)

Protein extracts have been separated in a one-dimensional, discontinuous SDS-PAGE [105]. The stacking gel contained 4% PAA, the separation gel 8-15% PAA, depending on the size of the proteins to be analyzed. The PageRuler[™] Prestained Protein Ladder (Thermo Fisher) was included as a size standard in each electrophoresis. The PAGE was conducted in 1x SDS-PAGE running buffer at 160-200V for 45-90 min. To achieve maximal separation of the proteins the run was not stopped until the loading dye incorporated in the sample buffer started leaving the gel.

c) Transfer to Membrane (Western Blot)

To enable immunological detection of proteins with specific antibodies, the separated proteins are transferred to a membrane using the wet blot technique. All Western blots described in this work

MATERIAL & METHODS

have been performed using a nitrocellulose membrane with a pore size of 0.22 μm (Whatman plc). First, the blotting cassette was positioned in a basin with the side facing the cathode on the bottom. All items used for the blotting sandwich were soaked in freshly prepared CAPS transfer buffer and positioned carefully one onto another to avoid the inclusion of air bubbles. The order of assembly, starting from the cathode was as following:

- sponge
- two blotting papers
- gel
- membrane
- two blotting papers
- sponge

The transfer was carried out at 90V for 90 min using a cooling coil and a magnetic stirrer to avoid melting of the gel and retain a pH of 10.3.

d) Immunological Detection of Target Proteins

Before incubation with the primary antibody the membrane was covered with blocking buffer and gently moved for at least 1 h to reduce unspecific binding events. The composition of the blocking buffer was chosen according to the preferences of the antibodies to be used (milk powder or BSA in PBS-T or TBS-T). Afterwards, the blocking buffer was washed away and the membranes were incubated overnight with the primary antibodies (see Table 3 at page 41) at 4°C, gently shaking. The next day, 3 washing steps à 5 min with the solution used for antibody dilution were performed, followed by 1 h of incubation in the secondary, fluorescence-labeled antibodies (LI-COR, 1:15000) and a second washing procedure before protein bands were detected using the Odyssey® Fc Imaging System (LI-COR Biosciences).

3.2.4.7. Chromatin Immunoprecipitation (ChIP)

To assess whether TFs are binding to the *IFNK* enhancer in vivo, a ChIP assay was performed. This was done using the SimpleChIP® Enzymatic Chromatin IP Kit from Cell Signaling Technology as advised in the manual. Briefly, NHK were seeded on 150 mm dishes and cultured until reaching near-confluency (3-4 days). After 4 h of treatment with 20 ng/ml TGF- β 1, proteins were cross-linked to the chromatin using a final concentration of 1% formaldehyde. Nuclei were prepared and chromatin fragmented as described in the manual and immunoprecipitation was performed for 4 h at 4°C using

10 µg of chromatin each. Each experiment was performed including a positive (histone H3) and a negative (rabbit IgG) control. The antibodies used for the CHIP assays are listed in Table 3 on page 41. Analysis of the enriched chromatin fragments was done using qPCR as described in section 3.2.5.3 on page 73. The results were converted to percentage input.

3.2.4.8. Immunofluorescence

For immunofluorescence analyses 80,000 C33A cells/well were seeded on cover slides in 12 well plates and transfected with the fluorescent protein-tagged HR-HPV E5 and STING expression plasmids the next day. The day after, the cGAS-deficient C33A cells were transfected with 5 µg/ml cGAMP or vehicle control to activate the STING protein. Four hours after cGAMP transfection, cells were fixed by addition of 4% paraformaldehyde and incubation for 15 min at room temperature. Afterwards, cells were washed three times with PBS and incubated in DAPI solution for 20 s, followed by another three washing steps with PBS and one washing step with H₂O. Afterwards, cover slides were gently placed on one droplet of mounting medium on a microscope slide and fixed using nail polish. The prepared slides were analyzed at room temperature using the DeltaVision OMX SR Imaging System (GE Healthcare) equipped with the 60x/1.42 NA (Olympus) objective and processed using the AcquireSR-softWoRx reconstruction and analysis software. Retrieved images represent z-stacks of 5-17 sections (depending on the volume of the respective cell) à 250 nm, which were afterwards pseudo-colored using the ImageJ software (LOCI, University of Wisconsin-Madison).

3.2.5. RNA Methods

In the following chapter, the methods used for analysis on RNA level are outlined.

3.2.5.1. Isolation of Total RNA from Mammalian Cells

To assess the impact of certain signaling pathways or TFs on transcription, the total RNA content of cultured cells, which were treated in different ways, was isolated. To do so, the RNeasy® Mini Kit from Qiagen was utilized. As a first step, cells were harvested as described in section 3.2.3.6 on page 64. Afterwards the cell lysate was passed through QIAshredder® columns (2 min, 21130 g, room temperature) to homogenize the sample and remove insoluble cell debris. Afterwards RNA isolation was carried out as described in the manual of the kit. The total RNA was eluted in 50 µl of RNase-free water and concentration as well as purity was determined using the NanoDrop™ 2000 spectro-

photometer. Only RNA with a 260/280 ratio of 2.0-2.2 was used for cDNA synthesis. During the making of this work all RNA samples met this criterion.

3.2.5.2. Synthesis of complementary DNA (cDNA)

The isolated RNA was subsequently reverse-transcribed to cDNA using the QuantiTect® Reverse Transcription Kit from Qiagen according to the manufacturer's instructions. The prepared cDNA was diluted with RNase-free water to yield a concentration of 5 ng/μl.

3.2.5.3. Quantitative Real-Time PCR (qPCR)

To compare the transcription of *IFNK* and other genes of interest between a control sample and a sample treated with a certain compound, qPCR was applied. With this method the amount of cDNA, which reflects the amount of mRNA at the time point of harvesting the treated cells, is measured in real-time, thus after each elongation step of the PCR. With qPCR relative as well as absolute quantification (when including a standard curve) are feasible. To answer the questions emerging during the making of this work, the measurement of relative changes in gene transcription were sufficient. The experiments have been performed with the LightCycler® 480 Instrument from Roche and the corresponding software using the LightCycler® SYBR Green I Master (Roche), a ready-to-use master mix containing an optimized Taq polymerase and the fluorescent SYBR green dye. With this system, quantification is achieved by the detection of the fluorescent signal emitted by the sequence-independent incorporation of the SYBR green dye in the dsDNA. In the logarithmic phase of DNA amplification, the detected fluorescent signal increases proportionally to the amount of DNA. Hence, the original amount of the gene of interest can be extrapolated from the recorded data. The results of each run are displayed as CP (crossing point) values, which displays the PCR cycle in which the fluorescence in the respective well exceeds the background fluorescence for the first time. CP values were converted to fold induction relative to the respective control treatment by applying the mathematic formula shown below developed by Michael W. Pfaffl [103].

$$\frac{(\text{primer efficiency}_{\text{target gene}})^{\Delta\text{CP target gene (control treatment - actual sample)}}}{(\text{primer efficiency}_{\text{reference gene}})^{\Delta\text{CP reference gene (control treatment - actual sample)}}$$

Technical duplicates of all samples were prepared and analyzed separately; the average values of these replicates were processed as the result of the respective biological replicate. All experiments were performed at least three times, in the case of NHK using cDNA derived from different donors.

MATERIAL & METHODS

The primer efficiency of each primer pair was determined prior to usage by using a 1:10 dilution series of untreated NHK cDNA. Only primers displaying a single melting curve peak, illustrating the production of a single amplicon, were used for subsequent experiments. Melting curve analysis was included in each experiment to verify the amplification of a single gene product.

3.2.6. Statistical Analysis and Creation of Figures

After processing the results of different experiments as described in the respective section the calculated values of the single biological replicates were used to do statistical analysis and create graphical representations of the data. This was done using the GraphPad Prism software (GraphPad Software Inc., San Diego, US; software version 8.1.0).

4. Results

Due to the fact that parts of this work have been published, some passages of the text represent exact quotes from this publication [13]. These passages are highlighted by italicized format.

4.1. Regulation of the *IFNK* Gene

C. Habiger, a former member of the laboratory, identified a putative regulatory element in the *IFNK* locus by comparing different epigenetic marks between NHK and other cell lines [94]. She started assessing its involvement in *IFNK* expression by cloning the putative regulatory region up to the start codon of the *IFNK* gene into the promoterless pGL3 plasmid, which encodes a Firefly reporter gene, thereby generating a pGL3 *IFNK* Prom reporter plasmid. 5'-deletion analysis indicated that elements downstream of -4743 bp relative to the *IFNK* start codon are needed for gene expression [94]. As a first hint to TFs possibly involved in *IFNK* regulation, she showed that a simultaneous mutation of three putative TFBS for AP-2, EGR2 and KLF5 reduces reporter activity to 31% of the wildtype construct in NHK [94].

4.1.1. Contribution of three DNase I Hypersensitive Regions to Reporter Activity

The analysis of the *IFNK* locus using the ENCODE database of the UCSC genome browser revealed that there are three DNase I hypersensitive (HS) regions located in the putative regulatory element of the *IFNK* gene [94], which will be termed HS 1 to HS 3 in the following. To address their role, deletion mutants of HS 1-3 and the region located between HS 1 and HS 2 (HS 1: -4811/-4660, HS 2: -4251/-4100, HS 3: -4046/-3895, del -4661/-4250) in the context of the -5631 *IFNK* construct were analyzed in NHK, in the spontaneously immortalized human RTS3b keratinocyte cell line and in human keratinocytes which have been immortalized by stable transduction with an HPV16 E7 expression plasmid (HK 16E7). The results depicted in Figure 5 are shown as normalized values (Firefly/*Gaussia* activity) relative to the activity of the reporter construct containing all 5631 bp upstream of the *IFNK* start codon (-5631). The activity of this construct was set to 100%.

RESULTS

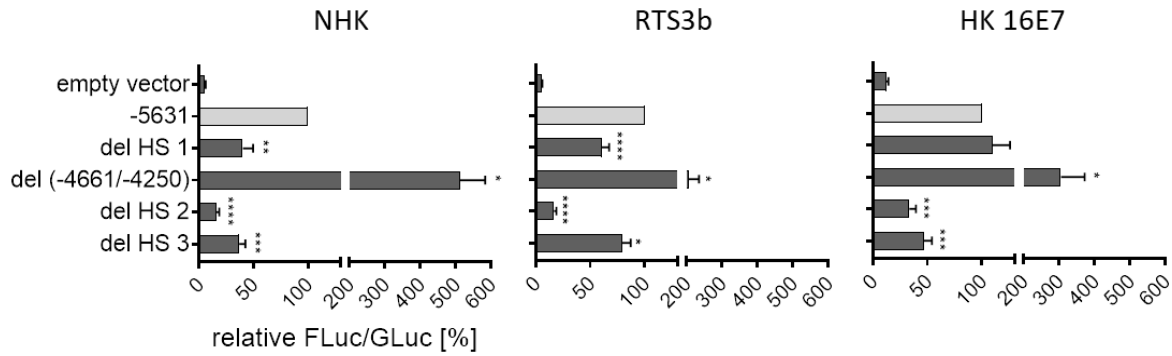


Figure 5: Deletion of DNase I HS regions from the putative regulatory element decreases reporter activity in NHK as well as in immortalized keratinocytes

Indicated cell types were transfected with different constructs listed on the left and luciferase activity was assayed 48 h post transfection. Luciferase activity is shown relative to the activity of the -5631 reporter construct (highlighted in light gray). Firefly luciferase (FLuc) activity was normalized to the expression of the co-transfected *Gussia luciferase* (GLuc) construct. Bars represent the average values and error bars the SEM. The average values for individual constructs are derived from $n \geq 4$ independent experiments. Significant deviations from the -5631 construct are denoted with asterisks (one-sample t-test: * < 0.05 , ** < 0.01 , *** < 0.001 , **** < 0.0001). del = deletion, HS = DNase I hypersensitive region. Italicized section and NHK diagram taken from the author's publication [13], slightly modified.

As shown in Figure 5, deletion of either HS region significantly decreased reporter activity in all analyzed cell types; with exception of the del HS 1 construct in HK 16E7. In contrast to this, deletion of the region between HS 1 and HS 2 enhanced reporter activity between 2-(RTS3b) and 5-fold (NHK) compared to the -5631 construct. The most prominent reduction was observed for deletion of the HS 2 region, which reaches from 16% to 17% remaining activity in NHK and RTS3b respectively to 33% reporter activity in HK 16E7. Deletion of HS 1 resulted in 40% activity in NHK, 60% in RTS3b and 110% activity in HK 16E7. Deletion of the third HS region led to a reduction to 37% reporter activity in NHK, 79% in RTS3b and 46% in HK 16E7. Overall, these findings indicate that all HS regions contribute to transcriptional activity.

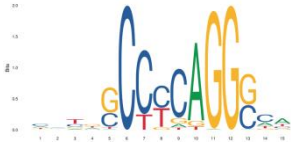



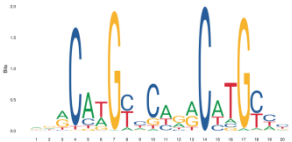
4.1.2. Identification and Analysis of putative Transcription Factor Binding Sites

As a next step the JASPAR CORE vertebrata database was used to identify putative TFBS (<http://jaspar.genereg.net>) in the HS regions (Table 14 on the next page).

RESULTS

Table 14: Candidate Transcription Factors derived from JASPAR Analysis

Matrix profiles are shown as position weight matrices, listing the accession number for the respective profile as well as the predicted binder. *Underlined nucleotides were mutated and analyzed by reporter or EMSA competition assays* (see Table 7 on page 48). Italicized sentence and table (modified) taken from the author's publication [13]

TF	Matrix profile JASPAR	Binding score	<i>IFNK</i> enhancer
AP-2	MA0524.1 – TFAP2C	11.9	GCCGCAGGGGA <u>GCCGCAGGGGA</u> (mt2_AP-2)
			
HOX	MA0485.1 – Hoxc9	15.8	AGCAATAAATCTT
			
AP-1	MA0099.1 – JUN::FOS	10.5	<u>CTGAATCA</u>
			
SMAD	MA0795.1 – SMAD3	15.7	<u>GTCTAGAC</u>
			
TP63	MA0525.1 – TP63	12.4	<u>ACATGTTCAGGCTTTCC</u>
		11.5	<u>TATGCACTGACATGCTA</u> (mt_TP63 #2)
			

Mutations introduced into these putative TFBS were used to assess the impact of the respective sequence stretches on reporter gene activity in different keratinocyte types (Figure 6 on the next page).

RESULTS

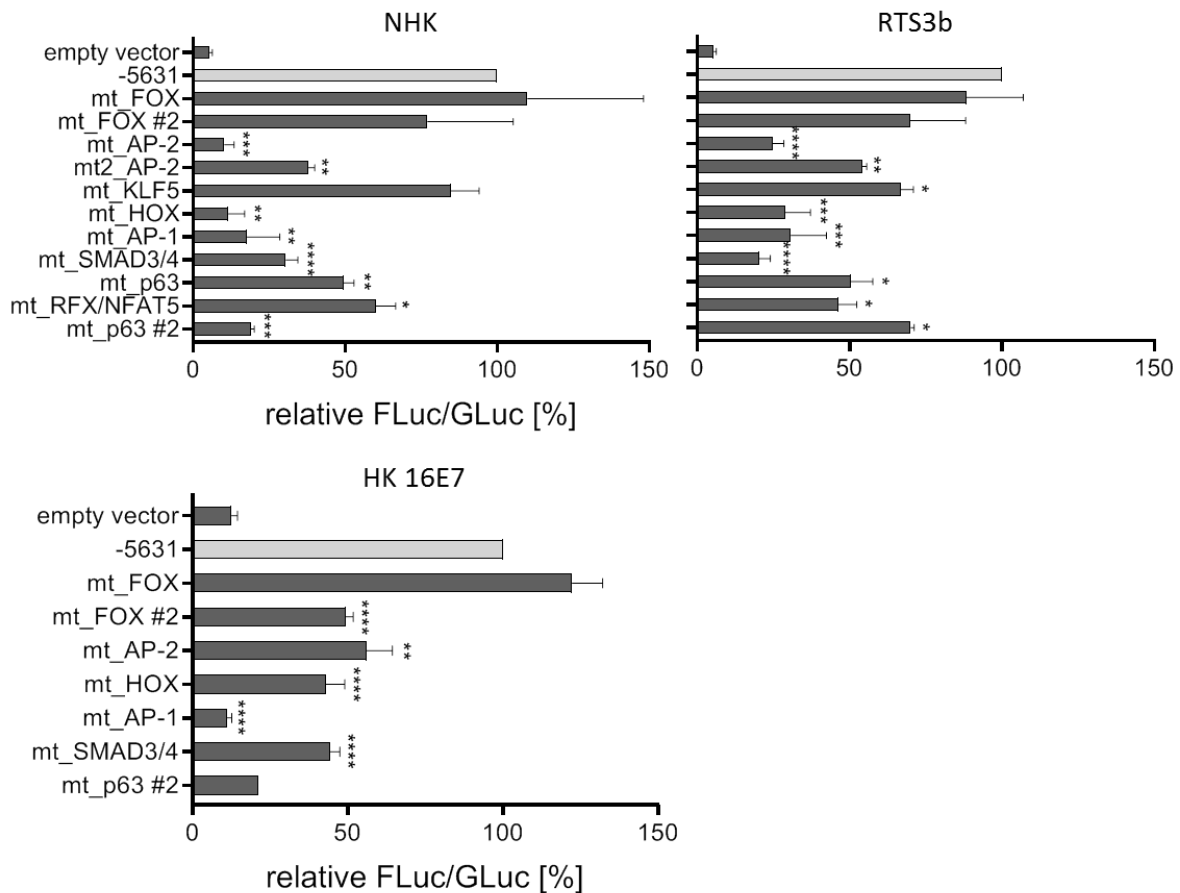


Figure 6: Mutation of several putative transcription factor binding motifs decreases *IFNK* promoter activity in keratinocytes

Indicated cell types were transfected with the constructs listed on the left and *luciferase activity* was assayed 48 h post transfection. *Luciferase activity* is shown relative to the activity of the -5631 reporter construct (highlighted in light gray). *Firefly luciferase (FLuc)* activity was normalized to the expression of the co-transfected *Gaussia luciferase (GLuc)* construct. Bars represent the average values and error bars the SEM. The average values for individual constructs are derived from $n \geq 3$ independent experiments (except for mt_p63 #2 in HK 16E7, which depicts a single measurement). Significant deviations from the -5631 construct are denoted with asterisks (one-sample t-test: * < 0.05, ** < 0.01, *** < 0.001, **** < 0.0001). mt = mutation. *Italicized section taken from the author's publication [13], slightly modified.*

In HS 1, four putative TFBS were identified. Mutation of two BS, which are predicted to be bound by TFs of the forkhead box protein family (FOX, position: -4794 to -4784 and -4752 to -4741 (#2)), did not result in significant reduction of reporter activity in either NHK or RTS3b (Figure 6). In HK 16E7, mutation of the second FOX BS (mt_FOX #2) resulted in 2-fold reduction of reporter activity (Figure 6). At position -4696 to -4681, a putative BS for family members of the transcription factor AP-2 was identified. Two different mutations were created, the first mutation (mt_AP-2) reduced reporter activity to only 10% compared to the -5631 construct in NHK, to 25% in RTS3b and to 56% in HK 16E7 (Figure 6). The second AP-2 BS (mt2_AP-2) mutation had a lower impact on reporter activity resulting in 38% activity in NHK and 54% in RTS3b and was not tested in HK 16E7. The fourth identified

RESULTS

putative TFBS in HS 1 is predicted to be bound by Krueppel-like factor 5 (KLF5). This BS partially overlaps with the AP-2 BS (position: -4689 to 4681) and is not affected in the mt2_AP-2 construct. Mutation of the putative KLF5 BS resulted in a non-significant reduction of only 15% in NHK and to a reduction of 33% in RTS3b (Figure 6). It was not evaluated in HK 16E7. In the second HS region, putative BS for TFs of the homeobox proteins (HOX, position -4204 to -4194), for TFs of the activator protein 1 (AP-1, position -4165 to -4158) family and an inverted tandem repeat BS for TFs of the SMAD family (position to 4149 to -4139) have been identified. Mutation of the putative HOX BS resulted in decrease of reporter activity to 12% or 29% in NHK and RTS3b, respectively, and to 43% in HK 16E7 (Figure 6). The mutant AP-1 construct led to a drop in reporter activity to 18% in NHK, 31% in RTS3b and 11% in HK 16E7 (Figure 6). Alteration of the adjacent, putative SMAD3/4 BS diminishes reporter activity to 30% in NHK, to 20% in RTS3b and to 44% in HK 16E7 (Figure 6). In the last HS region, HS 3, two putative BS for TFs of the p53 family (including p53, p63 and p73, termed p63 BS hereafter) were identified (position -4015 to -3996 and -3941 to -3922 (#2)). Between these two putative BS, a sequence motif which might be bound by TFs of the regulatory factor X (RFX) family or nuclear factor of activated T cells 5 (NFAT5) was discovered (position -3961 to -3942). Whereas changing the upstream located putative p63 BS results in 2-fold reduction of reporter activity in NHK and RTS3b, it was not tested in HK 16E7. Mutation of the second p63 BS diminished reporter activity to 19% in NHK, to 70% in RTS3b and to 21% in a single experiment in HK 16E7. The RFX/NFAT5 BS mutation led to 60% reporter activity in NHK and 46% in RTS3b (Figure 6). On the whole, the findings for the p53- deficient RTS3b cell line are in accordance with the findings for the primary keratinocytes. The only remarkable exceptions to this are the results for the second p63 binding site (mt_p63 #2), suggesting that p53 might bind to this BS and thereby activate the gene. However, later findings argue against a major contribution of p53 to *IFNK* activation (see section 4.1.9). In contrast to the HPV-negative RTS3b cell line, the HPV16 E7-immortalized keratinocytes show much more deviations from NHK in the reporter assays. This might be due to E7 as it interacts with a plethora of cellular proteins [79], among others with the SMAD proteins [106]. Nonetheless, they show the same trends for the most promising candidate TFs. On top, some of the mutational analyses were further supported by examining deletion mutants which exclude putative TFBS from the reporter construct. It could be shown, that deletion of the putative HOX BS leads to a significant reduction of reporter activity to 21% in NHK ($p < 0.0001$) but only to around 60% in RTS3b ($p < 0.001$) and HK 16E7 (not significant). Deletion of the proportions which contain either the AP-1 (11% in NHK, \approx 20% in others) or SMAD BS (approximately 40% in NHK and HK 16E7, 24% in RTS3b) led to significant reduction in all cell types. A deletion downstream of the analyzed putative TFBS in HS 2 resulted in significant decrease to 42% only in NHK (appendix: Figure 27 on page CXIX). To sum it up, the luciferase assays described so far suggested that *IFNK* expression depends on putative BS for AP-2 TFs in HS 1, HOX,

AP-1 and SMAD TFs in HS 2 and p53/p63 TFs in HS 3. Hence, as a next step, the sequence-specific binding of proteins derived from keratinocytes should be demonstrated.

4.1.3. Analysis of Protein Binding to Identified Binding Sites

To support the involvement of the HOX, AP-1, SMAD and p53/p63 TFs in *IFNK* regulation, nuclear extracts from NHK, RTS3b and HK 16E7 were prepared and used to perform EMSA experiments with labeled oligonucleotides containing the selected putative TFBS (Figure 7 on the next page). Despite repeated attempts, no sequence-specific binding to the putative HOX BS was observed. This was not caused by inferior quality of the nuclear extracts as judged by the appearance of bands (appendix: Figure 28A on page CXX) and sequence-specific binding of the used extracts to other BS. Varying the amount of competitor DNA for sequence-independent interactions did also not alter the resulting band pattern (appendix: Figure 28B on page CXX), indicating that the putative HOX BS might be a DNA stretch bound by proteins other than classical, sequence-specific TFs. However, for the putative AP-1 BS, two sequence-specific DNA-protein complexes could be observed for nuclear extracts derived from the three different keratinocyte types (Figure 7, arrowheads). The same seem to apply to the putative SMAD BS, even though, the faster migrating complex, which is visible in RTS3b and HK 16E7 cells, is not apparent in NHK (Figure 7). The uppermost signal in NHK is caused by labeled DNA stuck in the slots of the gel. The higher position of the putative SMAD band in the NHK gel compared to the position in RTS3b and HK 16E7 gels is caused by the higher percentage of the gel used for the NHK experiment (5% vs. 3% for the others). Repetition of the experiment and resolution in a 3% gel revealed the same relative position of the observed signal as seen for the immortalized keratinocytes (data not shown).

RESULTS

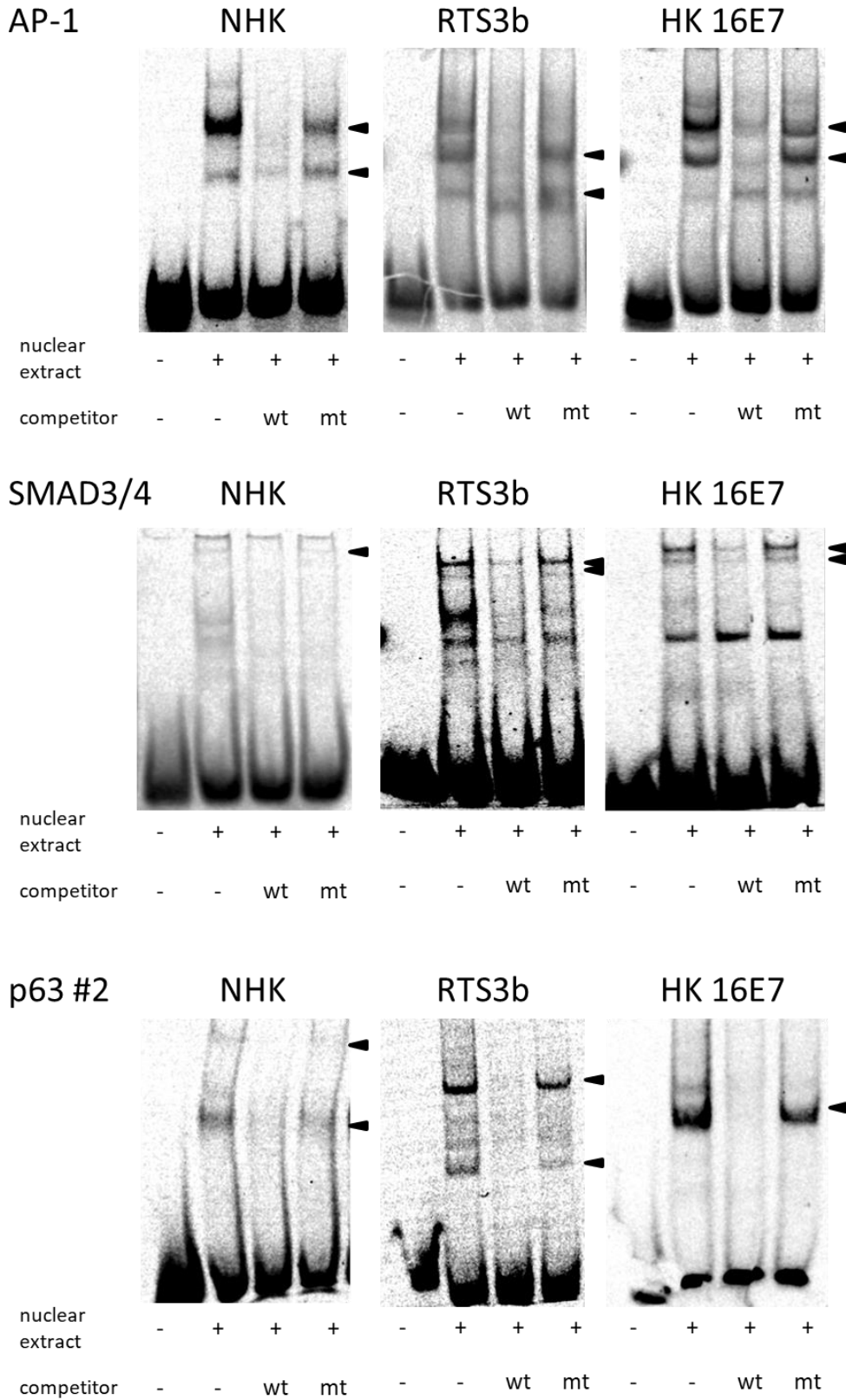


Figure 7: Proteins present in nuclear extracts from keratinocytes bind specifically to the putative binding sites for AP-1, SMAD and p63.

Legend on the next page

RESULTS

Figure 7: Proteins present in nuclear extracts from keratinocytes bind specifically to the putative binding sites for AP-1, SMAD and p63.

EMSA were performed with nuclear extract from cell types listed above the gels and DY681-labeled oligonucleotides displaying putative BS for the TFs listed on the left. *Unlabeled competitors were added in 100-fold excess. Specific shifts that were only competed by excess wildtype (wt) and not by mutant (mt) oligonucleotide are indicated by arrowheads.* NHK experiments were performed three times using extracts derived from three different donors. Italicized section and p63 #2 assay in NHK are taken from the author's publication [13], slightly modified.

In NHK and RTS3b, two different sequence-specific protein complexes binding to the second putative p63 BS were observed. In HK 16E7, only one sequence-specific complex was detected (Figure 7). Taken together, the data presented so far suggests that the loss of transcriptional activity observed in the reporter assays is due to the loss of binding of nuclear proteins to the putative AP-1, SMAD3/4 and the p63 BS in the *IFNK* enhancer. Experiments performed by C. Habiger also indicated that the AP-2 BS is specifically bound by AP-2 α and AP-2 γ [13].

4.1.4. Effect of Different Signaling Pathways on Endogenous *IFNK* RNA Expression

Some of the candidate TF, which were identified by the experiments outlined above, can be regulated by signal transduction pathways. To analyze the regulation of the endogenous *IFNK* gene, cultured keratinocytes were treated with substances that interfere with these signaling pathways. As the RTS3b cell line has been found to express *IFNK* only after treatment with DNA methyltransferase inhibitors (Frank Stubenrauch, unpublished data) the experiments were performed only in NHK and in HK 16E7 cells. Comparing the CP values for *IFNK* transcription in the control samples of all NHK and HK 16E7 experiments and normalizing them to the expression of the house keeping gene *PGK1* revealed that the E7-immortalized human keratinocytes express the same levels of endogenous *IFNK* as NHK do (Figure 8).

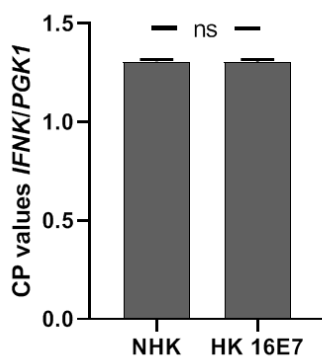


Figure 8: *IFNK* expression in HK 16E7 cells is not different from expression in NHK

Average CP values for *IFNK* expression obtained during qPCR analysis of both NHK (n=22, from 14 different donors) and HK 16E7 (n=20), which were not treated at all or only treated with the vehicle control, have been normalized to *PGK1* expression of the respective well and analyzed for differences using an unpaired, two-tailed t-test.

4.1.5. Effects of MAPK and TGF- β Signaling on *IFN κ* RNA Expression in NHK

Members of the AP-1 family and SMAD3/4 can be regulated by signal transduction pathways. The AP-1 TF is a dimeric complex composed of members from different protein families (JUN, FOS, ATF, MAF) whose activities can be regulated by different branches of the mitogen-activated protein kinase (MAPK) signaling network [107]. To address, whether MAPK signaling is involved in *IFN κ* expression in NHK, cells were treated with different compounds interfering with this signaling pathway and transcript levels were determined. The addition of 40 μ M T-5224, a small molecule inhibitor of FOS/JUN DNA-binding activity [108] for 24 h reduced *IFN κ* transcription to 34% in NHK (Figure 9A, page 85), suggesting that FOS and/or JUN family members are involved in *IFN κ* activation (italicized sections taken from the author's publication [13]).

The JUN family members Jun, jun-B and jun-D can be phosphorylated by Jun N-terminal kinases (JNK), which enhances their transactivation ability [109]. The JNK signaling pathway is activated among others by pro-inflammatory cytokines, TLR activation and with this, sensing of infection [109], making it an interesting candidate for *IFN κ* activation. Furthermore, JNKs can be activated by UV irradiation [109], as it has also been reported for *IFN κ* [36]. However, the addition of 4 μ M JNK-IN-8, an inhibitor of JNK1, 2 and 3 (thus labeled JNKi hereafter), did not alter *IFN κ* expression in NHK (Figure 9A). As JNK activity is implemented in the induction of TGF- β target genes in keratinocytes [110-112], the expression of the TGF- β target gene *SERPINE1* [113] was evaluated in parallel. Indeed, JNKi significantly reduced *SERPINE1* expression (2.8-fold, Figure 9C), showing the compound has been used at an effective concentration (italicized sections taken from the author's publication [13]).

A second branch of the MAPK signaling network comprises the pathway downstream of extracellular signal-regulated kinase (ERK) 1 and 2. ERK1/2 induce TFs which regulates the expression of many targets, among others the FOS TF [107]. Additionally, ERK1/2 phosphorylate different AP-1 members and thereby modulate their transactivation [114]. The ERK1/2 pathway can be stimulated by tetradecanoylphorbol-acetate (TPA) and ERK1/2 activity can be blocked by inhibitors such as SCH 772984 (labeled throughout the text as ERKi). The addition of 50 ng/ml TPA to NHK did not alter FOS consistently, but significantly decreased JUN expression 2.6-fold (data not shown). Importantly, TPA treatment reduced *IFN κ* expression 2-fold. Treatment with 1 μ M ERKi reduced FOS expression 7.7-fold in NHK (Figure 9D) and increased *IFN κ* expression 4.7-fold (Figure 9A). These findings are consistent with the observation that the inhibition of the tyrosine kinase activity of EGFR or of MEK activity leads to an increase of *IFN- κ* expression and ISG expression in NHK [29, 30], since ERK1/2 are activated by EGFR via MEK [115, 116]. The data generated for the MAPK signaling pathway indicates

RESULTS

that *IFNK* is negatively regulated by ERK1/2 and suggests that the putative AP-1 BS is not activated by TPA, ERK1/2 or JNK (italicized sections taken from the author's publication [13], slightly modified).

SMAD3 and 4 are crucial components of the TGF- β signaling network. Binding of TGF- β to the TGF- β receptor 1 (TGFBR1) and TGFBR2 induces TGFBR1 kinase activity which then phosphorylates SMAD2 and 3. Phospho-SMAD2 and 3 form complexes with SMAD4, which then enter the nucleus and bind to SMAD3/4 BS to regulate transcription [117]. To analyze whether the TGF- β pathway is involved in endogenous *IFNK* expression, NHK were treated with 20 ng/ml TGF- β 1 or 10 μ M of the TGFBR1 kinase inhibitor SB-431542 ([118]; labeled throughout the text as TGFBR1i). These treatments induced or repressed *SERPINE1*, an established TGF- β target gene [113] 10- and 4.6-fold, respectively (Figure 9C). *This indicates that the TGF- β pathway is constitutively activated in cultured NHK and can be further stimulated by adding exogenous TGF- β 1.* *IFNK* expression was induced 3.5-fold in NHK by TGF- β 1 and 3.6-fold repressed by TGFBR1i (Figure 9B); strongly suggesting that *IFNK* is a TGF- β target gene in keratinocytes. In addition, the ISG *IFIT1* was activated 3-fold by TGF- β and inhibited 1.9-fold by TGFBR1i (Figure 9D). *Sp100*, another ISG, known to be induced by IFN- κ [32], is weakly but significantly repressed upon inhibition and increased upon stimulation of the TGF- β pathway (Figure 9E). *This suggested that TGF- β -induced IFN- κ is biologically active.* To test, whether *IFNK* expression could be further enhanced, TGF- β and ERKi were applied together. As can be seen in Figure 9C and D, this combinatorial treatment still led to the induction or repression of the target genes of the respective compounds. Moreover, while the combination of TGF- β 1 and ERKi only weakly increased *SERPINE1* expression compared with TGF- β treatment alone and did not further decrease expression of the ERK target gene *FOS*, the observed effect on *IFNK* transcription was tremendous: *IFNK* RNA was induced 24.8-fold, conjointly with a 27.8-fold induction of *IFIT1* and 2.6-fold induction of *Sp100* (Figure 9D, E), suggesting that these ISGs are induced by IFN- κ . In contrast to this, *IFI16*, another ISG, was not induced by any of the treatments (data not shown; italicized sections taken from the author's publication [13]).

RESULTS

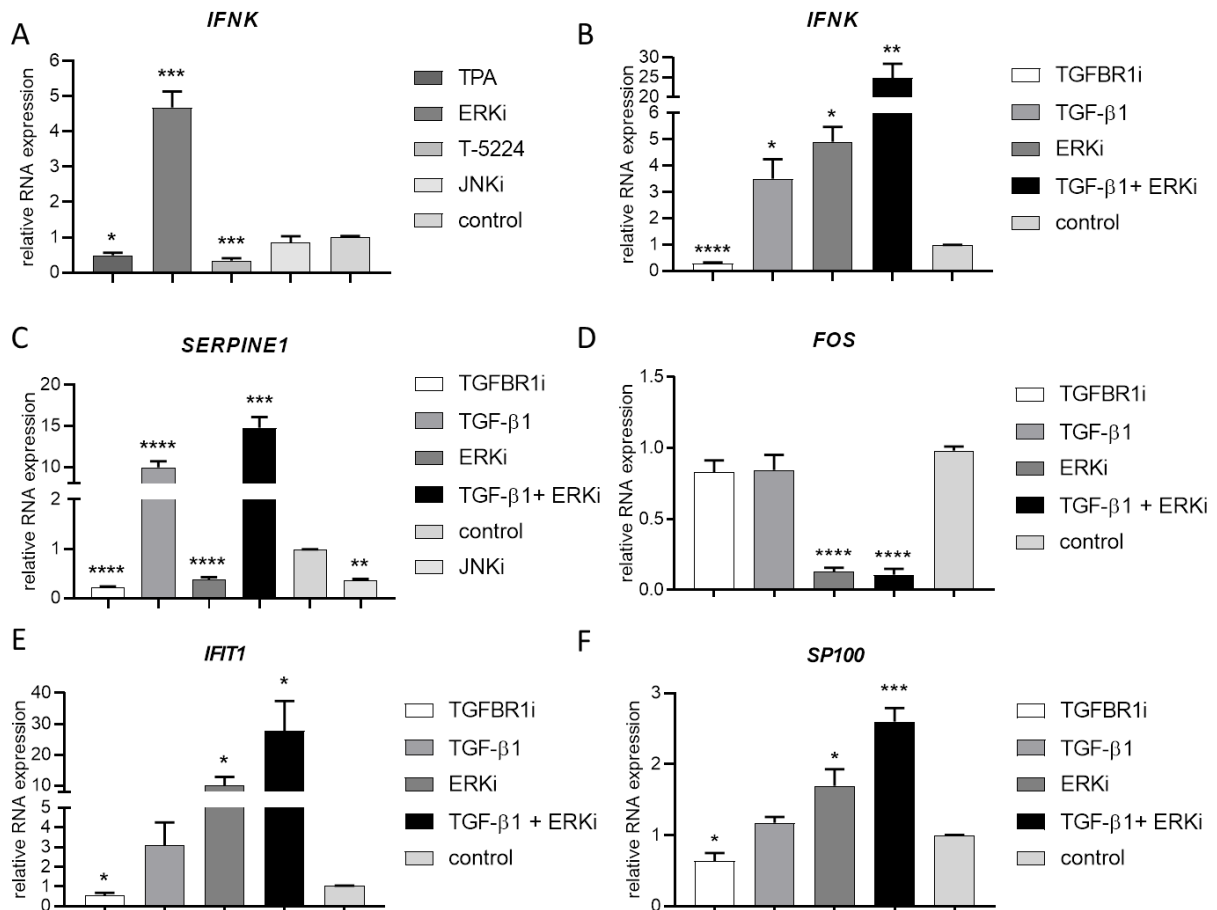


Figure 9: Analysis of NHK transcription reveals that endogenous *IFNK* is regulated by TGF- β 1 and ERK1/2 pathways

NHK were treated for 24 h with the indicated substances and transcripts of genes listed above the diagrams were quantified by qPCR using PGK1 as a reference gene and are given relative to the vehicle control. Error bars indicate the SEM. The average values in A were calculated from $n=3$ (TPA), $n=8$ (ERKi), $n=4$ (T-5224), $n=3$ (JNKi) and in B-F from $n=6$ independent experiments. Significant deviations from the vehicle control are highlighted with asterisks (paired *t*-test: * < 0.05 , ** < 0.01 , *** < 0.001 , **** < 0.0001). Italicized section and diagrams A, B, C (modified) and E are taken from the author's publication [13].

4.1.6. Effects of MAPK and TGF- β Signaling on *IFNK* RNA Expression in HK 16E7

In HK 16E7 the treatments interfering with the MAPK signaling pathway did not result in significant changes in *IFNK* expression, except for the treatment with the ERKi, which led to a 3-fold induction 24 h after treatment (Figure 10A), thus confirming the findings in NHK. However, in contrast to NHK, in which stimulation with TPA results in significant reduction in both *JUN* and *IFNK* transcription, *IFNK* transcription was induced 1.9-fold in HK 16E7 (Figure 10A on page 87).

RESULTS

Interestingly, *JUN* expression was increased 3.9-fold upon TPA treatment in these cells (data not shown), suggesting some involvement of Jun in the differences observed between HK 16E7 and NHK. Addition of TGF- β 1 induced (14.3-fold) and treatment with TGFBR1i decreased *SERPINE1* expression (2.7-fold, Figure 10C), suggesting that the TGF- β pathway can also be manipulated in HPV16 E7-containing keratinocytes. In contrast to its effect in NHK, in HK 16E7, the ERKi did not repress *SERPINE1* expression (Figure 10C). In accordance with this, the HPV16 E7 protein has been demonstrated to influence TGF- β 1-mediated gene regulation in NHK and immortalized HPV-negative keratinocyte cell lines [106, 119-121]. Stimulation or inhibition of the TGF- β pathway translated into a 2.6-fold induction or 5.6-repression of the *IFNK* gene in HK 16E7, respectively (Figure 10B). Combinatorial treatment with both, TGF- β 1 and ERKi, increased *IFNK* transcription 7.6-fold, but did not reach statistical significance and is more than three times less pronounced than in NHK (compare Figure 10B to Figure 9B). Except for the inhibition of TGF- β signaling, which decreases *IFIT1* 5.3-fold, none of the other treatments cause a significant change in *IFIT1* RNA levels in HK 16E7 (Figure 10D). *SP100* expression is reduced nearly 2-fold (to 54%) upon TGFBR1i treatment and not changed remarkably upon all other treatments (Figure 10E). As less than 30% reduction of *IFI16* expression was observed for TGFBR1i-treated samples (data not shown) and this compound had the most prominent effect on the other analyzed ISGs, *IFI16* expression was not further investigated. The more pronounced effect upon inhibiting TGF- β signaling in comparison to the effect upon stimulation suggests that the pathway is already activated and cannot be further stimulated. Even though, the HPV16 E7-immortalized cell line might be suboptimal to analyze MAPK and TGF- β signaling, the experiments still support the notion that the ERK1/2 axis negatively regulates *IFNK* expression, whereas TGF- β 1 activates expression of the *IFNK* gene.

RESULTS

HK 16E7

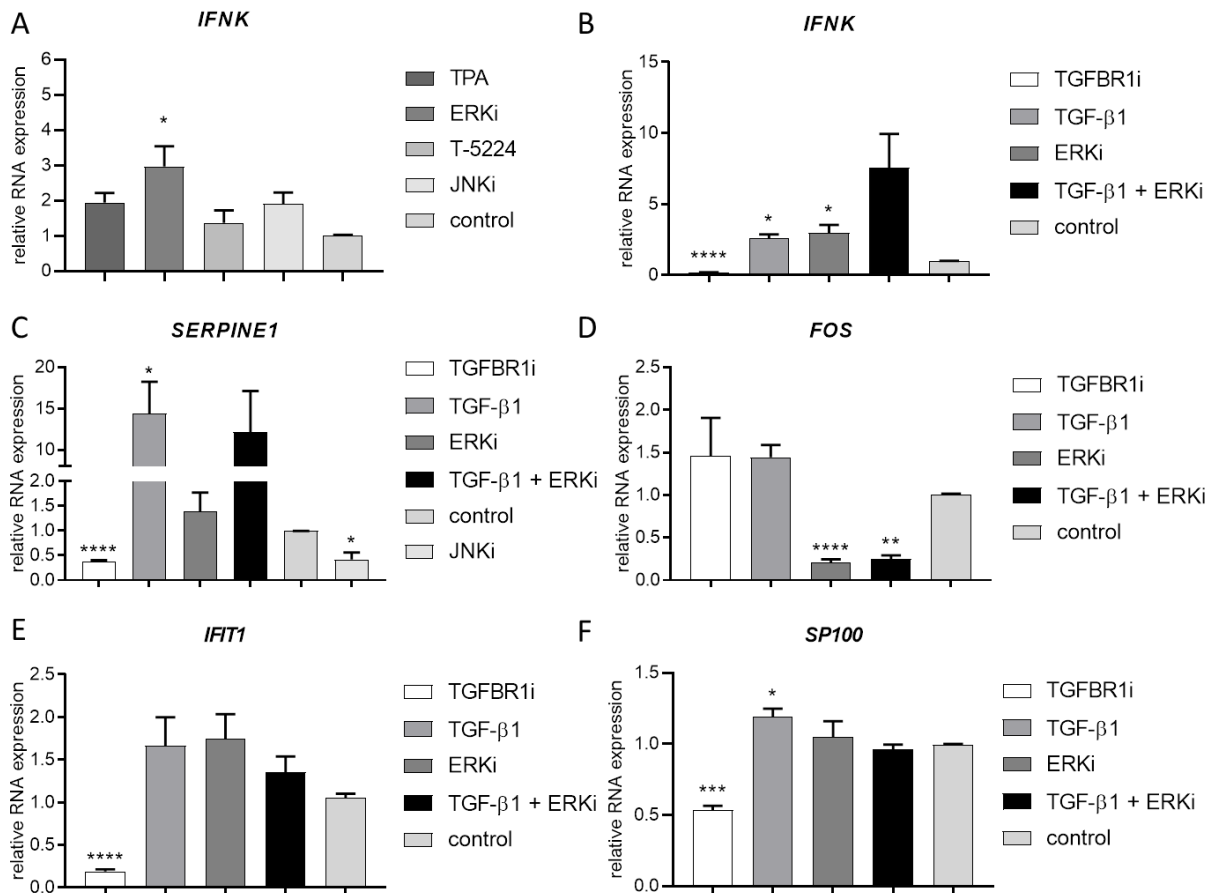


Figure 10: Influence of MAPK signaling on transcription in HK 16E7 differs from effects seen in NHK

HK 16E7 were treated for 24 h with the indicated substances and transcripts of genes listed above the diagrams were quantified by qPCR using *PGK1* as a reference gene and are given relative to the vehicle control. Error bars indicate the SEM. The average values in A were calculated from n=3 or n=5 (ERKi) independent experiments. In B-F average values of n=4 (TGF-β, TGFBRI), n=5 (ERKi) or n=3 (TGF-β + ERKi) independent experiments are depicted. Significant deviations from the vehicle control are highlighted with asterisks (paired t-test: * < 0.05, ** < 0.01, *** < 0.001, **** < 0.0001).

4.1.7. Analysis of IFN-κ on Protein Level

After having determined the influence of the ERK1/2 and TGF-β pathway on *IFNκ* transcription, the effect of these signaling axes on *IFNκ* protein level was evaluated. *IFNκ* is secreted and sequestered at the cell surface [122]. This sequestration is probably mediated by interaction with heparin sulfate glycosaminoglycans of the extracellular matrix, as already shown for other cytokines [123, 124]. Thus, intracellular and cell-bound levels of *IFNκ* protein were determined by Western blot using whole cell extracts obtained by RIPA lysis.

4.1.7.1. Analysis of IFN- κ , phospho-STAT1 and IFIT1 Expression in NHK

After 24 h of treatment with the different compounds, which have been found to enhance *IFNK* RNA levels, protein extracts were prepared from NHK and subjected to Western blot analysis. With this, transcriptional changes for *IFNK* (Figure 9B) could be confirmed at protein level (Figure 11). Moreover, an increase in STAT1 phosphorylation was observed in the samples displaying increased IFN- κ protein expression (Figure 11), strongly suggesting induction of IFNAR1/2 signaling. As already observed on transcript level (Figure 9D), the level of IFIT1 protein expression varies in accordance with the amount of IFN- κ protein (Figure 11), supporting the theory that this ISG is induced by IFN- κ .

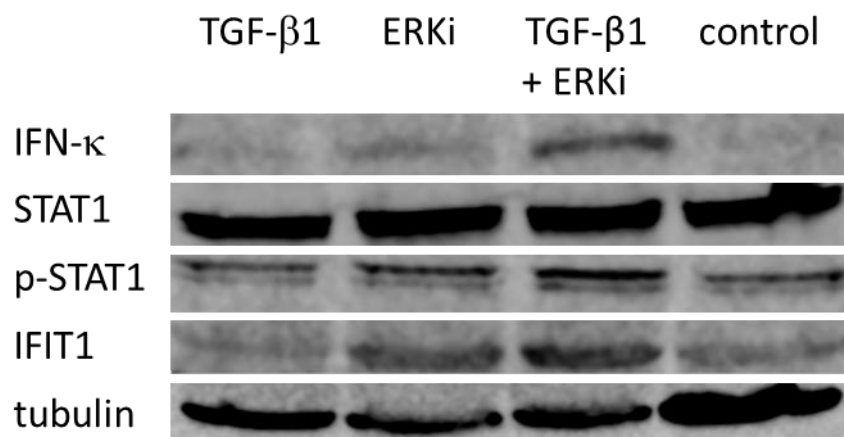


Figure 11: Stimulation of the TGF- β - and inhibition of the ERK1/2 pathway induces IFN- κ expression and is accompanied by increased phosphorylation of STAT1 and induction of the antiviral IFIT1 protein

Western blot analysis of NHK extracts treated for 24 h with the indicated substances using antibodies against IFN- κ , STAT1, phospho-Y701-STAT1, IFIT1, and tubulin as a loading control. The blot shown is representative of two independent experiments using extracts derived from different NHK donors. Italicized section and WB taken from the author's publication [13].

4.1.8. Regulation of putatively involved AP-1 Transcription Factors

The loss of activity of the mt_{AP-1} reporter construct and the treatment with T-5224 strongly suggested an involvement of JUN and/or FOS family members in IFNK gene activation. Published evidence indicates that AP-1 BS can mediate TGF- β responsiveness of promoters [125-128]. To test this, NHK were transfected with the -5631, the del HS 2, which lacks both the AP-1 and SMAD3/4 BS, the mt_{AP-1} or the mt_{SMAD3/4} reporter constructs (Figure 12). The addition of TGF- β 1 only

RESULTS

stimulated the -5631 construct 6.6-fold, but not the *mt_AP1*, *mt_SMAD3/4* or *del HS 2* constructs (Figure 12A). Consistent with this, addition of *TGFBR1i* only reduced the activity of -5631 construct 2.7-fold, but not of the mutant reporter constructs (Figure 12B). These data indicate that the AP-1 BS in the IFNK enhancer is also required for TGF- β responsiveness (italicized sections taken from the author's publication [13], slightly modified).

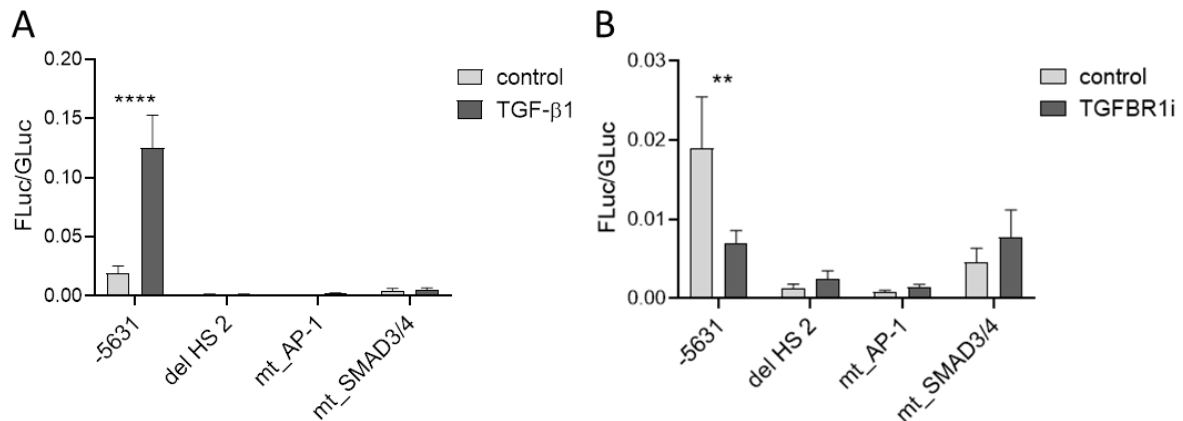


Figure 12: Manipulating the TGF- β pathway in NHK transfected with IFNK reporter constructs reveals that the AP-1 and SMAD binding sites constitute a TGF- β responsive element

NHK were transfected with the indicated reporter plasmids, TGF- β 1 (A) or TGFBR1i (B) were added 24 h later and luciferase activities were determined 24 h after treatment. Bars represent the average of $n=4$ independent experiments and error bars represent the SEM. Asterisks denote statistically significant differences from the vehicle control (multiple t-tests, corrected for multiple comparisons using the Holm-Sidak method: ** <0.01 , **** <0.0001). Italicized section and diagrams (modified) are taken from the author's publication [13].

To identify cis-elements required for activation by the ERKi, NHK were transfected with the -5631, del HS 1, del (-4661/-4250), del HS 2, del HS 3, and -3540 constructs and incubated with ERKi or the vehicle control for 24 h. This revealed that the -5631 construct was activated 3.1-fold, which is comparable to the endogenous gene (compare Figure 13 on the next page with Figure 9A). Similar activation levels were observed for the deletion constructs. The -3540 construct displayed only an activation of 1.7-fold but this was not significantly different from the activation of the -5631 construct (Figure 13). Taken together, this indicates that the ERKi does not target specific TFBS in the enhancer, but rather acts both on the enhancer and promoter of the IFNK gene (italicized sections taken from the author's publication [13], slightly modified).

RESULTS

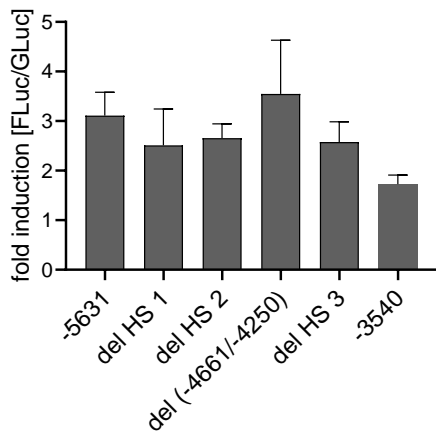


Figure 13: Inhibition of ERK1/2 in NHK transfected with different *IFNK* reporter constructs

NHK were transfected with the indicated reporter plasmids, ERKi was added 24 h later and luciferase activities were determined 24 h after treatment. Bars display fold induction relative to the vehicle control and represent the average of $n=3$ independent experiments + SEM. No significant deviations from the -5631 construct were observed (paired t -test). Italicized section and diagram (modified) taken from the author's publication [13].

4.1.9. Identification of Transcription Factors involved in *IFNK* Gene Activation

To identify the TFs responsible for *IFNK* expression, RNA interference was used. First, the involvement of AP-2 proteins should be assessed. The family of AP-2 TFs is made up of five different proteins, designated AP-2 alpha to epsilon in humans. According to the ARCHS4 RNA-seq database, *TFAP2A*, -C and -E are expressed in human keratinocytes (listed in descending order regarding their expression levels, [129]). *The levels of TFAP2A and -C could be efficiently reduced by siRNA, but IFNK expression was weakly induced by siTFAP2A and not significantly altered by siTFAP2C, respectively* (Figure 14A-C on page 92). Since the EMSA experiments of C. Habiger suggested that the AP-2 BS can interact with both AP-2 α and -2 γ , a combination of siTFAP2A and -C was tested but this also resulted only in a slight reduction to 79% of *IFNK* mRNA levels, which was not significant. Even though it is only very modestly expressed ([129], own observations), the effect of knocking down the third AP-2 candidate was also analyzed. However, *TFAP2E* alone or all three AP-2 proteins together, also had no influence on *IFNK* mRNA levels (Figure 14A). Thus, literature was consolidated again, revealing an interesting feature: *EGFR expression decreases upon TFAP2C knockdown in breast cancer cells [130, 131]. Indeed, knockdown of TFAP2A and -C separately or together significantly diminished EGFR mRNA expression* (Figure 14D on page 92). Since *the EGFR-MEK-ERK1/2 pathway inhibits IFN- κ expression, a possible explanation for the weak effects of the AP-2 α or AP-2 γ knockdown on IFNK expression is that this knockdown diminishes both activators and inhibitors of IFNK expression* (italicized sections taken from the author's publication [13]).

RESULTS

Knockdown efficiencies for the AP-1 family members FOS, FOSB, FOSL1, FOSL2, JUN, JUNB and JUND were between 8 and 45% (Figure 14B, C). Of those, only the knockdown of JUNB significantly reduced IFNK expression to 44%, whereas knockdown of FOSB induced IFNK expression 2.5-fold (Figure 14A). Here, it was interesting to see, that even though the knockdown efficiency of FOSB was rather low, a clear effect on IFNK transcription could be seen (Figure 14A-C). Moreover, in contrast to what might have been expected from TPA treatments, which concomitantly reduced JUN and IFNK transcription after 24 h (Figure 9), knockdown of JUN did not result in a change of IFNK expression after 48 h. Reduction of JUN transcript levels have been similar in both experiments (3.1-fold upon knockdown and 2.6-fold upon TPA treatment), arguing against a simple dosage effect. The knockdown experiment supports the notion that Jun is not directly involved in IFNK expression and the reduced gene activity upon TPA treatment is probably mediated via ERK1/2-induction of other regulators of transcription (italicized sections taken from the author's publication [13]).

To evaluate the impact of the SMAD proteins on *IFNK* expression, *SMAD4* expression was targeted. *SMAD4* is the co-SMAD, which assembles with TGF- β 1-activated SMAD2 and 3 proteins [117], and therefore should mirror effects of SMAD2, -3 and/or -4 knockdown. Indeed, *SMAD4* knockdown reduced *IFNK* mRNA expression to 53% (Figure 14A).

The last BS identified by reporter assays was predicted to be bound by p53 family members. P53 and p63 recognize similar consensus sequences and are both expressed at high levels in keratinocytes [129]. P63 is known to be involved in keratinocyte biology [132], but the reduced effect of the mt_p63 #2 construct on gene expression in the p53-deficient RTS3b cell line, suggested that p53 might also be involved in gene activation. Thus, knockdown of both *TP53* and *TP63* was tested, using siRNAs which target all existing isoforms. Despite similar knockdown efficiencies, a major effect on *IFNK* expression was only observed upon *TP63* knockdown (reduction to 47%), whereas the knockdown of *TP53* had only very minor effects (reduction to 76%; Figure 14A-C), suggesting that p63 plays a greater role in mediating *IFNK* expression in NHK.

RESULTS

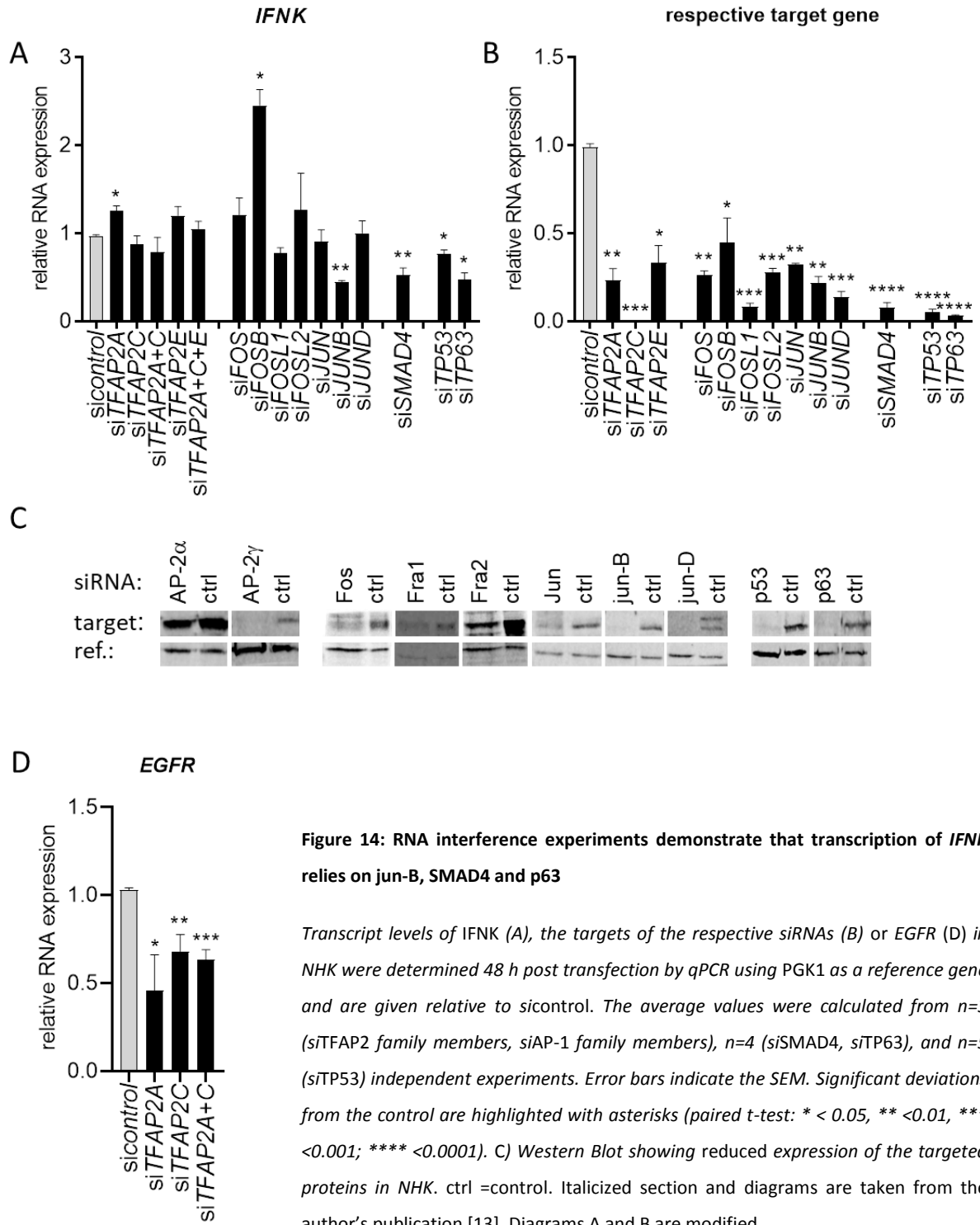


Figure 14: RNA interference experiments demonstrate that transcription of *IFNK* relies on jun-B, SMAD4 and p63

Transcript levels of *IFNK* (A), the targets of the respective siRNAs (B) or *EGFR* (D) in NHK were determined 48 h post transfection by qPCR using PGK1 as a reference gene and are given relative to sicontrol. The average values were calculated from n=3 (siTFAP2 family members, siAP-1 family members), n=4 (siSMAD4, siTP63), and n=5 (siTP53) independent experiments. Error bars indicate the SEM. Significant deviations from the control are highlighted with asterisks (paired t-test: * < 0.05, ** < 0.01, *** < 0.001; **** < 0.0001). C) Western Blot showing reduced expression of the targeted proteins in NHK. ctrl = control. Italicized section and diagrams are taken from the author's publication [13]. Diagrams A and B are modified.

In summary, the RNA interference data showed that *IFNK* transcription is induced 2.5-fold when *FosB* expression is decreased and reduced 2-fold upon knockdown of jun-B, SMAD4 or p63 TFs (Figure 14). These findings suggest that the *IFNK* gene is repressed by FosB and activated by jun-B, SMAD4 and p63.

RESULTS

4.1.9.1. Role of putative p53/p63 Binding Site in *IFNK* Enhancer

Not only p53, but also the other p53 family members can be stabilized and activated by DNA damage in certain settings [133], suggesting that putative target genes of these TF family might be upregulated when DNA toxins are applied. Thus, to further elucidate the involvement of p53 and p63 in *IFNK* transcription, NHK were treated for 24 h with etoposide, a topoisomerase II toxin, which causes DNA double-strand breaks. Indeed, *IFNK* transcription was 3.1-fold induced upon etoposide treatment (Figure 15A), even though this did not reach statistical significance. Next, to distinguish between p53 and p63, Nutlin-3a was applied. This compound specifically increases p53 protein amounts by disrupting the interaction between p53 and the E3 ubiquitin ligase MDM2 [134]. Interestingly, p53 stabilization repressed *IFNK* expression, suggesting p53 is not involved in activation of the gene (Figure 15B). *In line with observations that p53 can inhibit p63 expression in certain settings [135, 136], the levels of p63 protein were greatly diminished upon Nutlin-3a treatment (Figure 15C). These data suggest that IFNK is activated by p63 and repressed by p53 in keratinocytes (italized section taken from the author's publication [13]).*

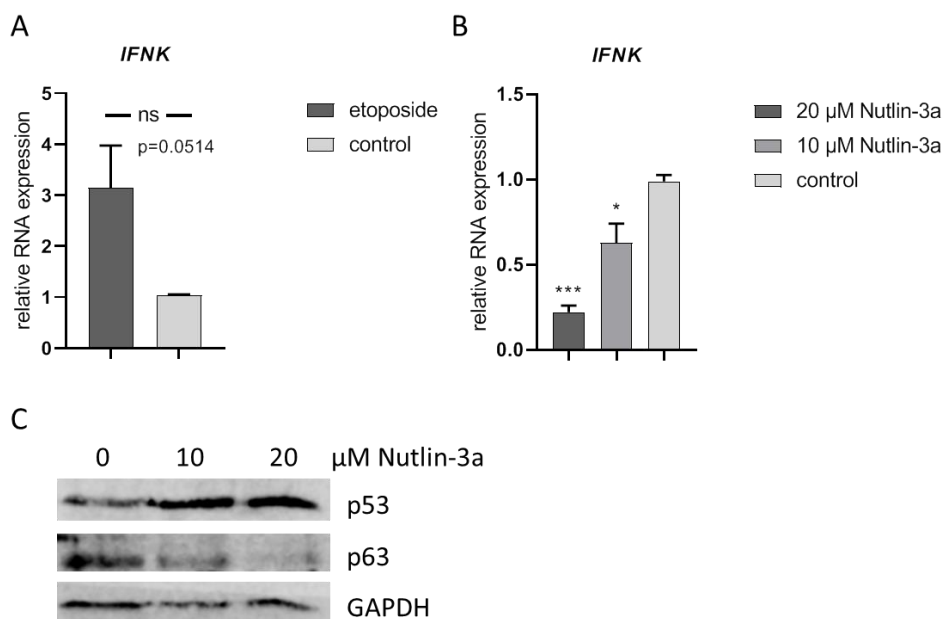


Figure 15: Compound treatments suggest that p53 represses and p63 activates *IFNK* expression in NHK

NHK were treated with etoposide (A) or Nutlin-3a (B) for 24 h and mRNA levels of *IFNK* were determined by qPCR using PGK1 as a reference gene and are given relative to the vehicle control. Averages were calculated from n=6 (A) or n=4 (B) independent experiments. Error bars indicate the SEM. Significant deviations from the vehicle control are highlighted with asterisks (paired t-test: * < 0.05, *** < 0.001). D) Western blot analysis of NHK extracts treated with 10 or 20 μ M Nutlin-3a for 24 h using antibodies against p53, p63 and GAPDH as a loading control. The blot shown is representative for two independent experiments using extracts derived from different NHK donors. Italicized section and diagrams B (modified) and C are taken from the author's publication [13].

4.1.10. Analysis of Transcription Factor Binding to the *IFNK* Enhancer in vivo

To establish that *AP-2 α* , *jun-B*, *SMAD4* and *p63* regulate *IFNK* expression by binding to the enhancer, data mining was performed for *p63* and chromatin immunoprecipitation (ChIP) experiments were carried out for *AP-2 α* , *jun-B* and *SMAD4*. Analyzing two published NHK/*p63* ChIP-Seq datasets revealed that fragments Chr9:27,519,197-27,520,919 [136] and Chr9:27,520,028-27,520,520 [137], which encompass the *p63* BS #1 and #2 (Chr9:27,520,318-27,520,411), are bound by *p63* in vivo.

ChIP experiments were carried out after stimulating NHK for 4 h with TGF- β 1 using antibodies to *AP-2 α* , *SMAD4* and *jun-B*. This revealed that *AP-2 α* binding to the HS 1 region is 16-fold enriched compared to the isotype control (IgG, Figure 16). In HS 2, *jun-B* as well as *SMAD4* proteins were found enriched 18-fold and 4-fold relative to IgG, respectively. Similar enrichment of *jun-B* and *SMAD4* binding was found in a published BS in the *SERPINE1* promoter (Figure 16, [112]). These results suggest that *AP-2 α* , *jun-B*, *SMAD4* and *p63* bind to the *IFNK* enhancer in vivo and activate *IFNK* expression (italicized section taken from the author's publication [13]).

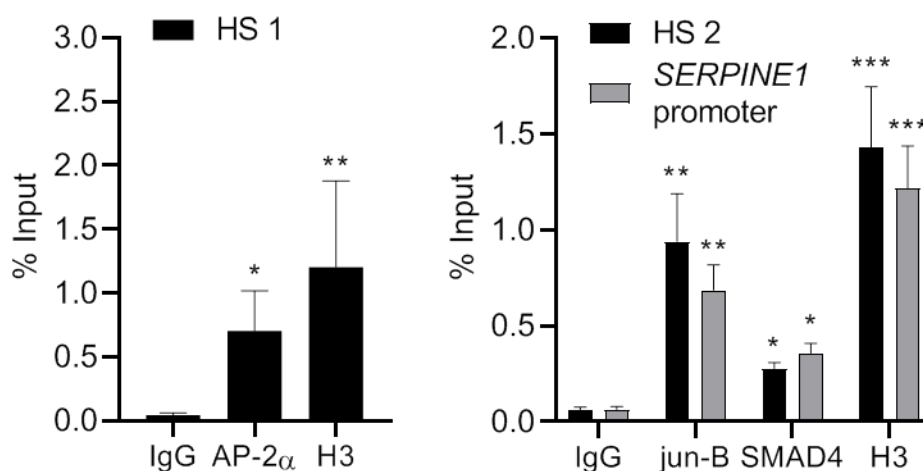


Figure 16: ChIP analysis in NHK showing enrichment of *AP-2 α* , *jun-B* and *SMAD4* in the *IFNK* enhancer

ChIP analyses were performed using chromatin isolated from NHK treated with TGF- β 1 for 4 h. Binding of *AP-2 α* , *jun-B*, *SMAD4* or histone 3 (H3) to HS 1, HS 2 or *SERPINE1* promoter DNA sequences was analyzed after immunoprecipitation with *AP-2 α* , *jun-B*, *SMAD4*, or H3 antibodies and then DNA sequences were quantified by qPCR. IgG served as a negative control. Bars represent the average of $n=3$ independent experiments and are shown relative to chromatin input. Error bars indicate the SEM. Asterisks highlight significant deviations from the respective IgG control (ratio paired t-test: * < 0.05, ** < 0.01, *** < 0.001). Italicized section and diagrams taken from the author's publication [13], slightly modified.

RESULTS

4.1.11. Effect of identified Transcription Factors on other Type I IFNs

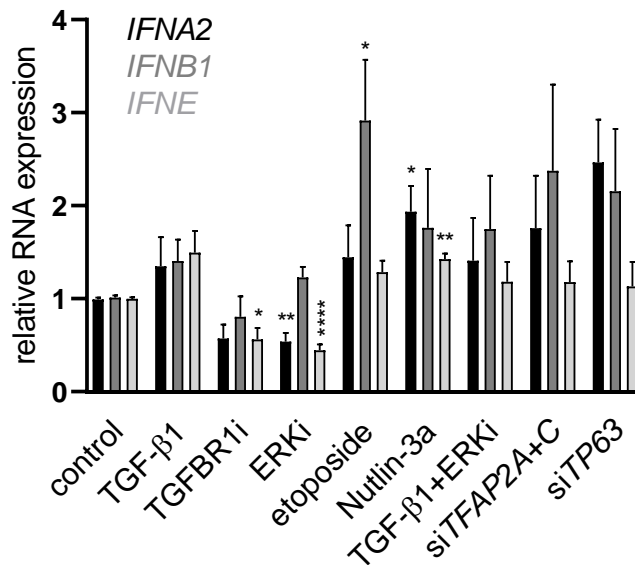


Figure 17: Effect of TGF-β1 and ERK1/2 pathway or TFAP2 and TP63 knockdown on expression of other type I IFN genes

NHK were treated with the indicated substances for 24 h or transfected with the indicated siRNAs for 48 h. IFNA2, IFNB1 and IFNE mRNA levels were determined by qPCR. Values given are relative to the vehicle control using PGK1 as a reference gene and represent averages from $n=8$ (TGF-β1, ERKi); $n=6$ (TGFBR1i, TGF-β1+ERKi, etoposide, $n=4$ (Nutlin-3a, siTP63) and $n=3$ (siTFAP2A+C) independent experiments. Significant deviations from the vehicle control are highlighted with asterisks (paired *t*-test: * < 0.05, ** < 0.01, **** < 0.0001). Italicized section and diagram (modified) are taken from the author's publication [13].

To address if the identified TFs also regulate other type I IFNs such as *IFNA2*, *IFNB1*, *IFNE* and *IFNW1* in NHK, transcription of these genes was determined from existing samples treated with TGFBR1i, TGF-β1, ERKi, etoposide, Nutlin-3a or transfected with siTFAP2A+C or siTP63. It turned out, that *IFNW1* expression is very low in these samples and falls below the detection limit of the Light Cycler 480 instrument in some cases. Thus, *IFNW1* RNA levels are not displayed in Figure 17 and were only analyzed in the initially tested samples. Expression of *IFNA2* and *IFNB1* was low, but above the detection limit. Expression levels of *IFNE* were very similar to *IFNK* levels (data not shown). The following observations have been made for the three other type I IFNs in NHK: *TGF-β* treatment did not significantly induce *IFNA2*, *IFNB1* or *IFNE* (Figure 17). *IFNE*, but not *IFNA2* or *IFNB1* expression was inhibited by TGFBR1i (Figure 17). However, the reduction of *IFNE* by TGFBR1i was much weaker (1.8-fold) compared to *IFNK* (3.6-fold, compare Figure 17 to Figure 9). In contrast to *IFNK*, ERKi reduced *IFNA2* and *IFNE* expression approximately 2-fold and had no effect on *IFNB1* transcription (Figure 17). Consistent with this, the combination of ERKi and TGF-β, which greatly enhances *IFNK* expression, did not induce *IFNA2*, -B1 or -E (Figure 17). Addition of etoposide induced *IFNB* expression 2.9-fold, which

RESULTS

is consistent with the finding that DNA damage induces the cGAS/STING pathway leading to *IFNB* expression in keratinocytes [17]. It did not have a significant effect on the other analyzed type I IFNs (Figure 17). Addition of 20 μ M *Nutlin-3a* weakly increased expression of *IFNA2* and *IFNE* (1.9- and 1.4-fold, respectively) which is in sharp contrast to the pronounced repression of *IFNK* (compare Figure 17 to Figure 15B on page 93). The knockdown of *TFAP2A+C* or *TP63* had no effect on *IFNE* expression but induced both *IFNA2* and *-B1* to similar, yet not statistically significant, extents (Figure 17). Taken together, these data strongly indicate that the regulation of *IFNK* expression by the *TGF- β 1*, *ERK1/2*, *p63* and *p53* pathways in *NHK* is unique for this type I IFN (italicized sections taken from the author's publication [13]).

4.2. Regulation of *IFNK* Expression in Pathological Settings

As outlined in section 2.1.3 on page 25, *IFN- κ* has been found to be abnormally expressed in several pathological settings. Thus, restoring physiological *IFN- κ* levels might help improving symptoms in the respective diseases. As a first step in this direction, it was analyzed, whether *IFNK* expression can be manipulated in disease-relevant settings.

4.2.1. *IFNK* Expression in HR-HPV-positive Keratinocytes

To address if *IFNK* expression can also be activated in the context of HPV infection, three different human keratinocyte cell lines with persistently, autonomously replicating *HPV16* genomes (*HK HPV16*; [91, 92]) were treated with *TGF- β 1*, *ERKi* or a combination thereof. *IFNK* expression could be induced 6.2-fold by *TGF- β* (Figure 18A), which is consistent with observations by Woodby and colleagues [38] and enhanced compared to *NHK* (3.5-fold, Figure 9B). On the other hand, *ERKi* and *ERKi+TGF- β* induced *IFNK* expression 2.8-fold and 11.8-fold, respectively (Figure 18A), which is weaker than in *NHK* (4.9- and 24.8-fold, Figure 9B). Consistent with an activation of the type I *IFN*-signaling pathway, the ISG *IFIT1* was significantly activated by all treatments and the extent of induction correlated well with the levels of *IFNK* (Figure 18A, B). The analysis of spliced viral transcripts *E6*1* and *E1[^]E4* revealed that *TGF- β* alone repressed both transcripts in a similar manner to 44 % and 37 %, respectively (Figure 18C). *ERKi* only significantly reduced *E6*1* but not *E1[^]E4* levels (Figure 18C), and these effects were weaker than with *TGF- β* alone (66% vs. 44%). The combination of *TGF- β* and *ERKi* repressed viral transcription slightly more efficient than *TGF- β* alone, but this was not significantly different (Figure 18C). In summary, these data show that *IFNK* can be more efficiently induced by the

RESULTS

combination of TGF- β 1 and ERKi in HPV16-positive cell lines and that this combination also represses viral transcription (italicized sections taken from the author's publication [13]).

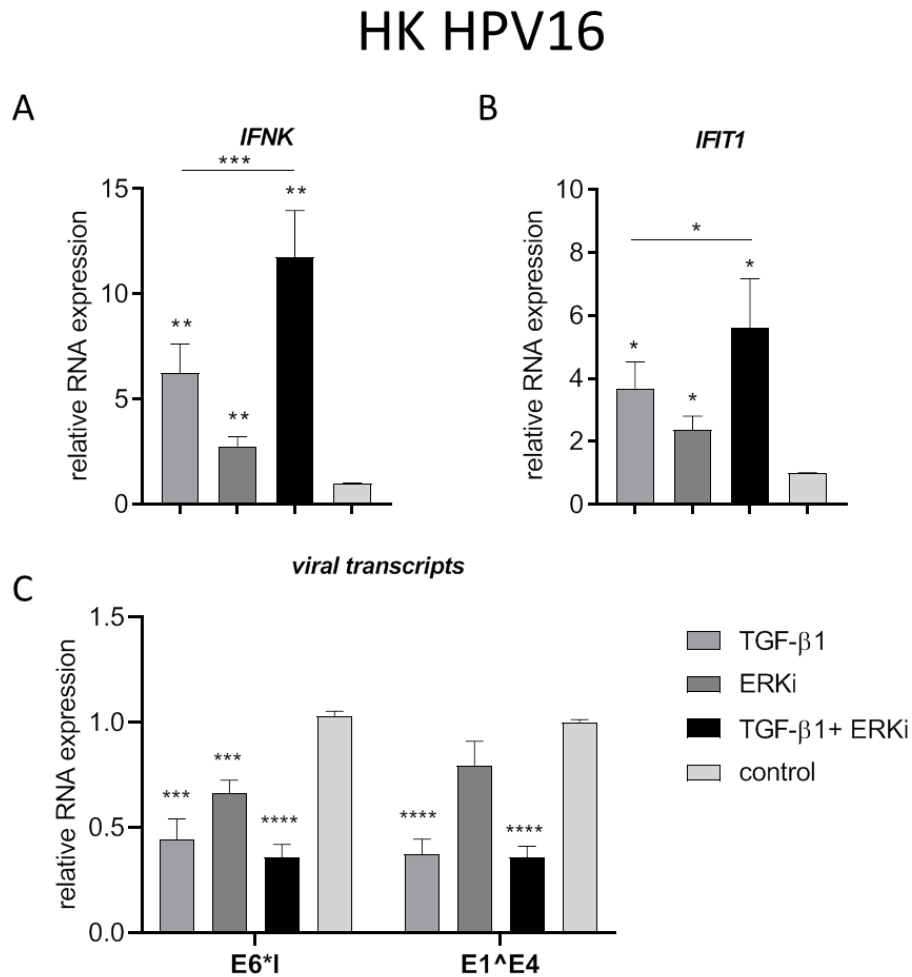


Figure 18: Analysis of transcription in HPV16-positive keratinocytes demonstrates that TGF- β 1 and ERKi induce *IFNK* and reduce viral transcription

RNA levels of *IFNK*, *IFIT1*, HPV16 *E6*1* and HPV16 *E1^E4* transcripts were determined by qPCR analyses after treatment of three different HPV16-positive cell lines with the indicated substances for 24 h ($n=3$ for each cell line). Values given are relative to the vehicle control using PGK1 as a reference. Error bars indicate the SEM. Significant deviations from the vehicle control are highlighted with asterisks (paired t-test: * < 0.05, ** < 0.01, *** < 0.001, **** < 0.0001). Italicized section and diagrams are taken from the author's publication [13].

To extend this knowledge to other HR-HPV types, a cell line, which carries autonomously replicating HPV31 genomes (HK HPV31), was treated in the same way. The effects on *IFNK* expression were much weaker than observed for the HPV16 cell lines (1.9-, 1.7- and 3.1-fold, Figure 19A) and not significantly different from the vehicle control. Nonetheless, the same trends could be observed: the

RESULTS

strongest induction was achieved with the combinatorial treatment. A significant induction of *IFIT1* expression could not be observed (Figure 19B), which is in line with a study that reported a nearly 10-fold repression of *IFIT1* in NHK transfected with HPV31 [138]. Looking at the viral transcripts, the *E6*1* transcript was reduced roughly 2-fold upon each treatment (to 37%, 55% and 44%, respectively, Figure 19C), whereas the levels of *E1^E4* transcript did not change significantly (Figure 19C). As these findings are derived from a single cell line and considerable donor-to-donor variations have been observed for the HPV16 cell lines, the results for the HK HPV31 cell line should be regarded as preliminary findings.

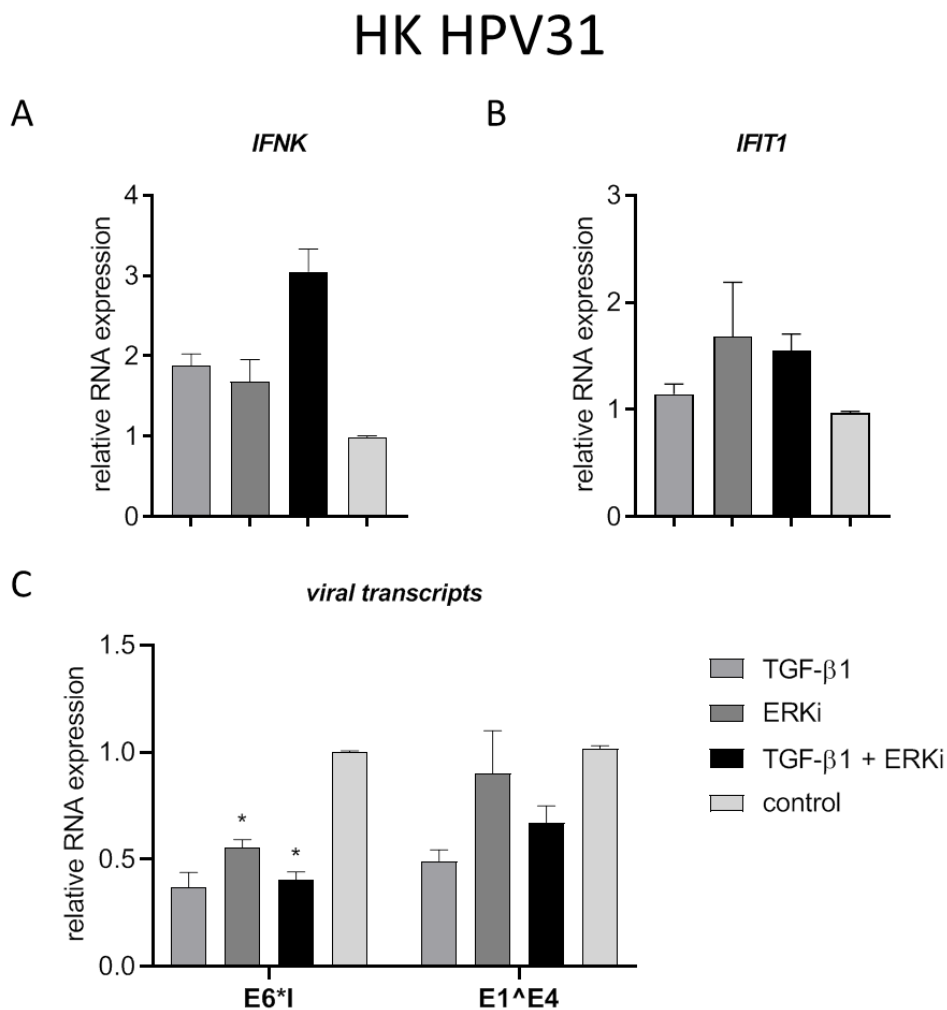


Figure 19: Analysis of transcription in HPV31-positive keratinocytes reveals the effect of TGF-β1 and/or ERKi on *IFNK* and viral transcription

RNA levels of *IFNK*, *IFIT1*, HPV31 *E6*1* and HPV31 *E1^E4* transcripts were determined by qPCR analyses after treatment of one HPV31-positive cell lines with the indicated substances for 24 h (n=2). Values given are relative to the vehicle control using *PGK1* as a reference. Error bars indicate the SEM. Significant deviations from the vehicle control are highlighted with asterisks (paired t-test: * < 0.05).

4.3. Influence of HR-HPV Proteins on cGAS/STING Signaling

The cGAS/STING pathway is responsible for sensing the presence of dsDNA in the cytoplasm and induce the expression of IFN- β (see section 2.1.2.2 on page 22). To test, whether HPVs have evolved means to counteract this pathway, the influence of different HR-HPV proteins on cGAS/STING signaling was analyzed. As HPVs infect NHK, a cell type for which the transfection efficiency is rather low, a reporter assay approach was considered.

4.3.1. Establishment of a cGAS/STING/*IFNB1*-Promoter Reporter Assay

First, the appropriate stimulus for induction of *IFNB1* was determined. NHK were stimulated with cGAMP, the second messenger molecule produced by the cGAS enzyme to activate STING, or with etoposide, an DNA damaging agent, reported to induce the cGAS/STING pathway in keratinocytes [17]. Endogenous *IFNB1* expression was analyzed at varying timepoints after treatment (Figure 20).

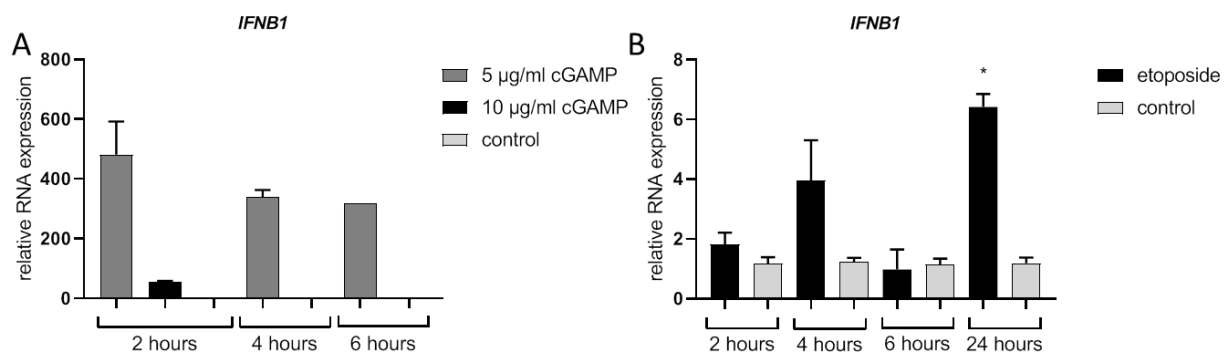


Figure 20: Impact of cGAMP and etoposide treatment on endogenous *IFNB1* expression in NHK

NHK were transfected (cGAMP) or treated (etoposide) with the indicated substances and harvested after the time points shown below the x-axis. *IFNB1* transcription was quantified by qPCR using *PGK1* as a reference gene and is given relative to the vehicle control. Bars represent the average of n=2 independent experiments (except for 10 µg/ml cGAMP, 6 h (n=1) and etoposide, 4 h (n=3)) + SEM. In B, significant deviations from the vehicle control are highlighted with asterisks (paired t-test, * < 0.05).

This analysis revealed that endogenous *IFNB1* transcription is highest 2 h post transfection of 5 µg/ml cGAMP, displaying a 480-fold induction (Figure 20). Transfection of 10 µg/ml cGAMP was not tolerated well by the cells, resulting in morphological changes and insufficient RNA yield for further analyses. Even though, cells did not appear to be stressed after treatment with the lower dosage of cGAMP for 2 or 4 h, the RNA yield decreased with time, and the cells displayed some morphological changes 6 h after transfection with 5 µg/ml cGAMP.

RESULTS

When looking at the etoposide treatment, it became obvious that it had strikingly weaker effects on *IFNB1* expression (Figure 20). However, etoposide does not directly activate the STING protein as cGAMP does, thus arguing for a delayed activation of the *IFNB1* gene. Induction and accumulation of DNA damage by etoposide treatment, as well as sensing of this damage and transmitting of the danger signal to the STING protein with subsequent *IFNB1* activation should take longer time than direct activation of the pathway. Indeed, *IFNB1* induction was most prominent 24 h after treatment (Figure 20). However, whereas the two samples displayed in Figure 20 resulted in an average 6.4-fold *IFNB1* induction, the induction observed for a higher number of independent donor-derived samples from the *IFNK* project (n=6) was much lower (2.9-fold), suggesting that the observed activation of *IFNB1* by DNA damage might not be reproducible with this magnitude in NHK from other donors. Nonetheless, another peak in *IFNB1* transcription was observed already 4 h after treatment, resulting in an average 4-fold induction. This increase was accompanied by remarkable variations between the three tested donors (2.1- to 6.6-fold) and did not reach statistical significance (Figure 20). As DNA damage activates several pathways in the cell, reasons other than DNA damage induced- STING signaling could also be responsible for the observed induction.

Due to the need for two consecutive transfections when using cGAMP and the weak effects of etoposide treatment on endogenous *IFNB1* transcription, another possibility of cGAS activation was considered: As cGAS recognizes dsDNA in the cytoplasm and transfection delivers such dsDNA directly into the cytoplasm, the impact of transfection on endogenous *IFNB1* transcription was assessed. This was done with NHK from a single donor transfected with two different preparations of the empty luciferase plasmid (pGL3 basic), resulting in a 31.4 - and 18.8-fold induction of the *IFNB1* gene two days after transfection (data not shown), suggesting that transfection alone is sufficient to induce the *IFNB1* promoter.

Thus, as a next step, activity of the pGL3 *IFNB1* Prom luciferase reporter was tested in the presence of different HPV proteins. To do so, NHK were transfected with 300 ng of pGL3 *IFNB1* Prom and 500 ng of empty expression vector (pSG5) or expression vectors for HPV16 proteins. Two days post transfection, luciferase activity was measured and plotted relative to the expression in the pSG5 co-transfected cells (Figure 21). Even though the *IFNB1* Prom reporter was considerably activated, no profound effects of the co-transfected HPV proteins could be observed (Figure 21). This was unexpected, as some studies suggest an involvement of HPV proteins in IFN- β expression. For example, it could be shown that HPV16 E6 binds IRF3, a TF involved in *IFNB1* activation, and interferes with IFN- β production in response to Sendai virus infection [78], suggesting that co-transfection with HPV16 E6 should diminish reporter activity. Moreover, DNA damage has been shown to induce IFN- β production via STING in keratinocytes [17] and the E1 protein is known to trigger DNA damage pathways [69].

RESULTS

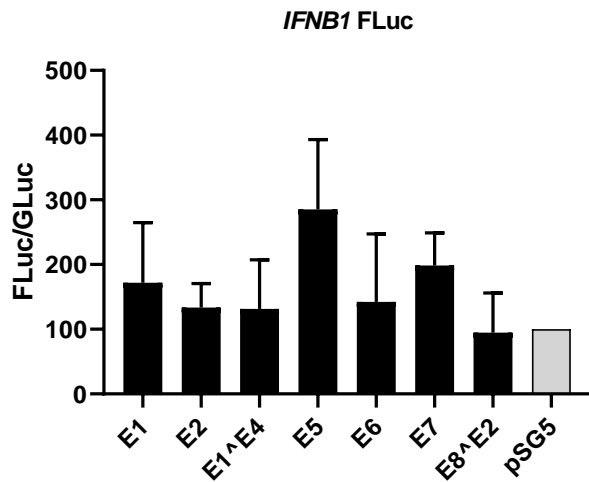


Figure 21: Co-transfection of different HPV16 protein expression plasmids with *IFNB1* Prom reporter in NHK

NHK were transfected with pGL3 *IFNB1* Prom reporter and expression plasmids for the indicated HPV16 proteins. Luciferase activity was assayed 48 h post transfection and is shown relative to the activity of the empty expression vector pSG5 (highlighted in light gray). Firefly luciferase (FLuc) activity was normalized to the expression of the co-transfected *Gussia* luciferase (GLuc) construct. Bars represent the average of n=3 independent experiments + SEM. No significant deviations from the pSG5 construct could be observed (paired t-test). cGAMP = cyclic GMP-AMP.

Thus, to optimize the system and evaluate whether the cGAS/STING pathway is indeed involved in the observed activation of the *IFNB1* reporter, the cGAS- and STING-deficient 293T cell line was used. These cells were co-transfected with the *IFNB1* Prom reporter and expression vectors for the different HPV proteins and complemented or not with cGAS and STING expression plasmids. A clear participation of cGAS and STING in *IFNB1* promoter activation could be shown, as all wells lacking cGAS and STING co-transfection displayed less than 2% of the FLuc/GLuc activity measured in the wells complemented with cGAS and STING (Figure 22).

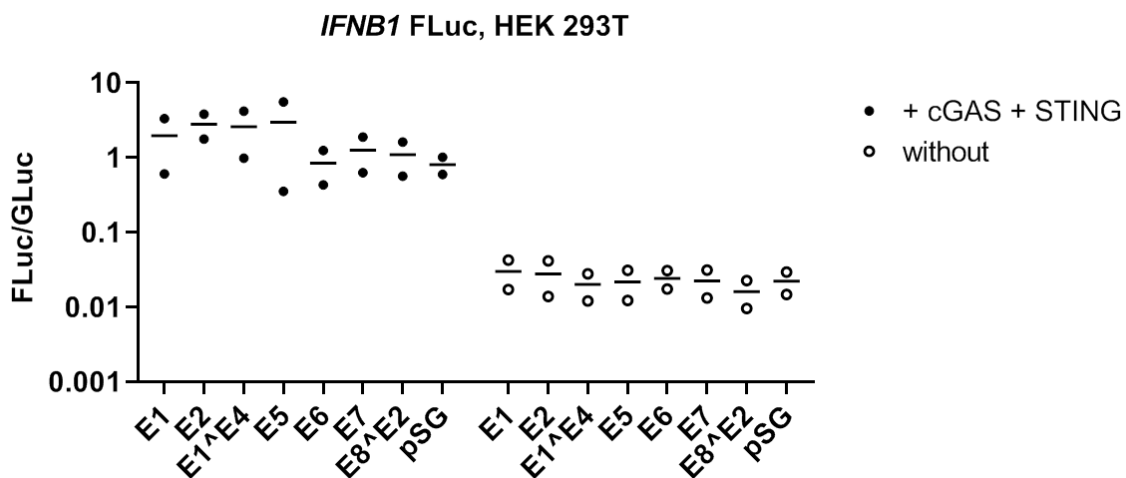


Figure 22: Effect of cGAS and STING expression on *IFNB1* Prom reporter in 293T cells

Legend on the next page

RESULTS

Figure 22: Effect of cGAS and STING expression on *IFNB1* r Prom reporter in 293T cells

293T cells were transfected with pGL3 *IFNB1* Prom reporter and the expression plasmids for the HPV16 proteins listed below the x-axis; with (filled circles) or without (open circles) additional transfection of cGAS and STING expression plasmids. Luciferase activity was assayed 24 h post transfection. Reporter activity is presented as Log10 of Firefly luciferase (FLuc) activity normalized to the activity of the co-transfected *Gaussia* luciferase (GLuc) construct. Circles illustrate average activity of two technical replicates from n=2 independent experiments, vertical line depicts the mean. cGAS = cyclic GMP-AMP synthase, STING = stimulator of IFN genes.

However, as 293T cells are kidney cells and express adenoviral proteins and the large T antigen of SV40, which have activities similar to HPV E6, E7 [139-145] and E1 [146-151], it was decided to test HPV-negative keratinocyte cell lines next. Hence, the RTS3b and C33A cell lines were transfected with the *IFNB1* Prom reporter and expression vectors for different HPV proteins, cGAS and STING. In RTS3b, no induction of the *IFNB1* promoter by cGAS and STING was observed (data not shown), excluding these cells from further analyses. In contrast, in C33A, co-transfection of cGAS and STING expression plasmids greatly induced activity of the *IFNB1* Prom reporter (Figure 23), strongly suggesting that C33A are STING-deficient. Without a functional STING protein, a functional cGAS enzyme could not induce *IFNB1* expression either, thus a statement about the cGAS status of C33A cells is not possible. The basal activity of the *IFNB1* Prom reporter in C33A cells was slightly higher than the activity observed in NHK, probably attributable to the higher transfection efficiency of C33A and arguing for an induction of the reporter by the transfection procedure also in this cell line.

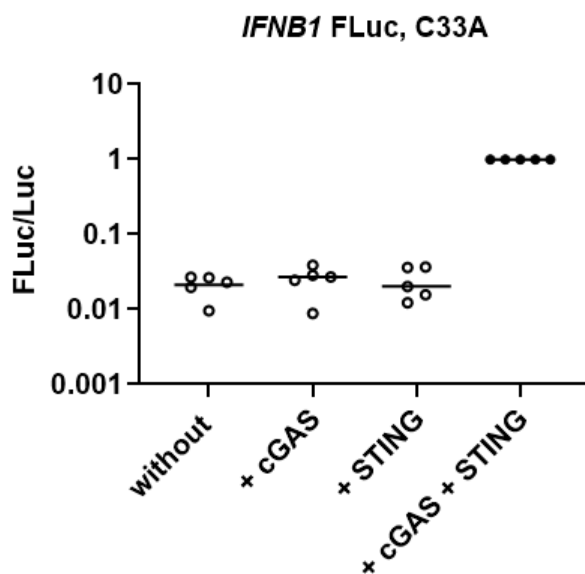


Figure 23: The C33A keratinocyte cell line relies on transfection of a STING expression plasmid to induce the *IFNB1* Prom reporter

C33A were transfected with the pGL3 *IFNB1* Prom reporter, cGAS and STING expression plasmids (filled circles), one of both or none of the expression plasmids (open circles). Luciferase activity was assayed 48 h post transfection and depicted as Log10 of Firefly luciferase (FLuc) activity normalized to the activity of the co-transfected *Gaussia* or *Renilla* luciferase (Luc). Circles illustrate average activity of two technical replicates from n=5 independent experiments, vertical line depicts the mean. cGAS = cyclic GMP-AMP synthase, STING = stimulator of IFN genes.

4.3.2. Influence of HR-HPV Proteins on STING-dependent *IFNB1* Reporter

Thus, as the *IFNB1* Prom reporter activation depends on cGAS/STING signaling and can be easily assessed in C33A keratinocytes, the influence of different early HR-HPV proteins on *IFNB1* Prom reporter activity was determined. As shown in Figure 24, co-transfection of the different expression plasmids (100 ng per well each) resulted in modest effects on *IFNB1* activation, with none of the proteins resulting in further activation of the gene. However, the 2.2-fold reduction of reporter activity upon transfection with the HPV16 E6 protein (Figure 24) indicated that the system per se can be used successfully, even though the expression levels of the different proteins might not be equal and therefore should be analyzed and adjusted in future studies. Nonetheless, some interesting observations could be made: The E2 protein of both HPV16 and HPV31 significantly reduced *IFNB1* Prom reporter activity (2- and 2.5-fold, respectively, Figure 24). The E5 protein of HPV16 did not reveal a consistent trend, but the two different HPV31 E5 constructs decreased *IFNB1* activation: Transfection of the YFP-tagged version significantly reduced reporter activity 2.7-fold and the non-tagged HPV31 E5 showed a tendency for reduction, which was confounded by one outlier (Figure 24). Whereas the E8^E2 protein of HPV16 did not uniformly influence the activity of the reporter, the E8^E2 protein of HPV31 decreased it 2.7-fold. Overall, it seemed that HPV31 proteins have a greater influence on *IFNB1* Prom reporter activity than their HPV16 counterparts.

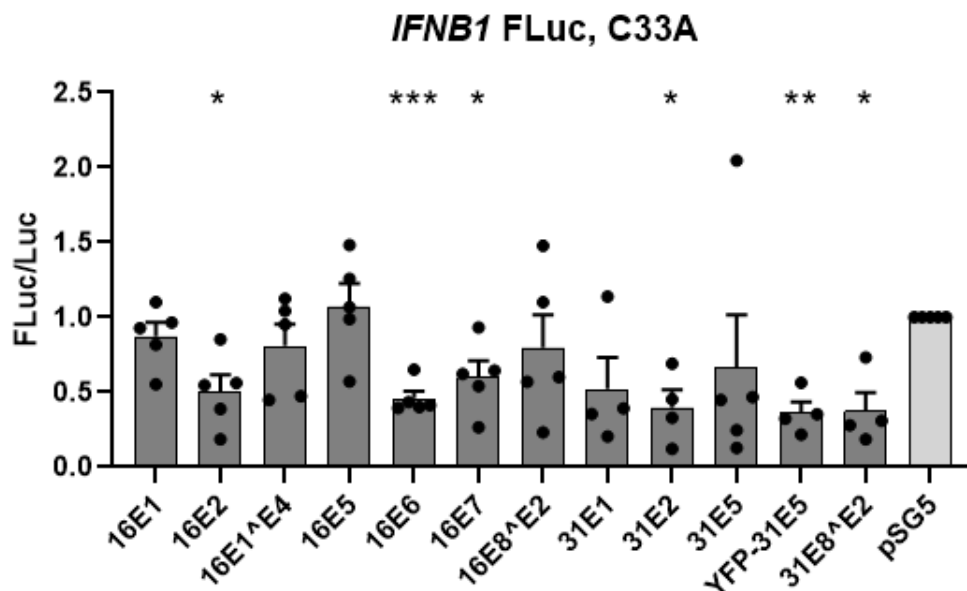


Figure 24: Influence of co-transfected expression plasmids for different HR-HPV proteins on *IFNB1* Prom reporter activity in C33A cells

Legend on the next page

RESULTS

Figure 24: Influence of co-transfected expression plasmids for different HR-HPV proteins on *IFNB1* Prom reporter activity in C33A cells

C33A were transfected with the pGL3 *IFNB1* reporter, cGAS and STING expression plasmids and the expression plasmids for the HPV proteins indicated below the x-axis. Luciferase activity was assayed 48 h post transfection. Reporter activity is presented as Firefly luciferase (FLuc) activity normalized to the activity of the co-transfected *Gaussia* or *Renilla* luciferase (Luc). Bars depict average of $n \geq 4$ independent experiments + SEM; circles illustrate average activity of two technical replicates. Asterisks highlight significant deviations from the pSG5 control (light gray; paired t-test, * < 0.05, ** < 0.01, < 0.001).

4.3.3. Localization of HPV E5 and STING

Due to the differences observed for HPV16 and HPV31 E5 and the fact that E5 proteins are transmembrane proteins which localize to the ER [76] comparable to STING [15], localization of these proteins was assessed. For this purpose, C33A cells were transfected with the mCherry-tagged murine STING expression plasmid and/or the YFP-tagged HPV E5 proteins of either HPV16 or HPV31. To the best of the author's knowledge, HPV31 E5 has not formally been proven to insert into membranes yet. As only a GFP-labeled version of the cGAS plasmid was available (which would be indistinguishable from the YFP-tagged HPV E5 proteins), cells were instead stimulated with 5 $\mu\text{g/ml}$ cGAMP 4 h before fixation to ensure pathway activation also in the possible absence of a functional cGAS protein. In cells transfected with the STING plasmid only (Figure 25A on the following page), a perinuclear localization of STING was observed. Moreover, some but not all of the cGAMP treated cells showed the appearance of dot-like STING structures near the nucleus (Figure 25A, compare row 3 to row 2), which might represent formation of STING oligomers upon pathway activation. Both HPV E5 proteins localized to perinuclear membranes as well as to the cytoplasm (Figure 25A). Scanning through the acquired sections (5-17 per image, data not shown) revealed that the cytoplasmic distribution is not even (as would be expected for a soluble protein) but seem to occur along the different membrane compartments in the cytoplasm. This fits to the reports for the E5 protein of HPV16, which has been found to localize also to Golgi- and mitochondrial membranes upon over-expression [76]. Importantly, significant co-localization of STING protein and both E5 proteins could be observed (Figure 25B). This was independent from and did not change upon treatment with cGAMP (Figure 25B). Additionally, resembling of the effect observed in the STING-transfected cells (Figure 25A, third row), some of the co-transfected cells displayed dot-like structures upon cGAMP stimulation (Figure 25C).

RESULTS

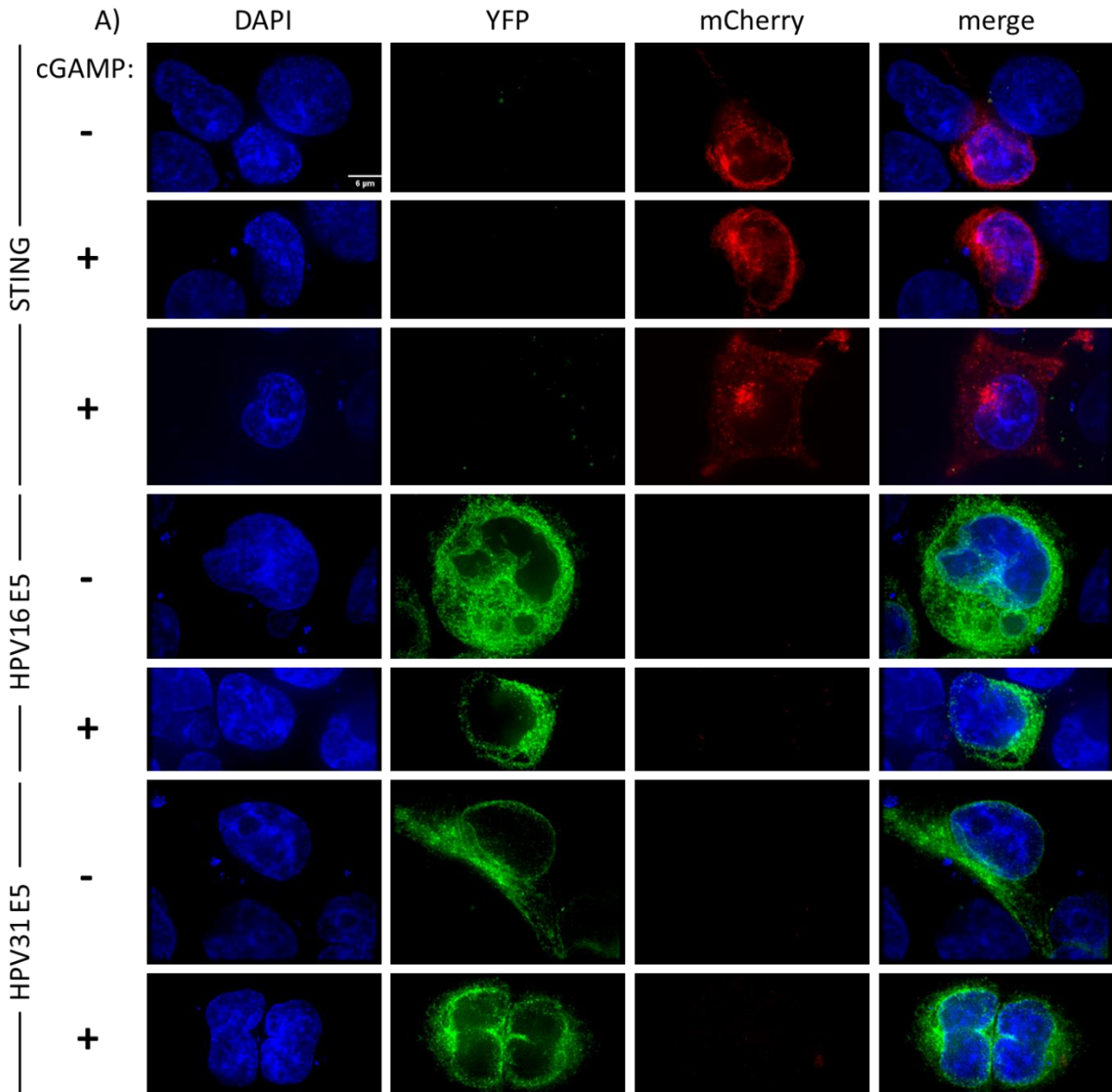


Figure 25: Immunofluorescence showing localization of STING or HR-HPV E5 proteins in C33A cells

C33A cells have been transfected with mCherry-STING (red) or YFP-HPV E5 (green) for 24 h and stimulated with 5 µg/ml cGAMP or vehicle control 4 h before fixation. DAPI staining (blue) was performed to visualize cell nuclei. Shown pictures are z-stacks and are representative for all observed cells from n=1 (HPV16) and n=2 (HPV31) independent experiment(s). A) Controls, transfected with either of the expression plasmids on their own. Respective plasmids are indicated at the left. Scale bar in the upper left picture represents 6 µm.

RESULTS

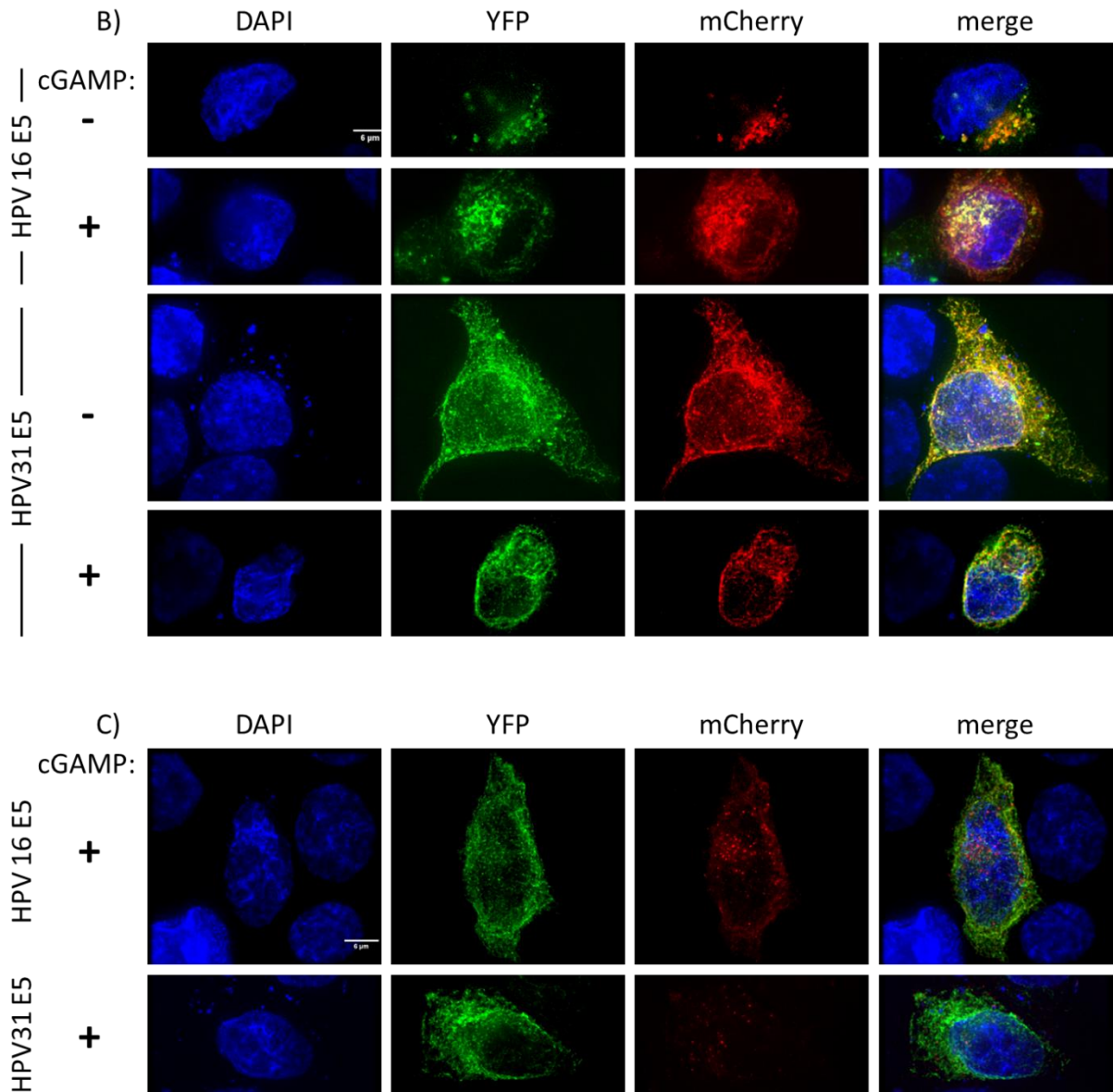


Figure 25: Immunofluorescence showing co-localization of HR-HPV E5 proteins and the STING protein in C33A cells

C33A cells have been transfected with mCherry-STING (red) or YFP-HPV E5 (green) for 24 h and stimulated with 5 $\mu\text{g/ml}$ cGAMP or vehicle control 4 h before fixation. DAPI staining (blue) was performed to visualize cell nuclei. Shown pictures are z-stacks B) Co-transfections, showing co-localization of E5 proteins with STING. Shown pictures are representative for all observed cells for n=1 (HPV16) and n=2 (HPV31) independent experiment(s). C) Cells with low STING expression showing accumulation of STING in the cytoplasm upon cGAMP stimulation. Pictures in C) illustrate rare observations. Respective HPV type is indicated at the left. Scale bar in the upper left picture represents 6 μm .

This could be seen best in cells displaying very low overall STING signals (Figure 25C), but might also be present in cells with higher expression rates or in non-stimulated cells (Figure 25B). In these cases, dot formation might be less obvious due to the higher overall signal intensity. If dot-like structures of STING signals can indeed be observed also in non-stimulated cells awaits further investigation.

5. Discussion

As mentioned earlier, major parts of this work have been published, thus, the discussion contains exact quotes from the author's publication [13], which are emphasized by italic typesetting.

The skin is the first barrier an invading pathogen has to overcome. It consists of a stratified epithelium, the epidermis, and the underlying dermis. *The major cell type in the epidermis is the epidermal keratinocyte.* In the dermis, fibroblasts, adipocytes and different immune cells can be found [152, 153]. Upon infection, the different cell types in the skin rapidly produce type I and type III IFNs to create a protective state [3, 4, 12]. In addition to these inducible IFNs, which are only generated in response to infection, keratinocytes constitutively express IFN- κ [9]. Keratinocytes express a large variety of PRRs and nucleic acid sensors to detect the presence of pathogens [154-156]. It has been found that the constitutive expression of IFN- κ sustains the basal expression of different ISGs, including the mentioned PRRs and different compounds of the type I and III IFN signaling pathways [23, 24, 33]. Thus, IFN- κ expression allows for a poised state of the epithelium, which enables the immediate reaction to infections. One infectious agent, which is very probably encountered upon onset of sexual activity, are HPVs. HPV is one of the most common sexual transmitted infectious agents [157] and a large majority of sexually active persons will acquire an infection with HPV at least once in their life time, leading to an approximately 12% prevalence of cervical HPV in asymptomatic women on a global scale [158]. Whereas most infections (\approx 90%) are cleared by the immune system, persistent infections with the HR-genotypes, such as HPV16, 18 or 31, can progress to cancer [159], demonstrating that these viruses have evolved strategies for long-term immune evasion. One of these strategies might be the down-regulation of IFN- κ expression by HR-HPVs [23, 24, 37, 39]. Thus, understanding the regulation of this unusual type I IFN might be useful to interfere with immune evasion of HPVs. Another strategy might be the down-modulation of DNA sensing pathways, one of which is the cGAS/STING signaling pathway ([15], italicized sections taken from author's publication, slightly modified).

5.1. Regulation of IFN- κ Expression

In this thesis it could be shown, *that IFN- κ expression is controlled by an enhancer element located 5 kb upstream of the IFNK gene, which consists of functional BS for AP-2 α/γ , jun-B, SMAD3/4 and p63 (Figure 26).* While it cannot be excluded that additional regulatory elements for IFNK expression exist,

DISCUSSION

the identified TFs provide a framework for both the cell type-specific expression of IFN- κ and its modulation by extracellular ligands and signal transduction pathways in keratinocytes (italicized section taken from the author's publication, slightly modified).

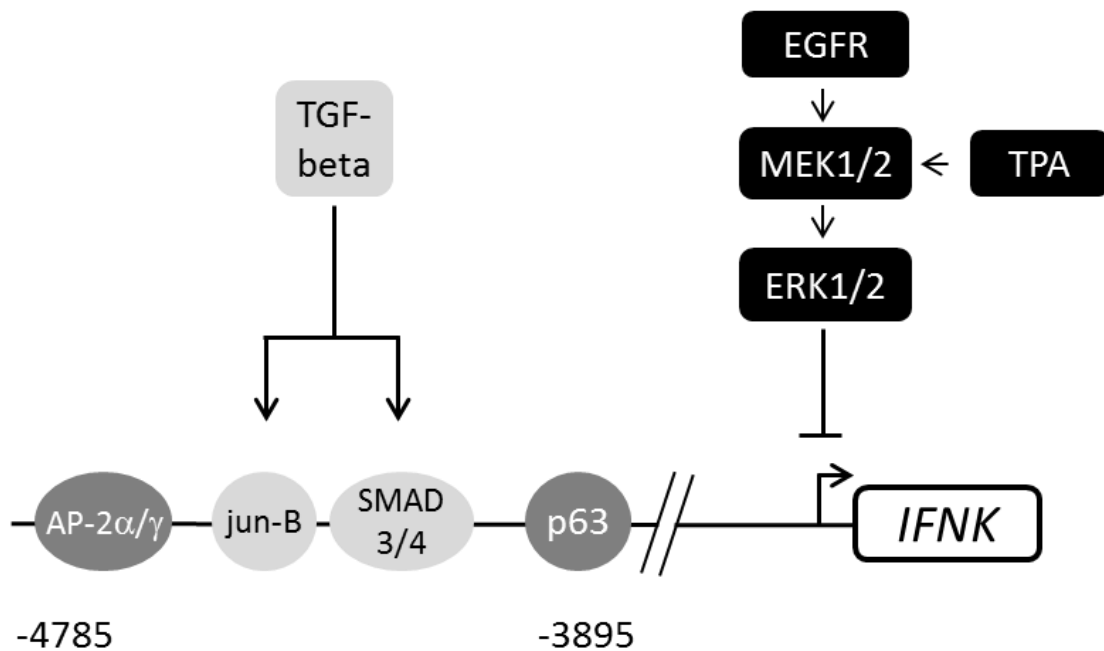


Figure 26: Model for the regulation of the *IFNK* gene in human keratinocytes

The *IFNK* enhancer spans a region of approximately 900 bp, starting at position -4785 relative to the *IFNK* transcription start site. It contains binding sites for the transcription factors AP-2, jun-B, SMAD3 and 4 and p63. The EGFR-MEK-ERK pathway has been found to negatively regulate *IFNK* transcription via a yet unknown mechanism. Figure taken from the author's publication [13].

With this, regulation of IFN- κ differs from the regulation of the classical type I IFN- α and - β which have been in the focus of type I IFN research. Whereas those IFNs are regulated by PRR-initiated pathways upon infection [3, 4], IFN- κ is regulated by a growth factor and a signaling pathway of the MAPK network, which is implemented in a plethora of different biological contexts [107, 160]. This finding demonstrates that environmental cues other than those generated upon infection can influence type I IFN expression and adds another layer of complexity to type I IFN regulation.

5.1.1. Putative Role of HMG-I Factors in *IFNK* Expression

Analysis of the regulatory element of the *IFNK* gene using the JASPAR database identified a putative BS for TFs of the HOX family at position -4204 to -4194, located in HS 2. Even though the mutation or deletion of this putative BS had a great impact on reporter gene activity in NHK (12% or 21% of the wildtype construct, respectively, Figure 6 on page 78, Figure 27 on page CXIX), no sequence-specific binding could be observed in subsequent EMSAs (Figure 28A on page CXX). As sequence-specific binding is a key feature of TFs [161], it is unlikely that the BS is bound by HOX proteins. However, unspecific binding occurs, even in the presence of increasing amounts of unspecific competitor oligo (0.5, 1.0 or 1.5 µg poly(dI:dC), Figure 28B), suggestive of another DNA-binding protein being involved in the observed effects on reporter gene activity. One possible candidate for such a DNA-binding protein would be a member of the high mobility group A protein (HMGA) family. These nuclear proteins are known to modulate the chromatin structure and are therefore also referred to as 'architectural, non-histone chromatin factors'. They are relatively small (around 100 amino acids) and are made up of an intrinsically disordered part, which allows for great flexibility of the protein, three so-called AT hooks, which mediate binding to short, AT-rich DNA sequences [162] and a highly acidic C-terminus. Moreover, they have been reported to arrange the binding of multiple proteins to enhancer and promoter regions, thus influencing gene expression [163]. The core sequence of the putative HOX binding motif in the *IFNK* enhancer consists of seven consecutive A or T nucleotides (AATAAAT, Table 14), hence representing a preferential target sequence for an AT hook. In addition to this sequence, several other stretches in the *IFNK* enhancer region contain four to eight sequential A/T bases and might therefore be bound by the other AT hooks of HMGA proteins [164]. Upon mutation of the supposed HOX BS, the AT-rich sequence is replaced, leaving only dispersed A and T nucleotides, which cannot be bound by AT hook-containing proteins any longer. Thus, the mutated plasmid used to assess reporter gene activity might have lost the supportive action of a structural protein, which binds DNA via AT hooks, and therefore display less activity than the wildtype construct. Interestingly, the HGMA protein has also been found to be part of an enhancer located in the regulatory region of integrated HPV18 genomes [165]. The HPV18 enhancer element is only active in epithelial cells [166] and might therefore confer epithelial specificity. In this enhancer, HGMA proteins were shown to interact with a heterodimer of the AP-1 factors jun-B and Fra2 [165], of which jun-B also binds to the *IFNK* enhancer. It has been demonstrated that binding of the HMGA proteins is as important for transcriptional activity of the HPV18 enhancer as a functional AP-1 BS [167]. Moreover, HMGA proteins have been found to initially assist in the assembly of TFs at the enhancer of the type I *IFNB1* gene, but are not contained in the final protein complex [168].

5.1.2. Signaling Pathways and Transcription Factors involved in *IFNK* Expression

Much knowledge about proteins assembling at an enhancer element and controlling gene expression has been derived from studies focusing on the inducible *IFNB1* gene. *Functional elements in the IFNK enhancer differ significantly from those in the IFNB1 enhancer. The size of the IFNB1 enhancer is only 55 bp and it is comprised of tightly clustered TFBS that form an enhanceosome [168], whereas the IFNK enhancer consists of multiple elements spread over 900 bp. The only common motif among both enhancers are BS for the AP-1 TF family. However, the IFNK AP-1 BS (TGAATCA) belongs to the TPA response element (TRE) family and is recognized by jun-B, whereas the IFNB1 AP-1 BS (TGACATAG) belongs to the cAMP response element family and is bound by Jun/ATF-2 [107, 169]. The data indicate that the AP-1 BS and SMAD3/4 BS both mediate TGF- β responsiveness of IFNK expression, consistent with findings that AP-1 TRE sequences can be found in the proximity of SMAD2/3 response elements [112, 125-128]. Furthermore, SERPINE1 expression requires the binding of both jun-B and SMAD2/3 to be strongly activated by TGF- β [112]. Taken together, this strongly suggests that IFNK is a bona fide TGF- β target in normal keratinocytes (italicized sections taken from author's publication [13], slightly modified).*

Despite the presence of the viral E7 protein, which interacts with a large number of cellular proteins [79, 121] and therefore has the capability to change cellular behavior, this finding was also supported by the experiments carried out in HK 16E7, in which addition of TGF- β increases and application of TGFBR1i decreases *IFNK* transcription (Figure 10B on page 87). Similarly, the stimulatory effect of the ERKi on *IFNK* transcription in NHK was also obvious in HK 16E7, whereas the other compounds interfering with MAPK signaling led to different effects (Figure 10A). Thus, even though these cells are not an ideal system to perform a detailed pathway analysis, they assisted in getting a first idea of potentially involved factors (reporter assays, EMSAs) and pathways, which could be confirmed using NHK. However, due to the remaining inconsistencies between the cell types used in the initial experiments it was decided to solely utilize NHK for all further experiments.

With these experiments, it became obvious that *AP-2 α/γ and p63 are important for constitutive IFNK expression. Interestingly, genome-wide analyses of keratinocytes revealed that AP-2 BS are significantly enriched near SMAD2/3 BS and that knockdown of TFAP2A changes the global transcription profile induced by TGF- β [127]. The data presented in this work show for the first time that p63 directly activates IFNK but not other type I IFNs in keratinocytes (Figure 14 on page 92, Figure 15 on page 93, Figure 17 on page 95). Interestingly, p63 regulates keratinocyte differentiation in conjunction with AP-2 α/γ and also functionally cooperates with AP-2 α/γ to activate the keratinocyte-specific C40 enhancer [170, 171]. In line with this observation, expression of $\Delta Np63\alpha$,*

DISCUSSION

the predominant p63 isoform in basal keratinocytes [172-174], and AP-2 α together with GRHL2 and c-myc is sufficient to reprogram mouse mesenchymal cells into keratinocyte-like cells [175]. A large body of additional evidence indicates that AP-2 α/γ and p63 are crucial players that regulate many aspects of keratinocyte biology [132, 172, 173, 176-179]. The TP63 gene encodes multiple p63 proteins, of which Δ Np63 α is the most abundant isoform in NHK [174]. In line with this, immunoblot analysis using an antibody that recognizes all p63 isoforms detected only one band with a molecular weight of approximately 70 kDa, which decreased upon siRNA treatment (Figure 14C on page 92) and thus most likely represents Δ Np63 α . In summary, these findings strongly support the concept that the combination of AP-2 α/γ , p63, jun-B and SMAD3/4 BS confers keratinocyte specificity and TGF- β inducibility of the IFNK enhancer (Figure 26 on page 108). Interestingly, IFNK expression can not only be activated but also be inhibited. The findings that the phorbol ester TPA represses and an ERKi activates IFNK expression (Figure 9A on page 85) are consistent with observations that inhibition of EGFR or MEK increases IFNK transcription [29, 30], strongly suggesting that the EGFR-MEK-ERK pathway negatively regulates IFN- κ expression. The mechanistic basis for this effect remains unclear. An ERK1/2-responsive element in the IFNK enhancer could not be identified using different reporter constructs lacking the respective binding sites, indicating that ERK1/2 does not inhibit IFNK expression via jun-B, SMAD3/4, AP-2 α/γ or p63. Further evidence that ERKi does not primarily activate the TGF- β pathway in NHK comes from the observation that the TGF- β target gene SERPINE1 is inhibited by ERKi (Figure 9C on page 85). A previous study reported that IRF1 is induced by PD168393, an EGFR inhibitor, and that knockdown of IRF1 attenuated IFN- κ expression in NHK [30]. Since the IFNK enhancer is not ERK1/2 responsive, it is unlikely that IRF1 directly binds to the enhancer. However, it cannot be excluded that functional IRF1 BS exist outside the IFNK enhancer (italicized sections taken from the author's publication [13], slightly modified).

5.1.3. IFNK in the Context of Infections

After having elucidated how IFN- κ expression is regulated in NHK, its regulation in diseased keratinocytes should be assessed. For this purpose, different keratinocyte cell lines, carrying episomal HPV16 or HPV31 genomes, were used. As only one HPV31 cell line was tested and significant donor-to donor variations for the HPV16 cell lines suggested that analyzing a single cell line might not reveal the complete picture, the discussion will focus on the results obtained for the three different HPV16 cell lines.

As outlined above, the ERK1/2 and TGF- β pathway regulate IFN- κ expression in NHK. *Interestingly, genome-wide analyses of HR-HPV induced cancers have revealed that both the EGFR-MEK-ERK1/2 and the TGF- β /SMAD4 pathway are significantly mutated in these cancers [180]. It is tempting to*

DISCUSSION

speculate that one consequence of these mutations is to limit IFN- κ expression. Moreover, TGF- β is involved in wound healing [181]. Therefore, activation of IFN- κ expression by the TGF- β pathway might be relevant in vivo when wounding occurs, because this increases the likelihood that basal keratinocytes may encounter pathogens such as HPV [64]. A recent study of the Bodily group suggested that TGF- β 1 activates IFNK expression only in HPV16-positive keratinocytes, but not in uninfected keratinocytes, by inducing the demethylation of a CpG island in the IFNK promoter [38]. In contrast, the presented work provides evidence that the TGF- β signaling pathway regulates IFN- κ expression in uninfected keratinocytes and that this is independent from promoter methylation but requires SMAD4 and jun-B BS in the enhancer. As pointed out above, the EGFR-MEK-ERK1/2 pathway inhibits IFN- κ expression. Since keratinocytes are cultivated in the presence of EGF, it is possible that differences in cell culture conditions account for the lack of induction of IFNK by TGF- β by the group of J. Bodily. On top, keratinocytes produce and are stimulated by TGF- β [182] and culturing keratinocytes in general might induce IFNK [183, 184], thus if further IFNK induction can be observed heavily depends on culture conditions. Nonetheless, the data presented here demonstrated that the combination of TGF- β and ERKi induces higher levels of IFN- κ than TGF- β alone not only in NHK, but also in HPV16-positive cells. While no obvious difference in the extent of repression of viral transcription could be seen between TGF- β or TGF- β + ERKi-treated HK HPV16, there is not only a significant increase in IFNK but also in ISG transcription. A very recent study by the Bodily group suggested that the HPV16 E5 protein takes part in IFNK regulation by inducing EGFR- and down-regulating TGF- β signaling pathways [31]. They confirm the activation of IFNK expression by TGF- β 1 in HPV16-positive cell lines. In addition, they report an increase of IFNK transcription upon treatment with hepatocyte growth factor as well as a weak activation upon treatment with EGF [31]. The effect of TGF- β 1 on IFNK transcription was already reported in the previous study of this group [38]. These results confirm that the IFNK gene is regulated by extracellular cues other than an infection. This is backed-up by their observation that inhibiting the JAK-STAT signaling pathway (which is activated upon sensing of infection in neighboring cells) does not significantly change IFNK levels in NHK or HPV16-positive cells. As already reported by Lulli and colleagues, also Scott and co-workers could observe a decreased IFNK expression in NHK upon inhibition of EGFR kinase activity [31]. They extended this analysis to HPV16-positive cell lines and obtained the same result, strongly supporting the findings regarding the inhibition of ERK downstream of EGFR presented here. Furthermore, they applied the same TGFBR1 inhibitor that has been used in this work to NHK and HPV16-positive cells, observing the same reduction of IFNK transcription [31]. Interestingly, they generated evidence that the HPV16 E5 protein might participate in IFN- κ down-regulation by increasing EGFR- and decreasing TGF- β signaling, which perfectly fits the observations described here in NHK when using artificial ways of manipulating these pathways and might explain the less pronounced effects of trying to

DISCUSSION

manipulate *IFNK* expression in cell lines harboring the full HPV16 genome and therefore expressing the E5 protein. After all, *IFNK* transcription can still be induced in human keratinocytes carrying HPV16 genomes by manipulating the pathways identified to regulate its expression in uninfected keratinocytes. This results in the induction of *IFIT1* and therefore most probably also enhances expression of other ISGs, as shown in other studies analyzing the impact of IFN- κ on ISG expression [9, 23, 32, 38]. The concomitant decrease of viral transcription and the antiviral activity of IFN- κ determined by other studies [9, 23, 32, 38], suggests that the knowledge about its regulation might be valuable for future antiviral applications. Moreover, since *IFN- κ can also act on immune cells such as monocytes and dendritic cells and induce several cytokines without the need for a co-stimulatory signal [25], an increase in the local IFN- κ concentration might be beneficial to induce and/or enhance immune responses to epitheliotropic viruses in general. This feature of IFN- κ would be consistent with immune-modulatory actions known for other type I IFNs [3, 4]. Thinking about the anti-HPV activity of IFN- κ and the possibilities to modulate its expression, further investigations using an animal model for PV infection would provide the required insights to decide whether reactivation of IFN- κ expression could be therapeutically exploited.*

5.1.4. IFN- κ in Skin Disorders

*In addition to HPV infections, several skin disorders are characterized by an aberrant type I IFN signature [185] and this often correlates with an altered IFN- κ expression (references hereafter). IFN- κ expression is upregulated in skin from allergic contact dermatitis and lichen planus-affected skin but is downregulated or absent from atopic dermatitis lesions [186]. For psoriasis, two conflicting reports exist: one study observed increased, whereas the other study reported decreased IFN- κ levels [28, 186]. Some of the mentioned skin diseases represent a major health problem. For example, psoriasis imposes a high impact on the quality of life of about 2% of the world's population (Status 2013, [187]) and only a symptomatic treatment but no cure are available so far (Status 2016, [188]). Thus, further research is urgently needed. Even though the research concerning the role of IFN- κ in skin diseases is only at its very beginning, several skin pathologies might turn out to be affected by dysregulated IFN- κ levels. Hence, knowing the mechanisms by which *IFNK* is regulated may offer new perspectives concerning the treatment of those skin disorders, for which a causative link to dysregulated IFN- κ expression can be established. Indeed, recently, increased IFN- κ expression was shown to contribute to the pathology of cutaneous lupus erythematosus (CLE) [33, 34]. CLE is characterized by a constant reactivation of innate immunity pathways and an elevated type I IFN signature. In Europe and North America four out of 100,000 persons are diagnosed to suffer from CLE every year (Status 2019, [35]). However, apart from being an isolated phenomenon,*

DISCUSSION

CLE can also manifest as a part of systemic lupus erythmatosus (SLE). Approximately 70-80% of SLE patients develop CLE. Even though the incidence of SLE is slightly lower than for isolated CLE, those patients add to the number of individuals which suffer from the type I IFN-mediated, cytotoxic inflammation of the epidermis, which results in disfiguring lesions and often also manifests in fatigue and fever [35]. Importantly, the group of Michelle Kahlenberg demonstrated that IFN- κ increases the type I IFN response in lupus keratinocytes and thereby enhances production of pro-inflammatory IL-6 [34] and promotes UVB-induced apoptosis in CLE skin [33]. Hence, the findings presented here may be used to manipulate IFN- κ expression in other pathological settings, apart from infectious diseases (italicized section taken from author's publication [13], slightly modified).

5.2. HR-HPV and cGAS/STING Signaling

5.2.1. Strategies of Immune Evasion

Persisting infections with HR-HPVs can lead to cancer [50], highlighting the capability of these viruses to circumvent the immune system. To do so, the virus must avoid being detected and/or counteract antiviral defense mechanisms of its host. HPVs do not lyse their target cells, thereby abrogating a possible source of viral antigens for antigen-presenting cells and there is no blood-resident stage of the virus, thus lymphocytes, antibodies or the complement system cannot encounter virus particles or antigens in the blood stream. In addition to these passive strategies, the virus employs several active strategies to suppress the immune system: It down-regulates the transcription of several genes which contribute to different aspects of antiviral immunity and influences several cellular proteins via protein-protein interactions. With such strategies HPVs can on the one hand avoid inflammation and thus generate an environment, which is less likely to elicit antiviral immune responses but supports immune tolerance and on the other hand directly repress several sensing mechanisms or antiviral effectors [189, 190].

5.2.2. The cGAS/STING Pathway in HPV Infection

The cGAS/STING pathway senses the presence of DNA molecules which either indicates that the cell has been infected or that self-DNA leaks into the cytoplasm as a consequence of cellular stress such as viral infection or DNA damage [15]. Upon activation of the pathway, IFN- β is produced, and induces the expression of different antiviral ISGs. With this, the pathway represents a major hurdle to viral infection and deficiencies in this pathway result in enhanced susceptibility to viral infection in laboratory animals as well as in humans ([15], see also section 2.1.2.2). To complete their life cycle,

DISCUSSION

HPV rely on the DNA damage response (DDR) [69]. The E1 protein has been demonstrated to induce the DDR, either alone or together with E2. The E7 protein is known to increase the transcription of and stabilize the products of genes involved in the DDR and initiate DDR pathways [69, 191]. Thus, it can be speculated that these proteins induce the cGAS/STING pathway, resulting in the production of IFN- β . However, this might hold true for E1, but for E7 it was shown that it counteracts STING activity. HPV18 E7 binds STING [80] and HPV16 E7 mediates degradation of STING, both resulting in decreased type I IFN production [81]. Very recently it has been demonstrated that the E7 proteins from HPV16 and 18 additionally repress cGAS expression [192]. This study also revealed another repression strategy of the E7 protein, as it showed epigenetic silencing of the respective loci [192]. Thus, taken together, the E7 protein most probably mediates an inhibitory effect on cGAS/STING signaling. Similar, the HPV16 E6 protein confers a negative effect on IFN- β production as it has been demonstrated to bind to and inhibit the function of the IRF3 TF [78], which is important for the induction of *IFNB1* expression [168]. In contrast to E7, there are no reports which claim that E6 might activate cGAS/STING signaling.

5.2.3. *IFNB1* Induction in various Cell Types

As one of the inducible type I IFN genes, the *IFNB1* gene is only transcribed at very low levels in the absence of appropriate stimuli in uninfected keratinocytes (among others: [23], see section 2.1.2.1). Thus, first of all, it was sought to determine the appropriate stimuli to assess IFN- β production in dependency of the different HPV proteins. Advantageously, it turned out, that plasmid transfection triggers *IFNB1* transcription sustainably enough to measure transcriptional changes even 2 days post transfection; hence reporter gene activity can be measured without the need for a further stimulus. As a next step, it was tried to evaluate the effect of co-transfection of different HPV proteins on *IFNB1* Prom reporter activity in NHK. Unfortunately, no consistent effects could be detected in several experiments. The reason for this remains unclear, but it is possible that the activation of the *IFNB1*-promoter by the transfected DNA precedes the expression of the viral proteins by several hours and thus cannot be efficiently inhibited. As an alternative, the cGAS/STING-deficient cell line was tested which was used previously for studies involving herpesviral proteins [96, 193]. While the transfection resulted in a robust, cGAS/STING-dependent reporter activation, no consistent response to the co-expressed HPV proteins was observed (Figure 22 on page 101). A caveat of 293T cells is that they express adenoviral proteins and the large T antigen of SV40 which have activities similar to the HPV E1, E6 and E7 proteins [139-151] and thus might mask the effects of the co-expressed HPV proteins. To overcome this, two HPV-negative keratinocyte cell lines were tested for their utilizability. Interestingly, in the C33A cell line co-transfection of cGAS and STING induced the *IFNB1*

Prom reporter similar to the induction observed in 293T cells (compare Figure 23 on page 102 to Figure 22); strongly suggesting the cell line is at least STING-deficient. As C33A cells are widely used in the field of papillomavirus research, this finding opens up possibilities to assess the impact of an important DNA sensor in an HPV-relevant cellular environment.

5.2.4. Impact of HPV Proteins on *IFNB1* Reporter

The HPV16 E6 protein, which has been reported to interfere with *IFNB1* induction [78], repressed cGAS/STING-dependent *IFNB1* Prom reporter activity (Figure 24 on page 103). Moreover, the E2 proteins of both, HPV16 and HPV31, significantly diminished reporter activity (Figure 24). The E2 protein functions as a transcriptional regulator [70] and might repress the activity of the *IFNB1* reporter indirectly by regulating the activity of other proteins involved in the activation of the *IFNB1* gene. The HPV31 E8^{E2} protein, which contains the C-terminal domain of the E2 protein and is known to negatively regulate transcription [70] also repressed *IFNB1* reporter activity, whereas the effect of HPV16 E8^{E2} co-transfection is ambiguous (Figure 24). The E7 protein of HPV16 which has been reported to repress STING [81, 192] also slightly but significantly reduced *IFNB1* Prom reporter activity (Figure 24). After all, further studies are needed to determine the amount of expression plasmid needed for optimal expression of the respective protein and see whether the repressive effect can be observed in a dosage-dependent manner. A suboptimal amount of E1 expression plasmid might also account for the lack of *IFNB1* induction. This induction was expected as overexpression of E1 is known to induce DNA damage which has been shown to induce STING-dependent *IFNB1* transcription in keratinocytes [17, 69]. Overall, all of the tested HPV31 proteins had a greater impact on reporter activity than the respective HPV16 proteins. This might be caused by different expression levels but could also reflect differences between the proteins from different HPV types and awaits further investigation.

5.2.5. HPV E5 and STING Signaling

As HPV16 E5 is inserted in the ER membrane and known to interact with other transmembrane proteins [76], it was possible that it modulates the activity of the ER-resident STING protein [15]. Indeed, immunofluorescence showed co-localization of HPV16 and STING at perinuclear membranes (Figure 25B on page 106). Nonetheless, the E5 protein of HPV16 did not affect STING-dependent reporter activity (Figure 24). In contrast to this, the E5 protein of HPV31 readily repressed *IFNB1* Prom reporter activity, even though the non-tagged version did not reach statistical significance due to one outlier (Figure 23). The HPV31 E5 protein also co-localizes with STING at perinuclear

DISCUSSION

membranes (Figure 25B), suggesting that it might interact with STING in the ER membrane, imposing a negative effect on signaling downstream of STING. In contrast to HPV16 E5, HPV31 E5 has not yet been analyzed in great detail [76]. Even though, this localization as well as the co-localization with the STING protein might have been expected, to the best of the author's knowledge, this work provides the first immunofluorescence staining of the HPV31 E5 protein with or without STING in perinuclear membranes. The E5 proteins of HPV16 and HPV31 are closely related [194]. Nonetheless, there are some differences in the amino acid composition of the putative transmembrane regions of HPV31 E5 compared to the transmembrane region of HPV16 E5 [194] which might lead to different intramembrane interactions with other transmembrane proteins such as STING. The E5 protein of HPV31 was shown to co-immunoprecipitate with Bap31 upon overexpression of both proteins in 293TT cells [195]. Bap31 is one of the most abundant transmembrane ER proteins and ubiquitously expressed, also in the skin (<http://www.proteinatlas.org>, February 2020, [196, 197]). It is a pro-apoptotic protein and has been shown to induce cell death following ER stress, among others in HeLa cells [198], indicating that there might be a connection of Bap31 to the STING pathway in keratinocytes.

After all, attempting to assess the influence of different HPV proteins on STING signaling will broaden the knowledge on immune evasion strategies of these viruses, which might be useful to combat persistent infections and decrease HPV-related cancer cases.

6. Appendix

6.1. Supplemental Figures

6.1.1. Internal Deletions of *IFNK* Reporter Constructs

Figure 27 on the next page displays the results of additional reporter assays, which support the supposed involvement of AP-1 and SMAD3/4 TFs in *IFNK* gene activation. First of all, the deletion of the sequence from -4786 to -4741, which contains the second putative FOX BS, whose mutation did not have a significant impact on reporter activity in NHK and RTS3b (Figure 6 on page 78), did not alter reporter activity in any of the tested cell types either. This demonstrates that the deletion of sequence stretches per se does not alter reporter gene activity and supports the hypothesis that FOX TFs are not involved in *IFNK* activation, even though the mutation had some influence on reporter activity in HK 16E7 (Figure 6). The deletion of DNA parts which enclose the BS for either AP-1 or SMAD TFs leads to significant decrease of reporter activity in all three cell types (from left to right: AP-1: 11%, 20%, 21%; SMAD: 41%, 24%, 42%; Figure 27), suggesting importance of these BS for gene activity. Deletion of the HOX BS reduced activity to 21% in NHK but only mildly (58%) or not significantly in the immortalized cell types. Deletion of the last nucleotides of HS 2, where no candidate TFBS have been identified, decreased reporter activity to 42% in NHK, suggesting that another factor mediating activity might bind there. In the immortalized keratinocytes, which were tested first, no significant reduction of reporter activity could be observed in this region (Figure 27) and JASPAR analysis did not deliver a promising BS for a keratinocyte-related TF in this sequence part, thus this finding was not further analyzed.

APPENDIX

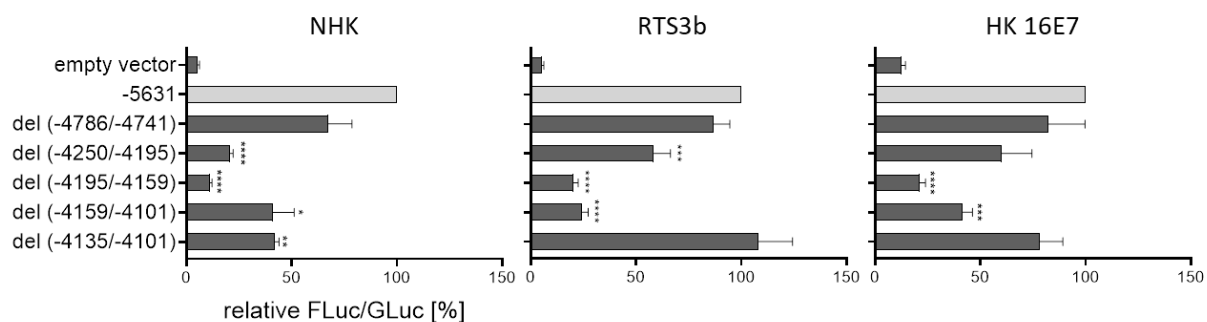


Figure 27: Deletion of sequences stretches encompassing putative TFBS influences reporter gene activity in human keratinocytes

Indicated cell types were transfected with the constructs listed on the left and luciferase activity was assayed 48 h post transfection. Luciferase activity is shown relative to the activity of the -5631 reporter construct (highlighted in light gray). Firefly luciferase (FLuc) activity was normalized to the expression of a co-transfected *Gussia* luciferase (GLuc) construct. Inset lists the TF which are predicted to bind to the DNA sequences deleted from the respective construct. Bars represent the average values and error bars the SEM. The average values for individual constructs are derived from $n \geq 3$ independent experiments. Significant deviations from the -5631 construct are denoted with asterisks (one-sample t-test: * < 0.05, ** < 0.01, *** < 0.001, ****). del = deletion.

6.1.2. Binding of Keratinocyte Proteins to the putative HOX BS

Figure 28A on the next page shows the sequence-independent binding of nuclear proteins derived from keratinocytes to the putative HOX BS. The absence of sequence-specific binding events to the 25 bp oligo strongly suggests that the observed reduction of reporter activity upon mutation of the predicted HOX BS (Figure 6 on page 78) is not due to the loss of TF binding. Figure 28B shows the impact of adding different amounts of poly(dI:dC). Increasing the amount of the competitor for unspecific DNA binding did not seem to alter the band pattern or intensity of HK 16E7 extracts. The same approach was tested with extracts derived from RTS3b, but the results remained inconclusive (data not shown).

APPENDIX

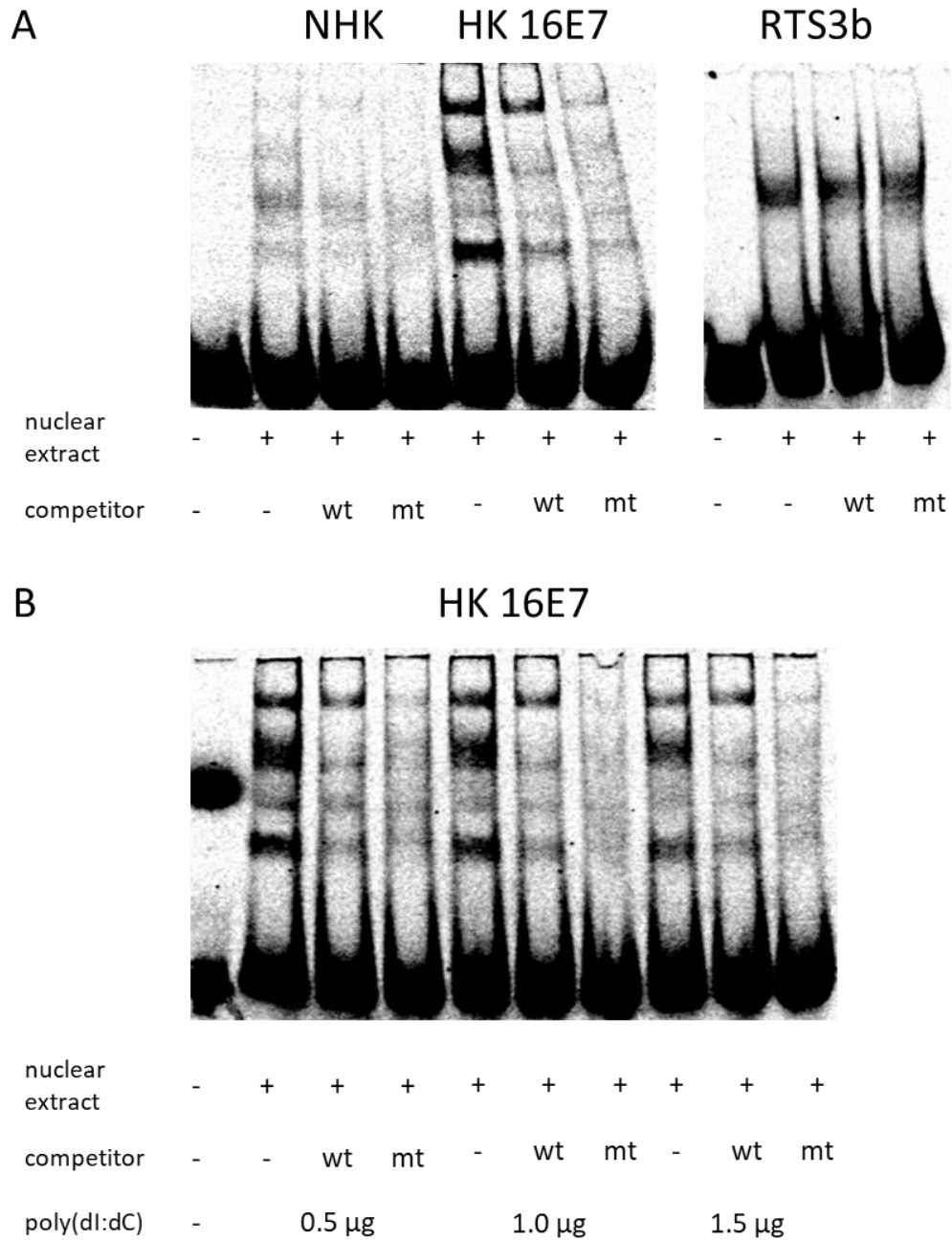


Figure 28: EMSA experiment with putative HOX binding site

EMSA was performed with nuclear extract from cell types listed above the gels and DY681-labeled oligos displaying the putative HOX BS. Unlabeled competitors were added in 100-fold excess. No specific shifts could be observed. A) Overview of results for different cell types, 1 µg poly(dI:dC) was used to prevent unspecific binding events. NHK experiment was performed only once and tried to be optimized using different nuclear extract preparations of both immortalized keratinocyte types. B) Varying amounts of competitor oligonucleotide for unspecific DNA binding (poly(dI:dC)) were added (n=1).

6.1.3. Effects of reduced Amounts of TGF- β on *IFNK* Transcription

Literature commonly suggests using concentrations of 5 ng/ml of TGF- β 1 in different, most often immortalized cell types. Due to personal experience with NHK, the dosage was increased 2- and 2.5-fold for the first experiment in NHK (n=1 each). However, this resulted in only 3.8-fold induction of the TGF- β target gene *SERPINE1*, which was much lower than expected, and inconsistent results regarding *IFNK* expression (3-fold downregulation with 10 ng/ml, unchanged with 12.5 ng/ml, data not shown). Thus, subsequent studies were performed with an increased concentration of 20 ng/ml. However, some remnants of freshly prepared NHK prompted me to investigate the effect of lower TGF- β doses: Indeed an 11.1- and 3.9-fold induction of *SERPINE1* and *IFNK* transcription, respectively, could also be achieved by adding 5 ng/ml TGF- β to the cells (Figure 29). Combination of this lower TGF- β concentration with 1 μ M of the ERKi resulted in a 21.1-fold induction of *IFNK*, concomitant with a 14.7-fold induction of *SERPINE1*. These findings are very similar to the results obtained with 20 ng/ml TGF- β and support the notion that TGF- β regulates the *IFNK* gene also at lower concentrations.

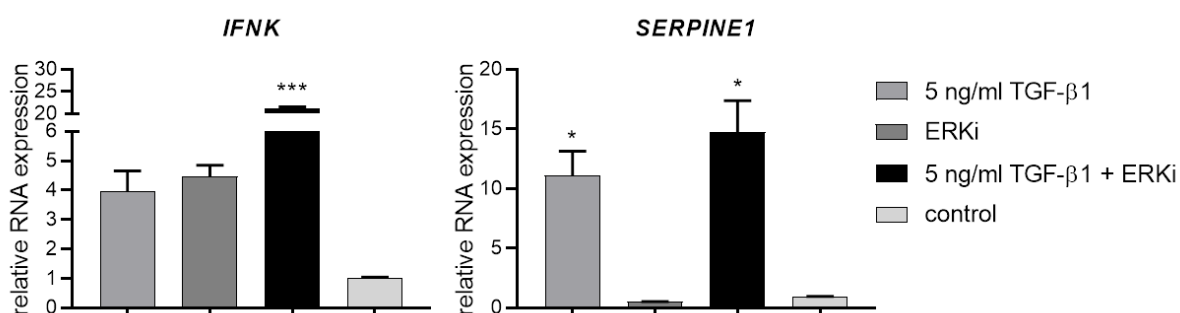


Figure 29: Treatment with 5 ng/ml TGF- β 1 results in similar induction of *IFNK* and *SERPINE1* transcription as achieved with 20 ng/ml TGF- β 1

NHK were treated for 24 h with the indicated substances and transcripts of genes listed above the diagrams were quantified by qPCR using *PGK1* as a reference gene and are given relative to the vehicle control. Error bars indicate the SEM. The average values were calculated from n=3 independent experiments. Significant deviations from the vehicle control are highlighted with asterisks (paired t-test: * < 0.05, *** < 0.001).

6.2. Curriculum Vitae

- 01/2017 - 06/2020: **Doctorate at the Institute for Medical Virology and Epidemiology of Viral Diseases, University Hospital Tübingen**
Regulation of IFN- κ Expression in Normal and HPV-positive Human Keratinocytes
- 10/2014 - 09/2016: **Study of Molecular Cellular Biology and Immunology at the Eberhard Karls University in Tübingen**
Additional subject: Parasitology
Master of Science: 1.05
Master thesis: 'Influence of non-coding mutation in the *DPH3* promoter on gene expression in skin cancer cell lines'; 1.0
- 10/2011 - 08/2014: **Study of Biology at the Eberhard Karls University in Tübingen**
Bachelor of Science: 1.2
Bachelor thesis: „Die Rolle von Elk-3 bei der retinalen Angiogenese und Homöostase des zerebralen Blutgefäßsystems“; 1.3
- 09/2010 - 08/2011: **Voluntary Social Year in the Crona Hospitals in Tübingen**
Nursing in the Urology Department
- 08/2010: **Internship in the Veterinary Clinic Domäne Ammerhof in Tübingen**
Accompanying veterinary doctors and nurses at their daily work
- 09/2001 - 6/2010: **Isolde-Kurz-Gymnasium Reutlingen**
Abitur: 1.4

6.3. Publications

Parts of the presented work have been published as following:

Klein, K., et al. (2020). "A TGF-beta- and p63-Responsive Enhancer Regulates IFN-kappa Expression in Human Keratinocytes." *J Immunol*: 1-11. [ji1901178](#).

6.4. Acknowledgement

In the following, I want to thank all the people who supported me during the making of this work.

First of all, I want to thank Prof. Dr. Frank Stubenrauch for giving me the opportunity to join his great working group and always being around when I needed scientific advice. We have had innumerable discussions which greatly contributed to the success of this work.

Furthermore, I want to thank Prof. Dr. Thomas Iftner who enabled me to graduate in the Virology Department and thereby broadening my knowledge on this fascinating topic.

I am very grateful that Prof. Dr. Stefan Stevanović agreed to supervise my work on behalf of the Faculty of Mathematics and Natural Sciences Tübingen and was willing to participate in my defense.

Moreover, Elke Straub, Aylin Yigitliler and all my other colleagues should be mentioned. Thank you for always supporting me, helping me with all the issues the daily work in a laboratory can bring and making me feel appreciated.

In addition, I want to warmly thank Dr. Ramona Businger who supported me with the handling of the fluorescence microscope and invested a lot of her precious time to ensure I gain optimal pictures.

I am glad Christina Habiger did great work in advance; this offered me the opportunity to directly start with this interesting project.

Last but not least, I would never have made it without the constant support of my loving family and boyfriend. You know, you mean the world to me.

7. References

1. Isaacs, A. and J. Lindenmann, *Virus interference. I. The interferon*. Proceedings of the Royal Society of London. Series B-Biological Sciences, 1957. **147**(927): p. 258-267.
2. Kirchner, H., et al., *Cytokine und Interferone, 1. Auflage, Spektrum*. 1993, Akademischer Verlag Heidelberg.
3. Fensterl, V., S. Chattopadhyay, and G.C. Sen, *No love lost between viruses and interferons*. Annual review of virology, 2015. **2**: p. 549-572.
4. McNab, F., et al., *Type I interferons in infectious disease*. Nature Reviews Immunology, 2015. **15**(2): p. 87-103.
5. Ortiz, A. and S.Y. Fuchs, *Anti-metastatic functions of type 1 interferons: Foundation for the adjuvant therapy of cancer*. Cytokine, 2017. **89**: p. 4-11.
6. Schneider, W.M., M.D. Chevillotte, and C.M. Rice, *Interferon-stimulated genes: a complex web of host defenses*. Annual review of immunology, 2014. **32**: p. 513-545.
7. Lazear, H.M., J.W. Schoggins, and M.S. Diamond, *Shared and distinct functions of type I and type III interferons*. Immunity, 2019. **50**(4): p. 907-923.
8. Hardy, M.P., et al., *Characterization of the type I interferon locus and identification of novel genes*. Genomics, 2004. **84**(2): p. 331-345.
9. LaFleur, D.W., et al., *Interferon- κ , a novel type I interferon expressed in human keratinocytes*. Journal of Biological Chemistry, 2001. **276**(43): p. 39765-39771.
10. Galani, I.E., O. Koltsida, and E. Andreakos, *Type III interferons (IFNs): emerging master regulators of immunity*, in *Crossroads between innate and adaptive immunity V*. 2015, Springer. p. 1-15.
11. Honda, K., et al., *IRF-7 is the master regulator of type-I interferon-dependent immune responses*. Nature, 2005. **434**(7034): p. 772-777.
12. Iversen, M.B. and S.R. Paludan, *Mechanisms of type III interferon expression*. Journal of Interferon Cytokine Research, 2010. **30**(8): p. 573-578.
13. Klein, K., et al., *A TGF- β - and p63-Responsive Enhancer Regulates IFN- κ Expression in Human Keratinocytes*. J Immunol, 2020: p. 1-11. j1901178.
14. Almine, J.F., et al., *IFI16 and cGAS cooperate in the activation of STING during DNA sensing in human keratinocytes*. Nature communications, 2017. **8**: p. 1-15. ncomms 14392.
15. Motwani, M., S. Pesiridis, and K.A. Fitzgerald, *DNA sensing by the cGAS–STING pathway in health and disease*. Nature Reviews Genetics, 2019. **20**(11): p. 657-674.
16. Mukai, K., et al., *Activation of STING requires palmitoylation at the Golgi*. Nature communications, 2016. **7**: p. 1-10. ncomms 11932.
17. Dunphy, G., et al., *Non-canonical activation of the DNA sensing adaptor STING by ATM and IFI16 mediates NF- κ B signaling after nuclear DNA damage*. Molecular cell, 2018. **71**(5): p. 745-760. e5.
18. Dansako, H., et al., *The cyclic GMP-AMP synthetase–STING signaling pathway is required for both the innate immune response against HBV and the suppression of HBV assembly*. The FEBS journal, 2016. **283**(1): p. 144-156.
19. Lam, E., S. Stein, and E. Falck-Pedersen, *Adenovirus detection by the cGAS/STING/TBK1 DNA sensing cascade*. Journal of virology, 2014. **88**(2): p. 974-981.
20. Sun, C., et al., *Evasion of innate cytosolic DNA sensing by a gammaherpesvirus facilitates establishment of latent infection*. The Journal of Immunology, 2015. **194**(4): p. 1819-1831.
21. Fung, K.Y., et al., *Interferon- ϵ protects the female reproductive tract from viral and bacterial infection*. Science, 2013. **339**(6123): p. 1088-1092.
22. Hermant, P., et al., *IFN- ϵ is constitutively expressed by cells of the reproductive tract and is inefficiently secreted by fibroblasts and cell lines*. PloS one, 2013. **8**(8): p. 1-9. e71320.

REFERENCES

23. Reiser, J., et al., *High-risk human papillomaviruses repress constitutive kappa interferon transcription via E6 to prevent pathogen recognition receptor and antiviral-gene expression*. Journal of Virology, 2011. **85**(21): p. 11372-11380.
24. Rincon-Orozco, B., et al., *Epigenetic silencing of interferon- κ in human papillomavirus type 16-positive cells*. Cancer research, 2009. **69**(22): p. 8718-8725.
25. Nardelli, B., et al., *Regulatory effect of IFN- κ , a novel type I IFN, on cytokine production by cells of the innate immune system*. The Journal of Immunology, 2002. **169**(9): p. 4822-4830.
26. Albertini, S., et al., *HPV18 Persistence Impairs Basal and DNA Ligand-Mediated IFN- β and IFN- λ 1 Production through Transcriptional Repression of Multiple Downstream Effectors of Pattern Recognition Receptor Signaling*. The Journal of Immunology, 2018. **200**(6): p. 2076-2089.
27. DeCarlo, C.A., et al., *IFN- κ , a novel type I IFN, is undetectable in HPV-positive human cervical keratinocytes*. Laboratory Investigation, 2010. **90**(10): p. 1482-1491.
28. Li, Y., et al., *Interferon Kappa Is Up-Regulated in Psoriasis and It Up-Regulates Psoriasis-Associated Cytokines in vivo*. Clinical, Cosmetic and Investigational Dermatology, 2019. **12**: p. 865-873.
29. Lulli, D., M. Carbone, and S. Pastore, *The MEK inhibitors trametinib and cobimetinib induce a type I interferon response in human keratinocytes*. International journal of molecular sciences, 2017. **18**(10): p. 1-13. 2227.
30. Lulli, D., M.L. Carbone, and S. Pastore, *Epidermal growth factor receptor inhibitors trigger a type I interferon response in human skin*. Oncotarget, 2016. **7**(30): p. 47777-47793.
31. Scott, M.L., et al., *Human Papillomavirus 16 E5 Inhibits Interferon Signaling and Supports Episomal Viral Maintenance*. Journal of Virology, 2020. **94**(2): p. e01582-19.
32. Habiger, C., et al., *Interferon kappa inhibits human papillomavirus 31 transcription by inducing Sp100 proteins*. Journal of virology, 2016. **90**(2): p. 694-704.
33. Sarkar, M.K., et al., *Photosensitivity and type I IFN responses in cutaneous lupus are driven by epidermal-derived interferon kappa*. Annals of the rheumatic diseases, 2018. **77**(11): p. 1653-1664.
34. Stannard, J.N., et al., *Lupus skin is primed for IL-6 inflammatory responses through a keratinocyte-mediated autocrine type I interferon loop*. Journal of Investigative Dermatology, 2017. **137**(1): p. 115-122.
35. Wenzel, J., *Cutaneous lupus erythematosus: new insights into pathogenesis and therapeutic strategies*. Nature Reviews Rheumatology, 2019. **15**(9): p. 519-532.
36. Dell'Oste, V., et al., *Altered expression of UVB-induced cytokines in human papillomavirus-immortalized epithelial cells*. Journal of general virology, 2008. **89**(10): p. 2461-2466.
37. Evans, M.R., et al., *Human papillomavirus 16 E2 regulates keratinocyte gene expression relevant to cancer and the viral life cycle*. Journal of virology, 2019. **93**(4): p. e01941-18.
38. Woodby, B.L., et al., *Induction of interferon kappa in human papillomavirus 16 infection by transforming growth factor beta-induced promoter demethylation*. Journal of virology, 2018. **92**(8): p. e01714-17.
39. Sunthamala, N., et al., *E2 proteins of high risk human papillomaviruses down-modulate STING and IFN- κ transcription in keratinocytes*. PloS one, 2014. **9**(3): p. 1-11. e91473.
40. Lo Cigno, I., et al., *The Nuclear DNA Sensor IFI16 Acts as a Restriction Factor for Human Papillomavirus Replication through Epigenetic Modifications of the Viral Promoters*. J Virol, 2015. **89**(15): p. 7506-20.
41. Saikia, P., V. Fensterl, and G.C. Sen, *The inhibitory action of P56 on select functions of E1 mediates interferon's effect on human papillomavirus DNA replication*. Journal of virology, 2010. **84**(24): p. 13036-13039.
42. Terenzi, F., P. Saikia, and G.C. Sen, *Interferon-inducible protein, P56, inhibits HPV DNA replication by binding to the viral protein E1*. The EMBO journal, 2008. **27**(24): p. 3311-3321.
43. Stepp, W.H., J.M. Meyers, and A.A. McBride, *Sp100 provides intrinsic immunity against human papillomavirus infection*. MBio, 2013. **4**(6): p. e00845-13.

REFERENCES

44. Stepp, W.H., et al., *Sp100 colocalizes with HPV replication foci and restricts the productive stage of the infectious cycle*. PLoS pathogens, 2017. **13**(10): p. 1-31. e1006660.
45. Egawa, N., et al., *Human papillomaviruses; epithelial tropisms, and the development of neoplasia*. Viruses, 2015. **7**(7): p. 3863-3890.
46. Knipe, D., et al., *Fields Virology*. 2007. **2**.
47. Van Doorslaer, K., *Evolution of the papillomaviridae*. Virology, 2013. **445**(1-2): p. 11-20.
48. Bernard, H.-U., et al., *Classification of papillomaviruses (PVs) based on 189 PV types and proposal of taxonomic amendments*. Virology, 2010. **401**(1): p. 70-79.
49. De Villiers, E.-M., et al., *Classification of papillomaviruses*. Virology, 2004. **324**(1): p. 17-27.
50. Gheit, T., *Mucosal and cutaneous human papillomavirus infection and cancer biology*. Frontiers in oncology, 2019. **9**: p. 1-22. 355.
51. Bruni, L., et al., *ICO/IARC Information Centre on HPV and Cancer (HPV Information Centre). Human Papillomavirus and Related Diseases in the World. Summary Report 22 January 2019*. 2019.
52. Walboomers, J.M., et al., *Human papillomavirus is a necessary cause of invasive cervical cancer worldwide*. J Pathol, 1999. **189**(1): p. 12-19.
53. Guan, P., et al., *Human papillomavirus types in 115,789 HPV-positive women: a meta-analysis from cervical infection to cancer*. International journal of cancer, 2012. **131**(10): p. 2349-2359.
54. Chaturvedi, A.K., et al., *Human papillomavirus and rising oropharyngeal cancer incidence in the United States*. Journal of clinical oncology, 2011. **29**(32): p. 4294-4301.
55. Gillison, M.L., et al., *Epidemiology of human papillomavirus-positive head and neck squamous cell carcinoma*. Journal of clinical oncology, 2015. **33**(29): p. 3235-3242.
56. Bodelon, C., et al., *Genomic characterization of viral integration sites in HPV-related cancers*. International journal of cancer, 2016. **139**(9): p. 2001-2011.
57. Hong, D., et al., *Viral E6 is overexpressed via high viral load in invasive cervical cancer with episomal HPV16*. BMC cancer, 2017. **17**(1): p. 1-8. 136.
58. Duggan, M.A., et al., *HPV DNA typing of adult-onset respiratory papillomatosis*. The Laryngoscope, 1990. **100**(6): p. 639-642.
59. Gissmann, L., E.M. De Villiers, and H.Z. Hausen, *Analysis of human genital warts (condylomata acuminata) and other genital tumors for human papillomavirus type 6 DNA*. International journal of cancer, 1982. **29**(2): p. 143-146.
60. Siti-Aishah, M., et al., *Detection of Human Papillomavirus Using In Situ Hybridization Technique in Vulvo-Vaginal Warts*. The Malaysian journal of medical sciences: MJMS, 2000. **7**(2): p. 27-31.
61. Doorbar, J., et al., *The biology and life-cycle of human papillomaviruses*. Vaccine, 2012. **30**: p. F55-F70.
62. McBride, A.A., *Mechanisms and strategies of papillomavirus replication*. Biological chemistry, 2017. **398**(8): p. 919-927.
63. Kines, R.C., et al., *The initial steps leading to papillomavirus infection occur on the basement membrane prior to cell surface binding*. Proceedings of the National Academy of Sciences, 2009. **106**(48): p. 20458-20463.
64. Roberts, J.N., et al., *Genital transmission of HPV in a mouse model is potentiated by nonoxynol-9 and inhibited by carrageenan*. Nature medicine, 2007. **13**(7): p. 857-861.
65. Schiller, J.T., P.M. Day, and R.C. Kines, *Current understanding of the mechanism of HPV infection*. Gynecologic oncology, 2010. **118**(1): p. S12-S17.
66. Schmitt, A., et al., *The primary target cells of the high-risk cottontail rabbit papillomavirus colocalize with hair follicle stem cells*. Journal of virology, 1996. **70**(3): p. 1912-1922.
67. Herfs, M., et al., *A discrete population of squamocolumnar junction cells implicated in the pathogenesis of cervical cancer*. Proceedings of the National Academy of Sciences, 2012. **109**(26): p. 10516-10521.

REFERENCES

68. Bergvall, M., T. Melendy, and J. Archambault, *The E1 proteins*. Virology, 2013. **445**(1-2): p. 35-56.
69. Bristol, M.L., D. Das, and I.M. Morgan, *Why human papillomaviruses activate the DNA damage response (DDR) and how cellular and viral replication persists in the presence of DDR signaling*. Viruses, 2017. **9**(10): p. 1-16. 268.
70. McBride, A.A., *The papillomavirus E2 proteins*. Virology, 2013. **445**(1-2): p. 57-79.
71. Jeckel, S., et al., *Identification of the E9^Δ E2C cDNA and functional characterization of the gene product reveal a new repressor of transcription and replication in cottontail rabbit papillomavirus*. Journal of virology, 2003. **77**(16): p. 8736-8744.
72. Stubenrauch, F., et al., *The E8 repression domain can replace the E2 transactivation domain for growth inhibition of HeLa cells by papillomavirus E2 proteins*. International journal of cancer, 2007. **121**(10): p. 2284-2292.
73. Stubenrauch, F., T. Zobel, and T. Iftner, *The E8 domain confers a novel long-distance transcriptional repression activity on the E8^Δ E2C protein of high-risk human papillomavirus type 31*. Journal of virology, 2001. **75**(9): p. 4139-4149.
74. Zobel, T., T. Iftner, and F. Stubenrauch, *The papillomavirus E8^Δ E2C protein represses DNA replication from extrachromosomal origins*. Molecular and cellular biology, 2003. **23**(22): p. 8352-8362.
75. Doorbar, J., *The E4 protein; structure, function and patterns of expression*. Virology, 2013. **445**(1-2): p. 80-98.
76. DiMaio, D. and L.M. Petti, *The E5 proteins*. Virology, 2013. **445**(1-2): p. 99-114.
77. Pol, S.B.V. and A.J. Klingelutz, *Papillomavirus E6 oncoproteins*. Virology, 2013. **445**(1-2): p. 115-137.
78. Ronco, L.V., et al., *Human papillomavirus 16 E6 oncoprotein binds to interferon regulatory factor-3 and inhibits its transcriptional activity*. Genes & development, 1998. **12**(13): p. 2061-2072.
79. Roman, A. and K. Munger, *The papillomavirus E7 proteins*. Virology, 2013. **445**(1-2): p. 138-168.
80. Lau, L., et al., *DNA tumor virus oncogenes antagonize the cGAS-STING DNA-sensing pathway*. Science, 2015. **350**(6260): p. 568-571.
81. Luo, X., et al., *HPV16 drives cancer immune escape via NLRX1-mediated degradation of STING*. The Journal of Clinical Investigation, 2019: p. 1-18. JCI129497.
82. Buck, C.B., P.M. Day, and B.L. Trus, *The papillomavirus major capsid protein L1*. Virology, 2013. **445**(1-2): p. 169-174.
83. Wang, J.W. and R.B. Roden, *L2, the minor capsid protein of papillomavirus*. Virology, 2013. **445**(1-2): p. 175-186.
84. Roden, R.B. and P.L. Stern, *Opportunities and challenges for human papillomavirus vaccination in cancer*. Nature Reviews Cancer, 2018. **18**(4): p. 240-254.
85. Auersperg, N., *Long-term cultivation of hypodiploid human tumor cells*. Journal of the National Cancer Institute, 1964. **32**(1): p. 135-163.
86. Scheffner, M., et al., *The state of the p53 and retinoblastoma genes in human cervical carcinoma cell lines*. Proceedings of the National Academy of Sciences of the United States of America, 1991. **88**(13): p. 5523-5527.
87. Yee, C., et al., *Presence and expression of human papillomavirus sequences in human cervical carcinoma cell lines*. The American journal of pathology, 1985. **119**(3): p. 361-366.
88. Jainchill, J.L., S.A. Aaronson, and G.J. Todaro, *Murine sarcoma and leukemia viruses: assay using clonal lines of contact-inhibited mouse cells*. Journal of virology, 1969. **4**(5): p. 549-553.
89. Graham, F.L., et al., *Characteristics of a human cell line transformed by DNA from human adenovirus type 5*. Journal of general virology, 1977. **36**(1): p. 59-72.
90. Yuan, J., et al., *The Scattered Twelve Tribes of HEK293*. Biomedical and Pharmacology Journal, 2018. **11**(2): p. 621-623.

REFERENCES

91. Straub, E., et al., *The viral E8^A E2C repressor limits productive replication of human papillomavirus 16*. Journal of virology, 2014. **88**(2): p. 937-947.
92. Straub, E., et al., *Characterization of the human papillomavirus 16 E8 promoter*. Journal of virology, 2015. **89**(14): p. 7304-7313.
93. Purdie, K.J., et al., *Malignant transformation of cutaneous lesions in renal allograft patients: a role for human papillomavirus?* Cancer research, 1993. **53**(21): p. 5328-5333.
94. Habiger, C., *Die Wirkung von Interferon-kappa auf karzinogene humane Papillomviren*. 2015, Eberhard-Karls-Universität zu Tübingen.
95. Lin, R., et al., *Selective DNA binding and association with the CREB binding protein coactivator contribute to differential activation of alpha/beta interferon genes by interferon regulatory factors 3 and 7*. Molecular and cellular biology, 2000. **20**(17): p. 6342-6353.
96. Stempel, M., et al., *The herpesviral antagonist m152 reveals differential activation of STING-dependent IRF and NF- κ B signaling and STING's dual role during MCMV infection*. The EMBO journal, 2019. **38**(5): p. 1-22. e100983.
97. Ausubel, F., et al., *Current Protocols in Molecular Biology (Greene/Wiley)*. 1990, Interscience, New York.
98. Mullis, K., et al. *Specific enzymatic amplification of DNA in vitro: the polymerase chain reaction*. in *Cold Spring Harbor symposia on quantitative biology*. 1986. Cold Spring Harbor Laboratory Press.
99. Vosberg, H.-P., *Molecular cloning of DNA*. Human genetics, 1977. **40**(1): p. 1-72.
100. Blacker, K.L., M.L. Williams, and M. Goldyne, *Mitomycin C-Treated 3 T 3 Fibroblasts Used as Feeder Layers for Human Keratinocyte Culture Retain the Capacity to Generate Eicosanoids*. Journal of investigative dermatology, 1987. **89**(6): p. 536-539.
101. Nikfarjam, L. and P. Farzaneh, *Prevention and detection of Mycoplasma contamination in cell culture*. Cell Journal (Yakhteh), 2012. **13**(4): p. 203-212.
102. Uphoff, C.C. and H.G. Drexler, *Detection of mycoplasma contamination in cell cultures*. Current protocols in molecular biology, 2014. **106**(1): p. 28.4. 1-28.4. 14.
103. Pfaffl, M.W., *A new mathematical model for relative quantification in real-time RT-PCR*. Nucleic acids research, 2001. **29**(9): p. e45-e45.
104. Burnette, W.N., *"Western blotting": electrophoretic transfer of proteins from sodium dodecyl sulfate-polyacrylamide gels to unmodified nitrocellulose and radiographic detection with antibody and radioiodinated protein A*. Analytical biochemistry, 1981. **112**(2): p. 195-203.
105. Laemmli, U.K., *Cleavage of structural proteins during the assembly of the head of bacteriophage T4*. nature, 1970. **227**(5259): p. 680-685.
106. Habig, M., et al., *E7 proteins from high-and low-risk human papillomaviruses bind to TGF- β -regulated Smad proteins and inhibit their transcriptional activity*. Archives of virology, 2006. **151**(10): p. 1961-1972.
107. Eferl, R. and E.F. Wagner, *AP-1: a double-edged sword in tumorigenesis*. Nature Reviews Cancer, 2003. **3**(11): p. 859-868.
108. Aikawa, Y., et al., *Treatment of arthritis with a selective inhibitor of c-Fos/activator protein-1*. Nature biotechnology, 2008. **26**(7): p. 817-823.
109. Bogoyevitch, M.A. and B. Kobe, *Uses for JNK: the many and varied substrates of the c-Jun N-terminal kinases*. Microbiol. Mol. Biol. Rev., 2006. **70**(4): p. 1061-1095.
110. Lamouille, S., J. Xu, and R. Derynck, *Molecular mechanisms of epithelial-mesenchymal transition*. Nature reviews Molecular cell biology, 2014. **15**(3): p. 178-196.
111. Santibañez, J.F., *JNK mediates TGF- β 1-induced epithelial mesenchymal transdifferentiation of mouse transformed keratinocytes*. FEBS letters, 2006. **580**(22): p. 5385-5391.
112. Sundqvist, A., et al., *JUNB governs a feed-forward network of TGF β signaling that aggravates breast cancer invasion*. Nucleic acids research, 2017. **46**(3): p. 1180-1195.
113. Dennler, S., et al., *Direct binding of Smad3 and Smad4 to critical TGF β -inducible elements in the promoter of human plasminogen activator inhibitor-type 1 gene*. The EMBO journal, 1998. **17**(11): p. 3091-3100.

REFERENCES

114. Yoon, S. and R. Seger, *The extracellular signal-regulated kinase: multiple substrates regulate diverse cellular functions*. Growth factors, 2006. **24**(1): p. 21-44.
115. Avruch, J., X.-f. Zhang, and J.M. Kyriakis, *Raf meets Ras: completing the framework of a signal transduction pathway*. Trends in biochemical sciences, 1994. **19**(7): p. 279-283.
116. Blumer, K.J. and G.L. Johnson, *Diversity in function and regulation of MAP kinase pathways*. Trends in biochemical sciences, 1994. **19**(6): p. 236-240.
117. Derynck, R. and E.H. Budi, *Specificity, versatility, and control of TGF- β family signaling*. Sci. Signal., 2019. **12**(570): p. 1-24. eaav5183.
118. Inman, G.J., et al., *SB-431542 is a potent and specific inhibitor of transforming growth factor- β superfamily type I activin receptor-like kinase (ALK) receptors ALK4, ALK5, and ALK7*. Molecular pharmacology, 2002. **62**(1): p. 65-74.
119. Moses, H.L., *TGF- β regulation of epithelial cell proliferation*. Molecular reproduction and development, 1992. **32**(2): p. 179-184.
120. Pietenpol, J.A., et al., *TGF- β 1 inhibition of c-myc transcription and growth in keratinocytes is abrogated by viral transforming proteins with pRB binding domains*. Cell, 1990. **61**(5): p. 777-785.
121. Songcock, W.K., S.-m. Kim, and J.M. Bodily, *The human papillomavirus E7 oncoprotein as a regulator of transcription*. Virus research, 2017. **231**: p. 56-75.
122. Buontempo, P.J., et al., *Antiviral activity of transiently expressed IFN- κ is cell-associated*. Journal of interferon & cytokine research, 2006. **26**(1): p. 40-52.
123. Ali, S., L.A. Hardy, and J.A. Kirby, *Transplant immunobiology: a crucial role for heparan sulfate glycosaminoglycans?* Transplantation, 2003. **75**(11): p. 1773-1782.
124. Fernandez-Botran, R., J. Yan, and D.E. Justus, *Binding of interferon γ by glycosaminoglycans: a strategy for localization and/or inhibition of its activity*. Cytokine, 1999. **11**(5): p. 313-325.
125. Chung, K.-Y., et al., *An AP-1 binding sequence is essential for regulation of the human 2 (I) collagen (COL1A2) promoter activity by transforming growth factor*. Journal of Biological Chemistry, 1996. **271**(6): p. 3272-3278.
126. Keeton, M.R., et al., *Identification of regulatory sequences in the type 1 plasminogen activator inhibitor gene responsive to transforming growth factor beta*. Journal of Biological Chemistry, 1991. **266**(34): p. 23048-23052.
127. Koinuma, D., et al., *Chromatin immunoprecipitation on microarray analysis of Smad2/3 binding sites reveals roles of ETS1 and TFAP2A in transforming growth factor β signaling*. Molecular cellular biology, 2009. **29**(1): p. 172-186.
128. Zhang, Y., X.-H. Feng, and R. Derynck, *Smad3 and Smad4 cooperate with c-Jun/c-Fos to mediate TGF- β -induced transcription*. Nature, 1998. **394**(6696): p. 909-913.
129. Lachmann, A., et al., *Massive mining of publicly available RNA-seq data from human and mouse*. Nature communications, 2018. **9**(1): p. 1366-1375.
130. De Andrade, J.P., et al., *EGFR is regulated by TFAP2C in luminal breast cancer and is a target for vandetanib*. Molecular cancer therapeutics, 2016. **15**(3): p. 503-511.
131. Park, J., et al., *The role of Tcfap2c in tumorigenesis and cancer growth in an activated Neu model of mammary carcinogenesis*. Oncogene, 2015. **34**(50): p. 6105-6114.
132. Botchkarev, V.A. and E.R. Flores, *p53/p63/p73 in the epidermis in health and disease*. Cold Spring Harbor perspectives in medicine, 2014. **4**(8): p. 1-12. a015248.
133. Levine, A.J., et al., *The p53 family: guardians of maternal reproduction*. Nature reviews Molecular cell biology, 2011. **12**(4): p. 1-7. 259.
134. Vassilev, L.T., et al., *In vivo activation of the p53 pathway by small-molecule antagonists of MDM2*. Science, 2004. **303**(5659): p. 844-848.
135. Gallant-Behm, C.L., et al., *Δ Np63 α represses anti-proliferative genes via H2A. Z deposition*. Genes development, 2012. **26**(20): p. 2325-2336.
136. McDade, S.S., et al., *Genome-wide characterization reveals complex interplay between TP53 and TP63 in response to genotoxic stress*. Nucleic acids research, 2014. **42**(10): p. 6270-6285.

REFERENCES

137. Kouwenhoven, E.N., et al., *Transcription factor p63 bookmarks and regulates dynamic enhancers during epidermal differentiation*. EMBO reports, 2015. **16**(7): p. 863-878.
138. Chang, Y.E. and L.A. Laimins, *Microarray analysis identifies interferon-inducible genes and Stat-1 as major transcriptional targets of human papillomavirus type 31*. Journal of virology, 2000. **74**(9): p. 4174-4182.
139. DeCaprio, J.A., et al., *SV40 large tumor antigen forms a specific complex with the product of the retinoblastoma susceptibility gene*. Cell, 1988. **54**(2): p. 275-283.
140. Dyson, N., et al., *The human papilloma virus-16 E7 oncoprotein is able to bind to the retinoblastoma gene product*. Science, 1989. **243**(4893): p. 934-937.
141. Lane, D.P. and L.V. Crawford, *T antigen is bound to a host protein in SV40-transformed cells*. Nature, 1979. **278**(5701): p. 261-263.
142. Linzer, D.I. and A.J. Levine, *Characterization of a 54K dalton cellular SV40 tumor antigen present in SV40-transformed cells and uninfected embryonal carcinoma cells*. Cell, 1979. **17**(1): p. 43-52.
143. Werness, B.A., A.J. Levine, and P.M. Howley, *Association of human papillomavirus types 16 and 18 E6 proteins with p53*. Science, 1990. **248**(4951): p. 76-79.
144. Sarnow, P., et al., *Adenovirus E1b-58kd tumor antigen and SV40 large tumor antigen are physically associated with the same 54 kd cellular protein in transformed cells*. Cell, 1982. **28**(2): p. 387-394.
145. Whyte, P., et al., *Association between an oncogene and an anti-oncogene: the adenovirus E1A proteins bind to the retinoblastoma gene product*. Nature, 1988. **334**(6178): p. 124-129.
146. Collins, K.L. and T.J. Kelly, *Effects of T antigen and replication protein A on the initiation of DNA synthesis by DNA polymerase alpha-primase*. Molecular and Cellular Biology, 1991. **11**(4): p. 2108-2115.
147. Conger, K.L., et al., *Human papillomavirus DNA replication interactions between the viral E1 protein and two subunits of human DNA polymerase alpha/primase*. Journal of Biological Chemistry, 1999. **274**(5): p. 2696-2705.
148. Han, Y., et al., *Interactions of the papovavirus DNA replication initiator proteins, bovine papillomavirus type 1 E1 and simian virus 40 large T antigen, with human replication protein A*. Journal of virology, 1999. **73**(6): p. 4899-4907.
149. Masterson, P.J., et al., *A C-terminal helicase domain of the human papillomavirus E1 protein binds E2 and the DNA polymerase alpha-primase p68 subunit*. Journal of virology, 1998. **72**(9): p. 7407-7419.
150. Melendy, T. and B. Stillman, *An interaction between replication protein A and SV40 T antigen appears essential for primosome assembly during SV40 DNA replication*. Journal of Biological Chemistry, 1993. **268**(5): p. 3389-3395.
151. Park, P., et al., *The cellular DNA polymerase alpha-primase is required for papillomavirus DNA replication and associates with the viral E1 helicase*. Proceedings of the National Academy of Sciences, 1994. **91**(18): p. 8700-8704.
152. Bhattacharjee, O., et al., *Unraveling the ECM-Immune Cell Crosstalk in Skin Diseases*. Frontiers in cell developmental biology, 2019. **7**: p. 1-24. 68.
153. Fuchs, E. and S. Raghavan, *Getting under the skin of epidermal morphogenesis*. Nature Reviews Genetics, 2002. **3**(3): p. 199-209.
154. Baker, B., et al., *Normal keratinocytes express toll-like receptors (TLRs) 1, 2 and 5: modulation of TLR expression in chronic plaque psoriasis*. British Journal of Dermatology, 2003. **148**(4): p. 670-679.
155. Kalali, B.N., et al., *Double-stranded RNA induces an antiviral defense status in epidermal keratinocytes through TLR3-, PKR-, and MDA5/RIG-I-mediated differential signaling*. The Journal of Immunology, 2008. **181**(4): p. 2694-2704.
156. Lebre, M.C., et al., *Human keratinocytes express functional Toll-like receptor 3, 4, 5, and 9*. Journal of Investigative Dermatology, 2007. **127**(2): p. 331-341.

REFERENCES

157. Weinstock, H., S. Berman, and W. Cates Jr, *Sexually transmitted diseases among American youth: incidence and prevalence estimates, 2000*. Perspectives on sexual and reproductive health, 2004. **36**(1): p. 6-10.
158. Bruni, L., et al., *Cervical human papillomavirus prevalence in 5 continents: meta-analysis of 1 million women with normal cytological findings*. Journal of Infectious Diseases, 2010. **202**(12): p. 1789-1799.
159. Nyitray, A.G. and M.R. Iannacone, *The epidemiology of human papillomaviruses*, in *Human Papillomavirus*. 2014, Karger Publishers. p. 75-91.
160. Guo, Y.J., et al., *ERK/MAPK signalling pathway and tumorigenesis*. Experimental and Therapeutic Medicine, 2020. **19**(3): p. 1997-2007.
161. Vaquerizas, J.M., et al., *A census of human transcription factors: function, expression and evolution*. Nature Reviews Genetics, 2009. **10**(4): p. 252-263.
162. Huth, J.R., et al., *The solution structure of an HMG-I (Y)-DNA complex defines a new architectural minor groove binding motif*. Nature structural biology, 1997. **4**(8): p. 657-665.
163. Sgarra, R., et al., *High Mobility Group A (HMGA): Chromatin Nodes Controlled by a Knotty miRNA Network*. International Journal of Molecular Sciences, 2020. **21**(3): p. 1-30. 717.
164. Reeves, R. and M.S. Nissen, *The AT-DNA-binding domain of mammalian high mobility group I chromosomal proteins. A novel peptide motif for recognizing DNA structure*. Journal of Biological Chemistry, 1990. **265**(15): p. 8573-8582.
165. Bouallaga, I., et al., *An enhanceosome containing the Jun B/Fra-2 heterodimer and the HMG-I (Y) architectural protein controls HPV18 transcription*. EMBO reports, 2000. **1**(5): p. 422-427.
166. Bouallaga, I. and F. Thierry, *Control of Human Papillomavirus type 18 transcription: role in carcinogenesis*. Recent Research Developments in Virology, 1999. **1**: p. 369-383.
167. Bouallaga, I., et al., *HMG-I (Y) and the CBP/p300 coactivator are essential for human papillomavirus type 18 enhanceosome transcriptional activity*. Molecular and cellular biology, 2003. **23**(7): p. 2329-2340.
168. Panne, D., T. Maniatis, and S. Harrison, *An atomic model of the interferon- β enhanceosome*. Cell, 2007. **129**(6): p. 1111-1123.
169. Falvo, J.V., et al., *Assembly of a functional beta interferon enhanceosome is dependent on ATF-2-c-Jun heterodimer orientation*. Molecular cellular biology, 2000. **20**(13): p. 4814-4825.
170. Antonini, D., et al., *An autoregulatory loop directs the tissue-specific expression of p63 through a long-range evolutionarily conserved enhancer*. Molecular cellular biology, 2006. **26**(8): p. 3308-3318.
171. McDade, S.S., et al., *Genome-wide analysis of p63 binding sites identifies AP-2 factors as co-regulators of epidermal differentiation*. Nucleic acids research, 2012. **40**(15): p. 7190-7206.
172. Koster, M.I., et al., *p63 is the molecular switch for initiation of an epithelial stratification program*. Genes development, 2004. **18**(2): p. 126-131.
173. Mills, A.A., et al., *p63 is a p53 homologue required for limb and epidermal morphogenesis*. Nature, 1999. **398**(6729): p. 708-713.
174. Yang, A., et al., *p63, a p53 homolog at 3q27-29, encodes multiple products with transactivating, death-inducing, and dominant-negative activities*. Molecular cell, 1998. **2**(3): p. 305-316.
175. Kurita, M., et al., *In vivo reprogramming of wound-resident cells generates skin epithelial tissue*. Nature, 2018. **561**(7722): p. 243-247.
176. Bennett, K.L., T. Romigh, and C. Eng, *AP-2 α Induces Epigenetic Silencing of Tumor Suppressive Genes and Microsatellite Instability in Head and Neck Squamous Cell Carcinoma*. PLoS One, 2009. **4**(9): p. 1-8. e6931.
177. Kousa, Y.A., E. Fuller, and B.C. Schutte, *IRF6 and AP2A Interaction Regulates Epidermal Development*. Journal of Investigative Dermatology, 2018. **138**(12): p. 2578-2588.
178. Oyama, N., et al., *Different properties of three isoforms (α , β , and γ) of transcription factor AP-2 in the expression of human keratinocyte genes*. Archives of dermatological research, 2002. **294**(6): p. 273-280.

REFERENCES

179. Yang, A., et al., *p63 is essential for regenerative proliferation in limb, craniofacial and epithelial development*. *Nature*, 1999. **398**(6729): p. 714-718.
180. Litwin, T., et al., *Somatic host cell alterations in HPV carcinogenesis*. *Viruses*, 2017. **9**(8): p. 1-22. 206.
181. Ramirez, H., S.B. Patel, and I. Pastar, *The role of TGF β signaling in wound epithelialization*. *Advances in wound care*, 2014. **3**(7): p. 482-491.
182. Barrientos, S., et al., *Growth factors and cytokines in wound healing*. *Wound repair and regeneration*, 2008. **16**(5): p. 585-601.
183. Kennedy-Crispin, M., et al., *Human keratinocytes' response to injury upregulates CCL20 and other genes linking innate and adaptive immunity*. *Journal of investigative dermatology*, 2012. **132**(1): p. 105-113.
184. Klingenberg, J.M., et al., *Engineered human skin substitutes undergo large-scale genomic reprogramming and normal skin-like maturation after transplantation to athymic mice*. *Journal of investigative dermatology*, 2010. **130**(2): p. 587-601.
185. Hile, G.A., J.E. Gudjonsson, and J.M. Kahlenberg, *The influence of interferon on healthy and diseased skin*. *J Cytokine*, 2018: p. 1-10. j.cyto.2018.11.022.
186. Scarponi, C., et al., *Analysis of IFN- κ expression in pathologic skin conditions: Downregulation in psoriasis and atopic dermatitis*. *Journal of interferon cytokine research*, 2006. **26**(3): p. 133-140.
187. Parisi, R., et al., *Global epidemiology of psoriasis: a systematic review of incidence and prevalence*. *Journal of Investigative Dermatology*, 2013. **133**(2): p. 377-385.
188. Chestnov, O., *World Health Organization: Global report on psoriasis*. 2016. 2016.
189. Steinbach, A. and A.B. Riemer, *Immune evasion mechanisms of human papillomavirus: an update*. *International journal of cancer*, 2018. **142**(2): p. 224-229.
190. Tindle, R.W., *Immune evasion in human papillomavirus-associated cervical cancer*. *Nature Reviews Cancer*, 2002. **2**(1): p. 59-64.
191. Banerjee, N.S., et al., *Human papillomavirus (HPV) E7 induces prolonged G2 following S phase reentry in differentiated human keratinocytes*. *Journal of Biological Chemistry*, 2011. **286**(17): p. 15473-15482.
192. Lo Cigno, I., et al., *Human Papillomavirus E7 Oncoprotein Subverts Host Innate Immunity via SUV39H1-Mediated Epigenetic Silencing of Immune Sensor Genes*. *Journal of Virology*, 2020. **94**(4): p. e01812-19.
193. Chan, B., et al., *The murine cytomegalovirus M35 protein antagonizes type I IFN induction downstream of pattern recognition receptors by targeting NF- κ B mediated transcription*. *PLoS pathogens*, 2017. **13**(5): p. 1-35. e1006382.
194. Bravo, I.G. and Á. Alonso, *Mucosal human papillomaviruses encode four different E5 proteins whose chemistry and phylogeny correlate with malignant or benign growth*. *Journal of virology*, 2004. **78**(24): p. 13613-13626.
195. Regan, J.A. and L.A. Laimins, *Bap31 is a novel target of the human papillomavirus E5 protein*. *Journal of virology*, 2008. **82**(20): p. 10042-10051.
196. Ng, F.W., et al., *p28 Bap31, a Bcl-2/Bcl-XL-and procaspase-8-associated protein in the endoplasmic reticulum*. *The Journal of cell biology*, 1997. **139**(2): p. 327-338.
197. Uhlén, M., et al., *Tissue-based map of the human proteome*. *Science*, 2015. **347**(6220): p. 394-403.
198. Machihara, K. and T. Namba, *BAP31 Inhibits Cell Adaptation to ER Stress Conditions, Negatively Regulating Autophagy Induction by Interaction with STX17*. *Cells*, 2019. **8**(11): p. 1-13. 1350.